이학박사학위논문

Studies on the modulation of autophagic proteolysis during oxidative stress

산화적 스트레스 상황 하에서 세포 내 오토파지에 의한 단백질 분해 조절에 대한 연구

2018년 8월

서울대학교 대학원

생물물리 및 화학생물학과

김 대 호

산화적 스트레스 상황 하에서
세포 내 오토파지에 의한
단백질 분해 조절에 대한 연구
Studies on the modulation of autophagic proteolysis during oxidative stress

지도교수 이 준 호

이 논문을 이학박사 학위논문으로 제출함

2018년 6월

서울대학교 대학원

생물물리 및 화학생물학과

김 대 호

김대호의 이학박사 학위논문을 인준함

2018년 6월

위 원 장 권 용 태 (인)

부 위 원 장 이 준 호 (인)

위 원 묵 인 희 (인)

위 원 이 민 재 (인)

위 원 최 철 용 (인)

Studies on the modulation of autophagic proteolysis during oxidative stress

A dissertation submitted in partial
Fulfillment of the requirement
for the degree of

DOCTOR OF PHILOSOPHY

to the Faculty of
Department of Biophysics and Chemical Biology
at
Seoul National University
by

Daeho Kim

Date Approved:

June, 2018

_____

_____

_____

_____

_____

ABSTRACT

Studies on the modulation of autophagic proteolysis during oxidative stress

Daeho Kim

Department of Biophysics and Chemical Biology

The Graduate School

Seoul National University

Reactive oxygen species (ROS) are baring an extra electron, and the electron has a potential to engage in various reactions with its electro-potential energy in the cells. But, when excessive ROS are generated in cells, these ROS react with cellular substances and induce oxidative stress to cells. In response to the stress, there are the oxidative stress scavengers and through these mechanisms, cells could have reduced the concentration of ROS in cells; however, these mechanisms are limitedly focused on decreasing the concentration of ROS in cell or only controlling the ROS that are used

in the mechanism that the one of scavenging is mainly involved in. Therefore, it is insufficient to explain the response mechanism for the managing excessive ROS and consequences of oxidative stress in cells.

DJ-1/PARK7 is known as a protein having various activities in cells which is involved in cell growth and differentiation, or, mitochondrial homeostasis related with Parkinson's disease, but, intriguingly, among the functions of DJ-1, it also has a role in ROS recognition and scavenging. Under the tumor necrosis factor-related apoptosis-inducing ligand (TRAIL) induced oxidative stress, DJ-1 modulates an autophagy receptor, p62, and it targets ubiquitin (Ub) conjugated proteins to autophagic proteolysis. In response to TRAIL induced oxidative stress, Cys46, Cys53, and Cys106 of DJ-1 are oxidized by ROS and, though the process, a part of excessive ROS is diminished. Moreover, oxidized DJ-1 is interacting with arginylated BiP (R-BiP), which is N-terminally arginylated by TRAIL, and oxidation of DJ-1 has a pivotal role while the interaction is occurred. This interaction of oxidized DJ-1 and R-BiP is in part similar to an assistance activity of co-chaperone to chaperone. In summary, the interaction of oxidized DJ-1 and R-BiP modulates self-oligomerization of autophagy receptor, p62/SQSTM1, and this mechanism may target the misfolded protein and unfolded protein or other materials generated by oxidative stress to autophagy and processes the cytotoxic substances.

Given that DJ-1 is involved in processing cytotoxic substances under oxidative stress, DJ-1 knocked down cells were impaired in removing substances by lysosomal protein degradation. Therefore, the deficiency of DJ-1 incurs vulnerability of cells when cells suffer the stress from TRAIL or other stress inducers. In this study, DJ-1 functions on the autophagic proteolysis modulation and cyto-protective role in TRAIL

induced oxidative stress were verified.

Keywords: Oxidative stress, macroautophagy, N-end rule pathway, N-terminal arginylation, p62, proteolysis, protein quality control

Student number: 2011-22826

CONTENTS

LIST OF FIGURES AND TABLES

ABBREVIATIONS

Ala	Alanine
ATE1	Arginyl-tRNA protein transferase 1
BiP	Binding immunoglobulin protein
CHIP	Carboxyl-terminus of Hsp70 Interacting Protein
CHOP	C/EBP homologous protein
Cys	Cysteine
DMSO	Dimethyl sulfoxide
EDTA	Ethylenediamine tetraacetic acid
EGFP	Enhanced green fluorescent protein
ER	Endoplasmic reticulum
ERAD	ER-associated degradation
FACS	Fluorescence-activated cell sorting
FADD	Fas-Associated protein with Death Domain
FLAG-DJ-1	FLAG-tagged DJ-1

GAPDH	Glyceraldehyde 3-phosphate dehydrogenase
HA	Hemagglutinin
HA-BiP	HA-tagged BiP
IRE1α	Inositol-requiring protein 1α
IP	Immunoprecipitation
JNK	c-Jun NH2-terminal kinase
kDa	Kilodalton
LC3	Light chain 3
LC-MS/MS	Liquid chromatography-tandem mass spectrometry
MEF	Mouse embryonic fibroblast
MOI	Multiplicity of infection
MTT	3-(4,5-dimethylthiazol-2-yl)-2,5-diphenyltetrazolium bromide
NAC	N-acetylcysteine
PARP-1	Poly (ADP-ribose) polymerase 1
PBS	Phosphate-buffered saline solution
PERK	Protein kinase R-like endoplasmic reticulum kinase
PDI	Protein disulfide isomerase

PMSF	Phenylmethane sulfonyl fluoride
	or phenylmethylsulfonyl fluoride
SQSTM1	Sequestosome 1
R-BiP	Arginylated BiP
ROS	Reactive oxygen species
RT-PCR	Reverse transcription polymerase chain reaction
SDS-PAGE	Sodium dodecyl sulfate polyacrylamide gel electrophoresis
SEM	Standard error of the mean
SOD	Superoxide dismutase
shRNA	Small hairpin RNA
siRNA	Small interfering RNA
TAP	Tandem affinity purification
TRAIL	Tumor necrosis factor-related apoptosis-inducing ligand
Ub	Ubiquitin
UPR	Unfolded protein response
UPS	Ubiquitin proteasome system
WT	Wild-type

Introduction

Newly synthesized peptides are produced at ribosome and delivered to endoplasmic reticulum (ER) to be undergone the folding by molecular chaperones (Buchberger, Bukau, & Sommer, 2010; Bukau, Weissman, & Horwich, 2006). The folding of peptides makes proteins to get the ability to function properly as a component of particular mechanism or a normal enzyme; however, when cells suffer cellular stress, the folding mechanism is affected by the stress and misfolded or unfolded proteins are generated because of the stress incurred from certain effect and these proteins effects as another reason for cellular stress (Figure 1) (B. Chen, Retzlaff, Roos, & Frydman, 2011; Kriegenburg, Ellgaard, & Hartmann-Petersen, 2012). To diminish misfolded proteins in the cell, proteasomal degradation, macroautophagy (hereafter autophagy) or chaperone mediated autophagy are engaged in for degrading the proteins and these mechanisms are defined as the protein quality control (Ciechanover & Kwon, 2015; X. Wang, Pattison, & Su, 2013).

Upon the degradation process for the protein, many of protein follow the N-end rule which is UBR box of the specific E3 ubiquitin (Ub)-ligase enzymes: N-recognin, such as UBR1, UBR2 or UBR4, recognize the single amino acid of N-terminus of the substrate proteins: N-degron, and mediates ubiquitination of the proteins. Through the recognition by N-recognin, the metabolic fate of the substrates are determined, and Ub -conjugated clients are destined to degrade by proteasome (S. T. Kim et al., 2013; Varshavsky, 2011). Based on the N-end rule, a single amino acid exposed on the N-terminus is the key molecule for determining the degrading rate for proteins and among

the amino acids arginine (Arg), histidine (His), isoleucine (Ile), leucine (Leu), lysine (Lys), phenylalanine (Phe), tyrosine (Tyr), and tryptophan called primary destabilizing residues (Cha-Molstad et al., 2015; Cha-Molstad et al., 2017; Ciechanover & Kwon, 2017; Ji & Kwon, 2017). In addition, aspartate (Asp) and glutamate (Glu), secondary destabilizing residues, are undergone the arginylation on their R groups, by ATE1 R-transferases in cells; still other amino acids asparagine (Asn) cysteine (Cys), and glutamine (Gln) need deamination (for asparagine and glutamine) or oxidation (for cysteine) on their R group and these are called tertiary destabilizing residues (Figure 2) (Gibbs, Bacardit, Bachmair, & Holdsworth, 2014; S. T. Kim et al., 2013; Wadas et al., 2016). Therefore, how well identified by N-recognin and how less steps needed to be converted for the N-recognin are the rate-limiting step for the ubiquitination by UBR proteins. (Ciechanover & Kwon, 2017; Ji & Kwon, 2017; Shim et al., 2018).

Even the condition without stresses, there are many misfolded proteins produced during the translation or folding of proteins in the ER, and these misregulated proteins are identified by ER residing molecular chaperones and targeted to ERAD (ER-associated protein quality control) with conjugating Ub tags to their clients and delivering to proteasomal degradation (Cha-Molstad et al., 2015; Shim et al., 2018). But under the cellular stress, ER residing BiP/GRP78/HSPA5 is translocated to cytoplasm and cytosolic BiP is Nt-arginylated on Glu19 (Nt-E19) by ATE1 coded R-transferase (Cha-Molstad et al., 2015; Ji & Kwon, 2017; Kwon et al., 1998; Shim et al., 2018; Tasaki et al., 2005).

Under the cellular stress, massive misfolded proteins are generated and are tend to form aggregates in cytoplasm, and aggregates themselves can be another cause of stress to cells. Many of these aggregates are not able to be degrade by proteasome and targeted

to macroautophagy and processed by lysosome (Ciechanover & Kwon, 2015, 2017). When the autophagy has been initiated, various kind of regulators and factor are recruited to ER membranes and forms omegasome, which is initiating step for constituting the phagophore, and breakaway from ER membrane, called phagophore (Green & Levine, 2014; Zaffagnini & Martens, 2016). During the cargo targeting and maturation of phagophore to autophagosome (Figure 3), ub-conjugates or aggregates are delivered to the membrane of phagophore and when protein cargos interact or are recognized by specific receptor is called selective autophagy (Dikic, 2017; Dikic & Elazar, 2018). Unlike non-selective or general autophagy, selective autophagy identifies specific protein cargos by its specific autophagic substrates (Figure 4) (Dikic & Elazar, 2018), such as ER residing molecular chaperone BiP, or stress specific autophagic receptors. Thereby, cells can response to specific cytosolic stress or other stresses initiated from cellular organelles; however, specific receptors for specific stresses are yet to be discovered.

ER residing molecular chaperone BiP is known as one of member of Hsp70 family (Chien et al., 2010; Gething, 1999; J. Wang, Lee, Liem, & Ping, 2017; J. Wang, Pareja, Kaiser, & Sevier, 2014). These family proteins are functioning with their partners called co-chaperones or co-factors, even alter their functions such as changing the role from folding the peptide to degrading the proteins (Figure 5) (Broadley & Hartl, 2009; Duncan, Cheetham, Chapple, & van der Spuy, 2015; Muller et al., 2013). Meanwhile, ER residing molecular chaperone BiP is translocated to cytosol and through Nt-arginylation of cytosolic BiP, R-BiP binds to ZZ domain of p62/SQSTM1/Sequestosome 1 and it activates the protein by resulting the self-oligomerization of p62 which is not introduced in normal condition. During the

interaction of R-BiP and p62, the complex facilitates recruiting protein aggregates and forming the complex including cargo proteins. This interaction also leads the interaction with MAP1LC3/LC3 (microtubule-associated protein 1 light chain 3) embedded on autophagic membranes, resulting the targeting of cargoes to lysosomal degradation. Thus, ER residing BiP is translocated to cytoplasm and its arginylation by N-end rule leads activation and oligomerization of autophagic receptor p62 with protein cargos and finally mediates lysosomal degradation by forming autolysosomes (Cha-Molstad et al., 2018; Cha-Molstad et al., 2017). However, BiP has multiple role in protein quality control (Cha-Molstad et al., 2018; Shim et al., 2018), and it may alter the partners as if the family protein Hsp70 does. Considering the point that BiP may get the enzymatic association with its a binding partner, it is still unknown that specific binding partners of BiP during the stress, which the co-chaperone like protein to BiP may response to specific stress should be dealt with.

Reactive oxygen species (ROS) or reactive nitrogen species (RNS) introduced by oxygen or nitrogen baring singlet electrons not fitting with the octet rule, and reactive electrons are prone to react with other substances needed to have extra electrons to stabilize themselves (Murphy, 2009). The ROS is shown in cells as following substances: O_2^- (superoxide radical), ●OH (hydroxyl radical), and H_2O_2 (hydrogen peroxide), and these are mainly generated by mitochondria (Y. Chen, Azad, & Gibson, 2009; Filomeni, De Zio, & Cecconi, 2015; Kiffin, Bandyopadhyay, & Cuervo, 2006; Scherz-Shouval et al., 2007). Although these ROS are known to be harmful for cell because of the activity; however, these substances are used in various reactions to initiate by giving electron energy for the reaction engaged in, for example, protein folding (Ray, Huang, & Tsuji, 2012). Meanwhile, the circumstance which the ROS or

other substance having unstable electron substances are overwhelming cellular environment is known as an oxidative stress on cells (Filomeni et al., 2015).

Oxidative stress is a symptom mainly caused by imbalance of the producing and scavenging system of ROS that supposed to be tightly controlled in the cell. ROS are naturally generated by mitochondria during the oxidative phosphorylation as a byproduct of the mechanism (Chance, Boveris, Oschino, & Loschen, 1973), but excessive production of ROS, due to dysfunction of mitochondrial enzymes or physiological imbalance may be resulted from other reasons, may cause translocation of mitochondrial ROS to cytoplasm (Murphy, 2009), and this translocation of ROS invokes oxidative stress (S. S. Cao & Kaufman, 2014; Filomeni et al., 2015; Tsutsui, Kinugawa, & Matsushima, 2011; H. Zhang et al., 2009). Obviously, the transportation of ROS is harmful for the cells; however, there is an anti-cancer ligand using the mechanism inducing the oxidative stress to cancer cells (Altman & Rathmell, 2012; Gibson, 2013; Ishdorj, Li, & Gibson, 2012; Patella et al., 2016; Silva, Pernomian, & Bendhack, 2012; Wen et al., 2013), called tumor necrosis factor-related apoptosis-inducing ligand (TRAIL) (Suzuki-Karasaki, Ochiai, & Suzuki-Karasaki, 2014; Suzuki et al., 2012). TRAIL binds to receptors mainly expressed in cancer cells: death receptor 4 (DR4) or death receptor 5 (DR5), on the membrane of cancer cells, and it mediates cell death in directly with activating caspases (Type I) (Schneider-Brachert, Heigl, & Ehrenschwender, 2013), or it leads the dysfunction of mitochondria, which results apoptotic cell death (Type II) (Guicciardi & Gores, 2009; Hu et al., 2006; Inoue & Suzuki-Karasaki, 2013; Johnstone, Frew, & Smyth, 2008; Suzuki-Karasaki et al., 2014). In HCT116: human colon tumor cell, TRAIL has been known as having a cell-killing effect on the cell and inducing apoptosis by causing dysfunction of mitochondria as

well as direct activation of caspases (D. H. Lee et al., 2016); through the mechanism, TRAIL may cause oxidative stress originated from mitochondria and it can be considered as an oxidative stress inducer for the certain environment.

To defense cells from oxidative stress, there are many canonical mechanisms and cell organelles to deal with the stress. For the scavenger systems for excessive ROS in cells, superoxide dismutase (SOD), glutathione and peroxiredoxin circuit, and peroxisome have been commonly known as systems abolishing the ROS in cells. SOD mainly located in cytoplasm and mitochondria, and it resolves excessive ROS in both of cellular compartments; however, it cannot handle all the excessive ROS that has been occurred by oxidative stress (Day et al., 2012; Ramis, Esteban, Miralles, Tan, & Reiter, 2015). Glutathione and peroxiredoxin circuit are responding to ROS in cytoplasm but the mechanism is quite suspended while massive ROS has been produced by which oxidative stress inducer or under pathological symptoms (Day et al., 2012). Peroxisome is a cell organelle for fatty acid metabolism; thus, it has many enzymes including resolving ROS, but this organelle is focused on diminishing ROS generated by the fatty acid metabolism or the control of concentration of the ROS in the peroxisome which could be used for the source of enzymatic energy for the reaction in peroxisome (Lodhi & Semenkovich, 2014). Consequently, these mechanisms are focusing on the getting rid of or decreasing the concentration of ROS in cellular environment, but these are insufficient to explain the response against oxidative stress including the process for handling misfolded proteins generated by imbalanced energy from ROS.

For other possibilities for scavenging ROS, in resent studies, DJ-1/PARK7 is known as another protein having an activity to reduce ROS in cell (Andres-Mateos et

al., 2007; Kinumi, Kimata, Taira, Ariga, & Niki, 2004; Mitsumoto et al., 2001; Wilson, 2011). DJ-1 has been investigated as one of the most abundant protein in human cells, and it mediates growth and differentiation of cells, or, intriguingly, transcriptional regulation which is related to oxidative stress response, and mitochondrial homeostasis which may be involved in Parkinson's disease (Choi et al., 2006; Guzman et al., 2010; Hayashi et al., 2009; Lev et al., 2009; McCoy & Cookson, 2011; Saito, 2014; Thomas et al., 2011; Wilson, 2011; Won et al., 2013). Among the various functions of DJ-1, DJ-1 also has scavenging activity against ROS by oxidation on its oxidation sites: Cys46, Cys53, and Cys106, partially similar to acting as a co-chaperone in quality control of proteins (Andres-Mateos et al., 2007; Hayashi et al., 2009; Kolisek et al., 2015; H. M. Li, Niki, Taira, Iguchi-Ariga, & Ariga, 2005; Ren, Fu, Wang, Mu, & Wang, 2011; X. Wang et al., 2012). During the scavenging ROS, on these oxidation sites, these cysteines follow the nature of sulfur oxidation mechanism, and when each of sites oxidized with three oxygens (Figure 6), these sites become irreversible and further mechanism has not been discovered (Andres-Mateos et al., 2007; Im, Lee, Junn, & Mouradian, 2010; Saito, 2014; Wilson, 2011; Zhou, Zhu, Wilson, Petsko, & Fink, 2006). Although many of studies focused on delivery of DJ-1 from cytoplasm to nucleus and the function as a transcription factor which induces genes to response ROS in the cell (Ariga et al., 2013; Bonifati et al., 2003; Mitsumoto et al., 2001; Taira et al., 2004; Zhou et al., 2006), detailed metabolic process, which is having a potential to be a co-chaperone to molecular chaperones involving in protein quality control, have been poorly understood. Moreover, DJ-1 insufficiency incurs excessive ROS in cell that rises a chance for malfunction of organelles for example mitochondrial dysfunction (Canet-Aviles et al., 2004; Kahle, Waak, & Gasser, 2009; R. H. Kim et al., 2005; H. M. Li et

al., 2005; Meulener, Xu, Thomson, Ischiropoulos, & Bonini, 2006; Mitsumoto et al., 2001; Taira et al., 2004).

Therefore, in the studies, the investigation was focused on the function of DJ-1 that is related to autophagic proteolysis to protect cells against TRAIL induced oxidative stress, which is specific to cancer cells. In addition, through the research, I realized DJ-1 is the binding partner of molecular chaperone BiP, also known as ER counterpart of Hsp70, as if it is a co-chaperone during protein quality control. Moreover, TRAIL induced oxidative stress may induce arginylation on N-terminal of BiP and R-BiP functions as an activator for p62 with DJ-1, which is a role in modulation among R-BiP and p62 during the protein quality control by autophagic proteolysis; by the way, this interaction may be adapted to not only degrading misfolded ub-conjugates, but also this interaction may explain the detailed mechanism of Keap1 degradation of Keap1-Nrf2 response system against oxidative stress.

Material and methods

Cell culture

DJ-1$^{-/-}$ and corresponding wild-type mouse embryonic fibroblast (MEF) cell lines were kindly given by Dr. Mark R. Cookson (NIH, Washington DC, USA). Dulbecco's modified eagle medium with the addition of 55 μM β-mercaptoethanol (Invitrogen, Carlsbad, CA, USA) was used for maintenance of MEFs. Human colon tumor derived HCT116 cells and human cervical cancer HeLa cells were cultivated in McCoy's 5A medium and Dulbecco's Modified Eagle's minimum essential medium, respectively. Each of media contained 10% fetal bovine serum (HyClone, Logan, UT, USA), 1 mM L-glutamine, and 26 mM sodium bicarbonate. All the cells were kept in a 37°C humidified incubator with 5% CO_2.

Reagents and antibodies

The autophagy inhibitor bafilomycin A1 was purchased from Sigma (St. Louis, MO, USA). Human TRAIL was purchased from PeproTech (Rocky Hill, NJ, USA), and vaccinia virus expressing murine TRAIL (vvmTRAIL) and its parental thymidine kinase-deleted virus VJS6 for MEFs was described previously (Ziauddin et al., 2010). The ROS inducer tert-butyl hydroperoxide was purchased from Sigma (St. Louis, MO, USA).

Followings are the information of antibodies used in the research: Anti-DJ-1, and anti-p62 were purchased from Santa Cruz Biotechnology (Santa Cruz, CA, USA). Anti-

GFP, anti-FLAG, anti-HA, anti-DJ-1, anti-VDAC, and anti-calnexin were purchased from Cell Signaling (Beverly, MA, USA). Anti-WIPI2 and anti-p62 were purchased from Abcam (Cambridge, UK). Anti-LC3 was purchased from Sigma (St. Louis, MO, USA) and MBL (Woburn, MA, USA). Anti-FK2 was purchased from Enzo (Farmingdale, NY, USA). Anti-β-actin antibody was purchased from MP Biomedicals (Solon, OH, USA) and Sigma (St. Louis, MO, USA). For the secondary antibodies, anti-mouse-IgG-HRP and anti-rabbit-IgG-HRP were purchased from Santa Cruz Biotechnology. For the immunostaining, Alexa Fluor 488 conjugated goat anti-rabbit IgG, and anti-mouse IgG, and Alexa Fluor 555 conjugated goat anti-rabbit IgG, and Alexa Fluor 555 goat anti-mouse IgG were purchased from Thermo Fisher Scientific (Waltham, MA, USA).

Production of anti-R-BiP antibody

The Rabbit polyclonal antibody specifically detecting arginylated form of BiP (R-BiP) was produced using the recombinant peptide sequence REEEDKKEDVGC according to the N-terminal of matured R-BiP through a custom service at AbFrontier Inc. (Seoul, South Korea) as previously reported (Cha-Molstad et al., 2015). R-BiP antibody is now commercially available at AbFrontier Inc. (Cat. AR05-PA0001) and EMD Millipore (Cat. # ABS2103, Temecula, USA).

Plasmids, cloning, and mutagenesis

HA tagged recombinant BiP and GFP tagged recombinant DJ-1 were cloned in pCMV-HA and pEGFP-N1, respectively. The QuikChange II XL mutagenesis kit (Agilent Technologies, Santa Clara, CA, USA) was used for the mutagenesis of DJ-1 on the

three cysteine sites.

The following primers were used for mutagenesis of the three cysteine residues on human DJ-1. Each of the cysteine was converted to alanine:

for the mutation cysteine in position 46:

5′- GAAAAGACCCAGTACAGgcTAGCCGTGATGTGGTC-3′

(the mutated nucleotide is lower case);

for the mutation of alanine in position 53:

5′- CCGTGATGTGGTCATTgcTCCTGATGCCAGCCTTG-3′

(the mutated nucleotide is in lower case);

for the mutation of alanine in position 106:

5′- CCTGATAGCCGCCATCgcTGCAGGTCCTACTGCTC-3′

(the mutated nucleotide is lower case).

FLAG tagged DJ-1 expression plasmid (p3x FLAG-DJ-1) was kindly provided by Dr. Guanghui Wang (University of Science and Technology of China).

Stable transfection and generation of stable cell lines

Stably expressing FLAG tagged recombinant DJ-1 was constructed by transfection of p3x FLAG-DJ-1 plasmid in HCT116 cells with using Lipofectamine 2000 reagent corresponding to the manufacturer's protocol (Invitrogen, Carlsbad, CA, USA). Transfected cells were selected with 1 mg/ml G418 (Merck Millipore, Darmstadt, Germany) for two weeks and then maintained in complete medium containing 500 μg/ml G418. Stable DJ-1 knocked down and cell with transfected with scramble shRNA were produced by transducing with lentivirus containing shRNA encoded against DJ-1 or non-specific shRNA, respectively (Santa Cruz, CA, USA). Transduced

cells were selected with 5 μg/ml puromycin (Merck Millipore, Darmstadt, Germany) and maintained in complete media.

DJ-1 complex purification and mass spectrometry analysis

A detailed tandem affinity purification (TAP) procedure was followed by previous report (Nakatani & Ogryzko, 2003). FLAG-DJ-1 stably expressing HCT116 cells were used in TAP purification and FLAG-DJ-1 and their protein complexes were immunoprecipitated with anti-FLAG M2 monoclonal antibody-conjugated agarose beads (Sigma, St. Louis, MO, USA). A subpopulation of affinity-purified protein complexes was separated by 12% SDS-PAGE and then the gel was undergone silver-staining. In-gel digestion using trypsin (Promega, Madison, WI, USA) was performed manually as previously described (Shevchenko, Tomas, Havlis, Olsen, & Mann, 2006). Trypsin digested peptides were desalted using a Ziptip C18 (Merck Millipore, Darmstadt, Germany) and were eluted from the Ziptip with 0.5 μL of matrix solution (α-cyano-4-hydroxycinnamic acid 5 mg/mL in 50% acetonitrile, 0.1% trifluoroacetic acid, and 25 mM ammonium bicarbonate) and then the solution containing peptides were spotted on a MALDI plate. MALDI-TOF mass spectra were acquired in reflectron positive ion mode, averaging 4000 laser shots per spectrum. LTQ mass spectrometer (Thermo Scientific, Hudson, NH, USA) equipped with a nanoelectrospray source (New Objective, Woburn, MA, USA) was used for LC-MS/MS analysis and the analysis was held in the Mass Spectrometry Facility of the University of Pittsburgh. To the identified peptide sequences, the Scaffold Viewer (Proteome Software, Portland, OR, USA) database search engine was used in matching tandem mass spectra.

Subcellular fractionation

Cells were harvested, and washed by centrifugation at 500 xg for 5 min with phosphate buffered saline (PBS) (with 2 mM of Na_3VO_4 and 2 mM NaF for the inhibition of phosphatases). For the homogenization, cells were resuspended in homogenization buffer (225 mM mannitol, 75 mM sucrose, 30 mM Tris-HCl pH 7.4, 0.1 mM EGTA and PMSF), and then those were gently disrupted by Dounce homogenization. Cell extracts were centrifuged twice at 600 xg for 5 min to remove nuclei and unbroken cells, and then the supernatant was centrifuged at 10,300 xg for 10 min to purify a crude extract of mitochondria. Next, for the lysosomal and plasma membrane fraction, the supernatant from 10,300 xg purification was centrifuged at 20,000 xg for 30 min at 4°C. Further centrifugation of the obtained supernatant at 100,000 xg for 90 min (70-Ti rotor, Beckman, Milan, Italy) at 4°C resulted in the isolation of ER (pellet) and cytosolic fraction (supernatant). To purify genuine mitochondria from crude mitochondrial fraction, the pellet was resuspended in isolation buffer (250 mM mannitol, 5 mM HEPES pH 7.4 and 0.5 mM EGTA), and the extract was undergone to Percoll gradient centrifugation (Percoll medium: 225 mM mannitol, 25 mM HEPES pH 7.4, 1 mM EGTA and 30% vol/vol Percoll) in a 10-ml polycarbonate ultracentrifuge tube. After centrifugation at 95,000 xg for 30 min (SW40 rotor, Beckman, Milan, Italy), a dense band containing purified mitochondria was recovered approximately 3/4 down the tube, washed by centrifugation at 6,300 xg for 10 min to remove the Percoll, and finally resuspended in isolation medium. When preservation of protein phosphorylation states was required, immediately after the recovery, 2 mM Na_3VO_4 and 2 mM NaF were added to each fraction.

Co-immunoprecipitation

Co-immunoprecipitation was carried out using protein G-coated sepharose beads (GE Healthcare, Chalfont St Giles, UK) following the manufacturer's instructions. For whole-cell extracts, cells were lysed in buffer containing 30 mM Tris-HCl (pH 7.4), 50 mM NaCl, and 1% NP-40 and cleared by centrifugation. Protein extractions in the ER fraction were carried out by adding 50 mM NaCl and 1% NP-40 to the homogenization buffer. All the buffers were supplemented with proteases and phosphatase inhibitors (2 mM Na_3VO_4, 2 mM NaF,1 mM PMSF, and protease inhibitor cocktail). Extracted proteins (1000 μg) were first precleared by incubating lysates with sepharose beads for 1 h at 4°C and the supernatant (referred to as Input) was incubated overnight with antibodies at 4°C. Precipitation of the immune complexes was carried out for 4 h at 4°C. Afterwards, beads were washed with 50 mM Tris-HCl pH 7.4, 0.1% NP-40 4°C supplemented with phosphatase inhibitors and PMSF. Samples were processed by SDS-PAGE and analyzed by standard western blotting technique.

Immunostaining assay

Cells were washed with PBS once, fixed in 4% paraformaldehyde at room temperature for 30 min, incubated in permeable / blocking solution (0.5% BSA or 5% Goat serum (Abcam, Cambridge, UK) in PBS) for 1 hour. After blocking, the incubation with primary antibodies or 200 nM MitoTracker® Green (Invitrogen, Carlsbad, CA, USA) was followed. Subsequently, goat anti-rabbit or mouse IgG with Alexa Fluor-conjugated secondary antibodies (Invitrogen, Carlsbad, CA, USA) were used. For confocal microscopy, a LSM700 laser scanning confocal microscope (Zeiss, Jena, Germany) was used and processed by ZEN 2012 (Version 1.1.13064.302) under 63x

water immersion objective.

Detection of ROS generation

MitoSOX™ Red reagent and CM-H2-DCFDA were used for evaluation of ROS generation, and these chemicals permeate live cells where it selectively targets mitochondria ROS (MitoSOX™, Invitrogen, Carlsbad, CA, USA), and cytosolic ROS (CM-H_2-DCFDA, Invitrogen, Carlsbad, CA, USA) following the manufacturer's protocol (Invitrogen, Carlsbad, CA, USA). For co-localization studies of mitochondria and ROS, cells were treated with MitoSOX™ Red (5 μM) and MitoTracker® Green (0.2 μM, Invitrogen, Carlsbad, CA, USA). Cells were loaded with MitoSOX™ Red and MitoTracker® for 30 min at 37°C, and then treated with TRAIL for 1 h at 37°C. Using a flow cytometer, MitoSOX™ Red was excited at 488 nm and fluorescence emission at 575 nm was measured. Relative fluorescence intensity was used as a measurement of mitochondrial superoxide production. For cytosolic ROS measurement, with pre-treated of TRAIL for 4 h at 37°C, cells were treated with 7 μM of CM-H_2-DCFDA for 30 min at 37°C.

Immunoblotting assay

As previously described (D. H. Lee, Sung, Bartlett, Kwon, & Lee, 2015), immunoblotting assay was performed. Cells were lysed with Laemmli lysis buffer and boiled for 10 min. The concentration of proteins was measured with BCA Protein Assay Reagent (Thermo Scientific, Hudson, NH, USA), and extracts were separated by SDS-PAGE, and were transferred to PVDF membranes. By using the chemiluminescence protocol (ECL, Amersham, Arlington Heights, IL, USA), immuno-reactive proteins

were visualized.

GST pull-down assay

For the expression of recombinant GST-tagged DJ-1, plasmids pGEX-GST and pGEX-GST-DJ-1 were transformed into E. coli DH5α. According to the manufacturers' procedure, glutathione agarose resin (Pierce™ GST Protein Interaction Pull-Down Kit, Thermo Scientific, Hudson, NH, USA) pretreated with equilibrium buffer was utilized to capture the proteins into complexes. Then, the complexes were incubated with lysate of HCT116 cells overexpressing FLAG or FLAG-DJ-1 treated with 5 ng/ml of TRAIL 4 h at 4°C for 2 h whether to check the exchange of endogenous DJ-1 and recombinant GST-tagged DJ-1. After that, elution buffer was used to separate the GST-DJ-1 binding protein complexes and the eluted protein complexes were analyzed using immunoblotting assay.

JC-1 mitochondrial membrane potential assay

After human TRAIL treatment, cells were stained using a JC-1 Mitochondrial Membrane Potential Detection Kit (Invitrogen, Carlsbad, CA, USA) for 10 min and analyzed using flow cytometry. Fluorescence intensity was measured with the FACScan flow cytometer (Beckman Coulter, Hialeah, FL, USA), and the resulting data were analyzed using Flowjo software (Tree Star, Inc, Ashland, OR, USA).

Survival assay

MTT assays were carried out using the Promega CellTiter 96 AQueous One Solution Cell Proliferation Assay (Promega, Madison, WI, USA). Cells were grown in tissue

culture-coated 96-well plates and treated as described in results. Cells were then treated with MTS/phenazine methosulfate solution for 2 h at 37°C. Absorbance at 490 nm was determined using an enzyme-linked immunosorbent assay plate reader.

Apoptosis assay

The translocation of phosphatidylserine, one of the markers of apoptosis, from the inner to the outer leaflet of the plasma membrane was detected by binding of allophycocyanin-conjugated annexin V. Briefly, cells untreated or treated with TRAIL were resuspended for 4 h in the binding buffer provided in the Annexin V-FITC Detection Kit II (BD Biosciences Pharmingen, San Diego, CA, USA). Cells were mixed with 5 μL Annexin V-FITC reagent and incubated for 30 min at room temperature in the dark. Staining was terminated and cells were immediately analyzed uisng flow cytometry.

RT-PCR analysis

Total RNA was isolated from untreated or TRAIL-treated cells using the RNAeasy Kit (Qiagen, Valencia, CA, USA) according to the manufacturer's protocol. Total RNA (2 μg) was used to generate complementary DNA using SuperScript III reverse transcriptase (Invitrogen, Carlsbad, CA, USA). All PCR reactions were performed in triplicate, and PCR products were subjected to a melting curve analysis. The expression of p62 was detected by TaqMan® Gene Expression Assays 20 (Hs01061917_g1, Thermo Scientific, Hudson, NH, USA) according to manufacturer’s protocol.

Statistical analysis

Statistical analysis was carried out using GraphPad Prism6 software (GraphPad Software, Inc., San Diego, CA, USA). The results were expressed as the mean of arbitrary values ± SEM. All results were evaluated using an unpaired Student's t test, where a p-value of less than 0.05 was considered significant.

RESULTS

TRAIL induced oxidative stress

TRAIL has been reported for an anti-tumor ligand which binds to tumor specific membrane receptor DR4 or DR5 (Kuang, Diehl, Zhang, & Winoto, 2000; Suliman, Lam, Datta, & Srivastava, 2001; Walczak et al., 1997; Wiley et al., 1995). Through binding with receptors on the membrane, there are two types of cell death signal cascade triggered by TRAIL; one of which is activating caspase to directly induce apoptosis and the other is influencing electron transfer systems in mitochondria and generate ROS to make oxidative stress to cells (Rudner et al., 2005; Suliman et al., 2001; S. Wang & El-Deiry, 2003). TRAIL sensitive cells affected by either or both of sequences, but human colon cancer derived HCT116 cells have been known that cells are influenced by mitochondria impairment rather than direct caspase activation (Inoue & Suzuki-Karasaki, 2013; Suzuki-Karasaki et al., 2014). To determine the generation of ROS by TRAIL in dose dependent manner, I performed fluorescence activated cell sorting (FACS) assay by using MitoSox specifically recognizing mitochondrial superoxide (Dickinson, Srikun, & Chang, 2010). Through the experiment, I could have verified that TRAIL generated mitochondrial superoxide by cytotoxic mechanism and the amount of ROS has been increased according to the concentration of TRAIL that has been treated. (Figure 7A and 7B). Meanwhile, it is also important to check that the generation of ROS had taken place; thus, I conducted further experiment to examine the location of superoxide and the cell organelle which the location is supposed to be

mostly in mitochondria, and signals of Mito-Tracker, indicative of mitochondria, and MitoSox were co-located with each other; therefore, I have concluded that signals from FACS is mostly from superoxide in mitochondria and it is indeed induced from TRAIL treatment. (Figure. 8A)

By the way, TRAIL generated mitochondrial ROS have a possibility that mitochondrial ROS are not transferred to cytoplasm and might have a chance to be resolved in mitochondrial matrix by dismutases in mitochondria. Thereby, it is needed to determine whether mitochondrial ROS moves on cytoplasm; I performed further experiment tagging cytoplasmic ROS with CM-H_2-DCFDA (Eruslanov & Kusmartsev, 2010), and it showed significant increase in the signal in TRAIL treated cells (Figure 8B). By contrast, when N-acetylcysteine (NAC) getting rid of cytoplasmic ROS in cells was treated, the TRAIL effect on ROS generation was meaningfully eliminated (Figure 8B); as a result, TRAIL induces mitochondrial ROS and the ROS is transferred to cytoplasm and it may cause cytosolic oxidative stress.

DJ-1 as a TRAIL induced oxidative stress reducer

In previous studies, it has been reported that there are many physiological roles on DJ-1 (Saito, 2014), and among these various function, DJ-1 has an activity to getting rid of reactive oxygen species (ROS) (Andres-Mateos et al., 2007; Kolisek et al., 2015; Lev et al., 2013; Lev et al., 2009; Wilson, 2011) in the cells. In this study, I also reproduced as well as shown in previous studies, as expected, (Inoue & Suzuki-Karasaki, 2013; D. H. Lee et al., 2016; Suzuki-Karasaki et al., 2014) and ROS induced by TRAIL located in mitochondria verified by co-localization of Mito-Tracker and MitoSox signals (Figure 8A). In addition, compared with normal cell, DJ-1 deficient

cells showed increased level of ROS production not only under TRAIL stress, but also without the treatment (Figure 9A and 9B), based on this result, I could have concluded that DJ-1 influences on the level of mitochondrial ROS under the oxidative stress as well as basal level.

However, the result from MitoSox is only limited to the ROS from mitochondria, as mentioned, so it is needed to elucidate whether DJ-1 influences transfer of ROS in mitochondria to cytosol (Giaime, Yamaguchi, Gautier, Kitada, & Shen, 2012), I have performed CM-H_2-DCFDA for detecting cytosolic ROS (Ling, Tan, Lin, & Chiu, 2011) and it showed also significantly accumulated when TRAIL was treated (Figure 8B). Thus, the treatment of TRAIL to HCT116 leads the induction of ROS not only in mitochondria; it produces excessive ROS in cytosol, as well. Interestingly, DJ-1 deficient cells showed more significant accumulation under TRAIL treatment and it was abolished when the antioxidant N-acetylcysteine (NAC) was treated. Therefore, DJ-1 protects from TRAIL induced oxidative stress both of mitochondrial superoxide and its derivatives in cytosol.

The binding partner of DJ-1 under TRAIL induced oxidative stress

To understand the ROS protecting mechanism of DJ-1 under the oxidative stress, I performed tandem affinity immunoprecipitation assay with using HCT116 cell lines that are stably overexpressing FLAG or FLAG-DJ-1, and pulled down the proteins interacting with DJ-1 under TRAIL treatment. Proteins came out with recombinant DJ-1 were analyzed by liquid chromatography-tandem mass spectrometry (LC-MS/MS) (Figure 10A). In this analysis, there were chaperone proteins such as the ER-residing molecular chaperone BiP, and its cytosolic counter-partner Hsp70 and still other

cytosolic chaperones HSPA8 (HSC70), Hsp90 as well as the E3 ubiquitin-protein ligase TRIM21 and the eukaryotic translation initiation factor 4B eIF4B protein (Table 1). Among these proteins, I chose BiP the mechanism interacting DJ-1. To identify the cytosolic interaction between ER-residing chaperone BiP and DJ-1, I transiently transfected recombinant FLAG-DJ-1 and HA-BiP in HCT116 and found its binding under overexpression of both binding components (Figure 10B); in addition, to figure out the endogenous interaction between BiP and DJ-1 induced by TRAIL, I employed immunoprecipitation with endogenous protein and the interaction was induced under TRAIL induced oxidative stress (Figure 10C). Thus, I could have concluded that the ROS protecting mechanism of DJ-1 is related to interacting with ER-chaperone BiP and the location that its interaction has been occurred is still needed to be determined.

R-BiP induction by TRAIL and interaction with DJ-1

BiP is known as ER-residing molecular chaperone and mostly function as a protein folder locating in ER lumen (Gething, 1999); however, it has been reported that BiP is also located in non-ER compartment such as cytosol, mitochondria or plasma membrane (Gonzalez-Gronow, Selim, Papalas, & Pizzo, 2009; Y. Zhang, Liu, Ni, Gill, & Lee, 2010). In recent studies, subpopulation of BiP is arginylated on its N-terminal Glu19 (Nt-E19) by ATE1-encoded R-transferase under certain stresses such as ER stress (Figure 11) or cytosolic dsDNA induced immune reaction as a part of innate immunity (Cha-Molstad et al., 2015); in contrast, arginylated BiP (R-BiP) is not detectable in cell without a stress. Based on previous study, it was necessary to verify whether TRAIL induced oxidative stress induces R-BiP; through the immunoblotting assay and using R-BiP detectable antibody, TRAIL treatment was able to arginylate on

N-terminus of BiP and accumulated timely manner of treatment, indeed, TRAIL induced stress significantly elevated the level of R-BiP (Figure 12A). To determine the location where BiP and DJ-1 interact with, I conducted fraction assay using with differential centrifugation and changing the concentration of buffers to check the place among the cell organelles indicative of their marker proteins, and TRAIL induced R-BiP was shown in cytosol, exclusively, as expected, and DJ-1 is located both cytosol and mitochondria, but has not been detected in ER compartment, which is the place BiP mainly locates (Figure 12B); therefore, it is suggesting that ER-residing molecular chaperone BiP is translocated from ER to cytosol with arginylation on its N-terminus, then interacts with DJ-1 which has been taken place in cytosol.

Further verification for interaction of R-BiP and DJ-1, recombinant DJ-1 was transiently expressed in both HCT116 (Figure 13A) and HeLa cells (Figure 13B) and R-BiP and DJ-1 are interacting inevitably under TRAIL induced oxidative stress; thus mature BiP is transferred to cytosol and arginylated on its N-terminus by ATE1-encoded R-transferase then arginylated BiP interacts with DJ-1. In addition to co-IP assay from cell extract, I performed GST-pull down assay using bacterial overexpressed recombinant GST-DJ-1 and it also interacts with R-BiP when TRAIL was treated in HCT116 (Figure 13C). Thus, these results indicate DJ-1 binds with R-BiP, possibly as if co-chaperone.

Importance of arginylation on BiP in interaction with DJ-1

BiP is known as a N-terminal rule substrate and it is arginylated when the cells are suffering ER stress. Because of the stress, mature BiP is coming out from ER and arginylated by ATE1 in somewhere else in cytoplasm (Cha-Molstad et al., 2015; Shim

et al., 2018). But it remains to be a question that whether mature “cytosolic” BiP or “arginylated” cytosolic BiP is important. This claim is important because it is necessary to examine BiP is molecular chaperone and it has its own high affinity to other protein; thus it is needed to be segregate the possibility of non-specific binding on their interaction between cytosolic BiP and DJ-1. To diminish the possibility, I employed Ub-X-BiP-GFP system which is exposing R-BiP-GFP (Arg-BiP-GFP) representing arginylation or Val-BiP-GFP (V-BiP-GFP) after cleavage by deubiquitination enzyme (DUB) (Cha-Molstad et al., 2018; Cha-Molstad et al., 2015; Cha-Molstad et al., 2017) (Figure 14A). N-terminal arginine exposed BiP has an affinity to bind ZZ domain of p62 which the interaction can induce further activity on autophagy, but V-BiP, mimicking mature BiP, does not attain the binding affinity to p62; therefore, I expected, there is an impairment on forming the complex with DJ-1 when arginine is converted to valine. After co-immunoprecipitation with anti-GFP antibody, there is an interaction between overexpressed recombinant DJ-1 and R-BiP-GFP, but the interaction was impaired when V-BiP-GFP was pulled out (Figure 14B). Thus, I could have found that cytosolic BiP is only interacting DJ-1 with arginine exposed both of normal and TRAIL induced stress condition; therefore, I concluded that DJ-1 interacts with BiP in cytoplasm and interacting with arginylated form of BiP is rather important then its stickiness what molecular chaperones usually have and may influence in non-specific binding to a protein interested.

Oxidation of DJ-1 under the oxidative stress the function of oxidized DJ-1

It has been known that there are three oxidation sites in DJ-1 which are Cys46, Cys53, and Cys106 (Andres-Mateos et al., 2007; Ren et al., 2011; Saito, 2014; Saito et

al., 2014). Among these sites, Cys106 is known as most important for reacting the ROS in cytoplasm and to determine whether DJ-1 is oxidized by TRAIL, I checked oxidation of DJ-1 on Cys106 by specific antibody that detects oxidized Cys106 (Ariga et al., 2013; Saito, 2014). Oxidation on Cys106 of DJ-1 was detected and the signal of oxidation was abolished by antioxidant chemical N-acetylcysteine (NAC) (Figure 15A and 15B). But this result is not sufficient for verifying the oxidation on DJ-1 is indeed from TRAIL induced oxidative stress, because TRAIL can cause other cytosolic stresses and the stresses may influence on DJ-1 oxidation as a secondary effect. To generalize the oxidative stress and rule out the other possibilities. I used tert-butyl hydroperoxide to induce cytosolic oxidative stress and DJ-1 was oxidized and, similar to the result from TRAIL, and the signal was also diminished by NAC as shown (Figure 15C); therefore, not only the specific case from TRAIL, DJ-1 is generally oxidized by ROS in the cell.

To further understand whether oxidation of DJ-1 is important in interaction of R-BiP-DJ-1, I transiently co-transfected R-BiP-GFP and FLAG-DJ-1 or mutated DJ-1 which are C46A, C53A, and C106A plasmid. Wild type DJ-1 and C46A mutated DJ-1 only can interact with R-BiP during TRAIL induced oxidative stress (Figure 16A). Thus, oxidation of DJ-1 on its 106th cysteine occurs as a result of oxidative stress and oxidized DJ-1 has a pivotal role in interacting with arginylated BiP which is from ER.

Interaction of oxidized DJ-1 and autophagic receptor p62

Given that TRAIL induced oxidative stress causes the N-terminal arginylation of BiP, and the cellular stress leads to accumulation of BiP in cytoplasm and induces interaction with DJ-1. The previous studies showed that cytosolic R-BiP interacts with ZZ domain of p62 and it modulates accumulation of p62 under ER stresses (Cha-

Molstad et al., 2018; Cha-Molstad et al., 2015; Cha-Molstad et al., 2017). To verify TRAIL induced oxidative stress mediates the interaction between R-BiP and p62, I performed co-IP assay with overexpressed recombinant FLAG-DJ-1 in HCT116 cells, and it showed that p62 was pulled out with R-BiP when TRAIL was treated to cells (Figure 13A); moreover, it was also shown in TRAIL treated HeLa cells (Figure 13B). Thereby, I could assume that DJ-1 is interacting with p62 directly or indirectly at least via R-BiP, and the mechanism has a possibility to expand to other cellular environment.

I have showed that oxidation of DJ-1 the critical point of while the interaction of DJ-1 and R-BiP. Moreover, the interaction of DJ-1 and R-BiP was abolished in mutation of Cys53 and Cys106 (Figure 16A). Among these cysteines, Cys106 is the key of the oxidation related mechanisms; therefore, I compared the interactions between overexpressed recombinant FLAG-DJ-1/R-BiP and FLAG-DJ-1^{C106A}/R-BiP (Figure 16B). There is impairment on interaction of DJ-1/R-BiP, and DJ-1/p62 when DJ-1 was mutated. The results indicated that the interaction of DJ-1/R-BiP is affected by oxidation of DJ-1 on its Cys106 and, through the oxidation on Cys106, DJ-1 could have interacted with p62.

Importance of DJ-1 while the interaction of R-BiP and p62

I found DJ-1 is interacting with both of R-BiP and p62, but it is necessary to elucidate if DJ-1 is deficient in the interaction with R-BiP and/or p62. Or it has a worth to verify whether the interaction of DJ-1/R-BiP/p62 is the artifact caused by overexpression of each of components; thereby, I pulled down the endogenous p62 I could have detected with R-BiP and BiP only in IPed sample with TRAIL treatment (Figure 17A), and when autophagy was blocked by pharmaceutical treatment,

bafilomycin A1, TRAIL and bafilomycin A1. co-treated IP sample showed the interaction of DJ-1 and p62 (Figure 17B). But, when DJ-1 was knock down in HCT116 cells, the interaction of R-BiP and p62 was diminished; therefore, I could have assumed DJ-1 is important factor on R-BiP and p62 interaction.

Moreover, I have compared the level of R-BiP, BiP, and p62 in TRAIL and bafilomycin A1 single or double treatment, all the level of proteins was elevated in DJ-1 deficient cell; thus, DJ-1 may function as controlling the level of each autophagic related protein or the degradation of autophagic substrate (Figure 17A and 17B). As a result, I shortly concluded under TRAIL induced oxidative stress, ER residing BiP is translocated into cytoplasm, and arginylated by ATE1, then DJ-1 is oxidized by the stress and interacts with R-BiP and activated p62; moreover, this assembly may function in response to oxidative response mechanism that is related to autophagic proteolysis. (Figure 18)

DJ-1, a modulator of R-BiP / p62 autophagic puncta formation

Based on this study, DJ-1 and p62 are interacting each other via R-BiP, but it does not indicate somewhat physiological function in the cell. To elucidate the meaningful role of the 3-way interaction of DJ-1/R-BiP/p62, I conducted immunostaining to figure out the location of the interaction and the role and function of the interaction (Figure 15). R-BiP puncta were induced under TRAIL treatment in the normal cells, and the colocalization of p62 puncta and TRAIL induced R-BiP puncta were detected when autophagic flux was pharmaceutically blocked by bafilomycin A1 (Figure 19). By contrast, when *DJ-1* was knocked down, R-BiP puncta were not induced by TRAIL, nor colocalization with p62 was not detected in *DJ-1* deficient cells (Figure 20A).

Moreover, the formation of p62 puncta co-treated with TRAIL and bafilomycin A1 was significantly decreased in *DJ-1* depleted cell (Figure 20B, 20C and 20D); therefore, these results indicate that DJ-1 has a role in the response to TRAIL, the induction of R-BiP puncta as a result for the response to TRAIL, and I could have thought of which DJ-1 has a function on constituting p62 aggregation or autophagic puncta in the cell.

To examine the function of DJ-1 on aggregation or self-oligomerization of p62, I performed protein aggregation assay using the non-reducing SDS-PAGE that conserves disulfide bond-linked oligomers and aggregates, and the gel separates its higher molecular weight species. The result showed that the part of p62 formed its oligomers or aggregates but DJ-1 depleted extracts didn't show oligomers nor aggregates of p62 under the blockage of autophagy and TRAIL and bafilomycin A1 co-treatment (Figure 17A), as well as, I have found that DJ-1 also forms higher molecular weight species when TRAIL, bafilomycin A1 or both were treated (Figure 21A), and these formation of oligomer of DJ-1 was quite similar to tBHP induced DJ-1 oligomers (Figure 21B). Thus, I concluded that DJ-1 makes higher molecular weight species when cells suffer oxidative stress induced by TRAIL or other oxidative stress inducers, and autophagic receptor p62 also constitutes aggregation and the aggregation is induced by oxidative stress but this aggregation is impaired in DJ-1 deficiency; all together, decrease of p62 and R-BiP puncta might be linked to the impairment of aggregation and oligomerization of DJ-1 and p62.

DJ-1, the function as a modulator of cargo targeting

I have characterized the aspect of p62 and R-BiP puncta when TRAIL was treated and by comparing the puncta of p62 and R-BiP, I could have assumed the function of

DJ-1. However, still remained question is whether DJ-1 has a role in not only the interacting of p62 or R-BiP and effecting on formation of the puncta but still other functions in autophagy. The reason needed to be claimed is p62 puncta only can represent the accumulation of protein cargo or the interaction of the mass of proteins with p62. Therefore, it is necessary to focusing on other autophagic markers and I examined LC3 to elucidate the function of DJ-1 on autophagy.

LC3 is the protein binds with autophagic membrane via C-terminal truncation and lipidation, subsequently, thereby, it constitutes autophagic puncta when it located in closed form of autophagosome. In *DJ-1* deficient cells, LC3 puncta was significantly deceased even when there was basal level of autophagic flux which was blocked by bafilomycin A1 without other stresses (Figure 22A and 22B).

In addition, when TRAIL was treated and oxidative stress was occurred, I could have found the induction of both LC3 and p62 puncta in normal cells but $p62^+$ and/or $LC3^+$ puncta were deceased in DJ-1 deficient cells, and, because of the decrease of both of puncta, co-localization of p62 and LC3 puncta was diminished (Figure 22C); therefore, I could have thought DJ-1 not only effect on aggregation of p62 but also it has a function on targeting the cargo proteins to autophagosomes which are represented by LC3 puncta.

But still there is a question on protein degradation mediated by autophagic degradation; matured autophagosome are fused with lysosome and forms autolysosome (Huber & Teis, 2016; Zaffagnini & Martens, 2016). Even though the formation of LC3 puncta represents the autophagosome; however, it does not mean the degradation of the vesicle because there is still remaining the step for the degradation: the fusion with lysosome. Thus, I additionally conducted immunostaining and puncta assay using with

PLEKHM1. PLEKHM1 has been known as a linker between autophagosome and lysosome and mediates the fusion of those vesicles (Marwaha et al., 2017; McEwan et al., 2015). As a linker and making the fusion of both vesicles, it can be shown as puncta and *DJ-1* deficient cells showed significantly reduced puncta of PLEKHM1 (Figure 23A), as expected; as a result, there were deceased $LC3^{+}$ autophagosomes, and because of diminution, there were less autophagosomes to be fused with lysosomes and theses have been shown as less puncta of PLEKHM1.

Meanwhile, there is another point about autophagic biogenesis. In immunostaining data, it seems to decrease not only number of the puncta but total level of LC3 in the cytoplasm when *DJ-1* was knock down. To examine the amount of LC3, I performed immunoblotting assay and the data from whole cell lysates showed even elevation on the level of LC3 (Figure 23B); in addition, I used another phagophore maker WIPI2, which participates in the formation of phagophore, the precursor of autophagosome (Dooley et al., 2014; Polson et al., 2010). Immunostaining assay of WIPI2 indicated that the generation of phagophore and the biogenesis mechanism is rather normal or elevated even in *DJ-1* knocked down cells (Figure 23C). Therefore, I could have assumed that decreases shown in p62 or LC3 puncta are not related with autophagosome biogenesis and it is rather related with other points such as cargo targeting toward autophagosomes.

Cargo delivery defect in DJ-1 deficient cells

In TRAIL treated condition, it has been shown that oxidative stress or other cellular stresses are occurred and misfolded protein would be generated as a result of the stresses. To diminish the effect from the stress, misfolded or other malfunctioning

proteins are tagged by ubiquitin and Ub-conjugated proteins are intended to degraded by lysosomal degradation in the protein quality control (Huber & Teis, 2016).

During the process, p62 is one of the receptor for the protein degradation, which is also related to autophagic proteolysis (Lim et al., 2015; Wurzer et al., 2015). Based on the data, DJ-1 may have a function on cargo targeting to autophagosome; I examined DJ-1 effect on the subpopulation of Ub-conjugates during TRAIL treatment. Ub-conjugated proteins were excessively accumulated in DJ-1 knock down cells (Figure 24A) and the cytosolic puncta of FK2 representing Ub-species in the cells were highly stored in DJ-1 deficient cells comparing with normal cells (Figure 24B, 24C and 24D).

In autophagic proteolysis, Ub-conjugated proteins bind with p62 and collected to autophagosome, I compared the formation of $FK2^+$ $p62^+$ puncta under TRAIL treatment, in DJ-1 deficient cells, FK2 signal is co-located with p62 but the subpopulation of FK2 without interacting p62 was shown in DJ-1 knock down cells whereas it has not been shown in the normal cells (Figure 25A), indicative of the impairment on cargo collection and accumulation toward p62. In addition, to investigate the targeting of cargo proteins to LC3 which binds to autophagosome while autophagic proteolysis, Ub-conjugated proteins formed autophagic puncta and colocalized with $LC3^+$ puncta in normal cells, but the interaction was impaired in DJ-1 deficient cells (Figure 25B). Therefore, DJ-1 effects on the cargo targeting to autophagic vesicles, and it is not related with biogenesis of autophagosomes.

Autophagic proteolysis defect in DJ-1 deficient cells

Under the oxidative stress, transcriptional factor Nrf2 activates many of antioxidant genes to reduce the damage caused by oxidative stressors. But in normal conditions,

Nrf2 is degraded by proteasome via ubiquitination by E3 ligase Keap1 (Deshmukh, Unni, Krishnappa, & Padmanabhan, 2017; Ichimura et al., 2013; Katsuragi, Ichimura, & Komatsu, 2015; Komatsu et al., 2010). When cells undergone by oxidative stress, Keap1 is delivered to autophagosome by interacting with p62 and degraded by autophagic proteolysis, which is retaining Nrf2 and leading the transcription of target genes (Ichimura et al., 2013; Katsuragi et al., 2015; Komatsu et al., 2010). To elucidate the role of DJ-1 in the modulation of autophagic proteolysis of normally folded proteins, I performed immunostaining puncta analysis, and it showed that TRAIL induced $Keap1^{+}$ autophagic vacuoles were significantly decreased in DJ-1 deficient cells and, because of decrease, co-localization of $Keap1^{+}$ and $p62^{+}$ puncta also have been diminished (Figure 26A) without markedly difference in the level of Keap1 in the DJ-1 knocked down cells, characterized by immunostaining analysis (Figure 26B). A similar result has been shown in tBHP (Figure 27) treated DJ-1 knocked down cell, as expected; therefore, these results support that DJ-1 has a function on p62 engaged autophagic proteolysis and it influences not only misfolded protein, but it manages the degradation mechanism of a protein supposed to be processed for further the mechanism.

Mitochondria deficiency in DJ-1 deficient cells

In previous research, DJ-1 has a cyto-protective function during the cellular stress including mitochondrial impairment, ER stress, and other cell death processes such as apoptosis (Fu et al., 2012; Giaime et al., 2012; Kolisek et al., 2015; McCoy & Cookson, 2011; Thomas et al., 2011; Won et al., 2013). Moreover, TRAIL is anti-cancer ligand and selectively annihilates cancer cell by triggering mitochondrial dysfunction, ER

stress, and apoptosis in HCT116 cells; all of which oxidative stress has been included (Inoue & Suzuki-Karasaki, 2013; Suzuki-Karasaki et al., 2014; Suzuki et al., 2012). Thus, I performed further experiments to examine the physiological importance of DJ-1 for the process dealing with TRAIL induced oxidative stress.

Given that DJ-1 prevents cell death under TRAIL treatment, I have checked the membrane potential of mitochondria using with JC-1 dye representing the membrane potential by its color. Red fluorescence indicates healthiness of membrane of mitochondria; in contrast, green represents decrease of membrane potential and implies that cell is in the middle of apoptosis (Perelman et al., 2012). TRAIL treated cells indicated increase of green signals when it was detected by FACS and, upon the deficiency of DJ-1 in HCT116 cells, more subpopulation of cells presented more green fluorescence than normal cells with TRAIL treatment (Figure 28A, 28B and 28C). Similar aspect has also been shown in DJ-1 knocked out mouse embryonic fibroblasts (MEFs) (Figure 29A, 29B and 29C).; therefore, there is a protective role of DJ-1 in mitochondria dysfunction induced by loss of mitochondrial membrane, which might have been related to DJ-1 function on engaging in autophagic modulation.

Protective role of DJ-1 under ER stress

It has been reported that mitochondria and ER are linked with each other, and they exchange the elements containing meaningful signals and pathways such as ER stress and apoptosis (Ardail et al., 2003; Fujimoto & Hayashi, 2011). To elucidate the signal transfers from mitochondria to ER, I examined ER stress by specific maker to the stress. Unfolded protein response is one of the implication of ER stress that ER stress also mediates not only misfolding of protein, but it also triggers unfolding of protein in ER.

Co-IP analysis of BiP showed that TRAIL lead the dissociation of luminal BiP from PERK as well as IRE1α, two sensors of the UPR (Figure 30A and 30B), which BiP, PERK and IRE1α are interacting with among the proteins without the stress (Balchin, Hayer-Hartl, & Hartl, 2016; Carrara, Prischi, Nowak, Kopp, & Ali, 2015; A. S. Lee, 2005; J. Li & Lee, 2006), suggesting that, as expected, TRAIL induced stress influenced on ER, even if it has been directly or indirectly connected to mitochondrial stress.

Next, to verify ER stress responses in MEFs, MEFs was infected with vaccinia virus that carries mouse TRAIL (vvmTRAIL) (Ziauddin et al., 2010). Immunoblotting analysis confirmed that vvmTRAIL also induced ER stress as determined by markers representing ER stress which are cleavage of poly (ADP-ribose) polymerase-1 (PARP-1), the phosphorylation of eIF2α and c-Jun NH2-terminal kinase (JNK), and elevation of the levels of ATF4 and C/EBP homologous protein (CHOP) (Figure 31A). Moreover, DJ-1 knocked out MEFs presented more sensitive to virus carrying TRAIL treatment as compared normal cells and prone to get through the apoptosis (Figure 31B). In addition, quantitative RT-PCR analysis also showed that the expression of *ATF4*, *CHOP*, and *BiP* were also elevated when TRAIL was treated and the levels were drastically up-regulated (Figure 31C); thus, altogether with these evidences, the deficiency of DJ-1 makes cell to be sensitive to TRAIL induced stresses, and, due to the impairment, cells may venerable to the stress encountered.

The goal of TRAIL treatment to cancer cell is to trigger the apoptosis in cancer cells by using its therapeutic activity as an anticancer ligand (Johnstone et al., 2008). Immunoblotting analysis indicated that stably expressing *DJ-1* shRNA in HCT116 presented more cleavage of PARP-1 and caspase 8 while the stable cell line stably

overexpresses recombinant DJ-1 (DJ-1-GFP) became resistant to TRAIL-induced apoptosis (Figure 32). These result was further supported by FACS analysis of annexin V-stained *DJ-1* knockdown cells (Figure 33A and 33B). In addition, the result was correlated with when viral TRAIL was treated on *DJ-1* knock out MEFs. When it comes to targeting the cancer cells, it might be inefficient to diminish the cancer cell; in contrast, these results demonstrate that DJ-1 contributes to preventing apoptosis caused by TRAIL.

Not only in the TRAIL treatment, it is needed to be generalized the case and to determine whether DJ-1 plays a general protective role against ER stress, ER stressor thapsigargin was treated +/+ and *DJ-1*$^{-/-}$ MEFs for the comparison the effect of DJ-1 on ER stress. *DJ-1*$^{-/-}$ MEFs showed hypersensitive to thapsigargin, and it supports other evidences have been shown in previous, (Figure 34A); consistently, cell viability test using MTT (3-(4,5-dimethylthiazol-2-yl)-2,5-diphenyltetrazolium bromide) assay showed that *DJ-1*$^{-/-}$ MEFs were more vulnerable to thapsigargin compared with +/+ MEFs (Figure 34B). Thus, DJ-1 protects cells from ER stress caused by TRAIL and other stressors.

Protective role of N-end rule substrate BiP under TRAIL induced stress

Given that TRAIL induces Nt-arginylation on BiP (Figure 14A), ATE1-encoded R-transferases mediate Nt-arginylation of sets of ER-residing molecular chaperones such as BiP, calreticulin, and protein disulfide isomerase (Cha-Molstad et al., 2015). Getting the clue from previous research, I focused on whether BiP and ATE1 R-transferase also have a protective role against TRAIL induced stress in cells. Knockdown of ATE1 using siRNA strongly inhibited the formation of N-terminal

arginylation on BiP in TRAIL-treated cells that correlated with the increase of PARP1 cleavage (Figure 35A). The pro-survival activity of ATE1 was further supported by the MTT assay using *ATE1* knockdown cells (Figure 35B). These results suggest that Nt-arginylation protects the cell from TRAIL.

Based on the findings that DJ-1 is having its activity in part engaged in the interaction with R-BiP and/or, possibly indirectly, p62 (Figure 13A), BiP has a chance to participate in cellular stress responses that defensing against TRAIL induced stress. By using small interfering RNA (siRNA) in HCT116 cells, *BiP* was strongly knockdown, and deficiency of BiP deteriorated TRAIL-induced apoptosis with measuring PARP-1 cleavage and MTT assay, respectively (Figure 35C and 35D). Reciprocally, when BiP was overexpressed, reduced PARP1 cleavage was shown and cancer cell killing activity of TRAIL was rather suppressed (Figure 35E and 35F). These results suggest that Nt-arginylation may be a post-translational modification that protects the cell from various oxidative stresses.

Figure 1. A schematic diagram of protein quality control. Newly synthesized peptides are delivered to molecular chaperone and folded by folding machinery. But when misfolded proteins or protein aggregates are generated, these proteins are degraded by either proteasomal degradation or autophagy.

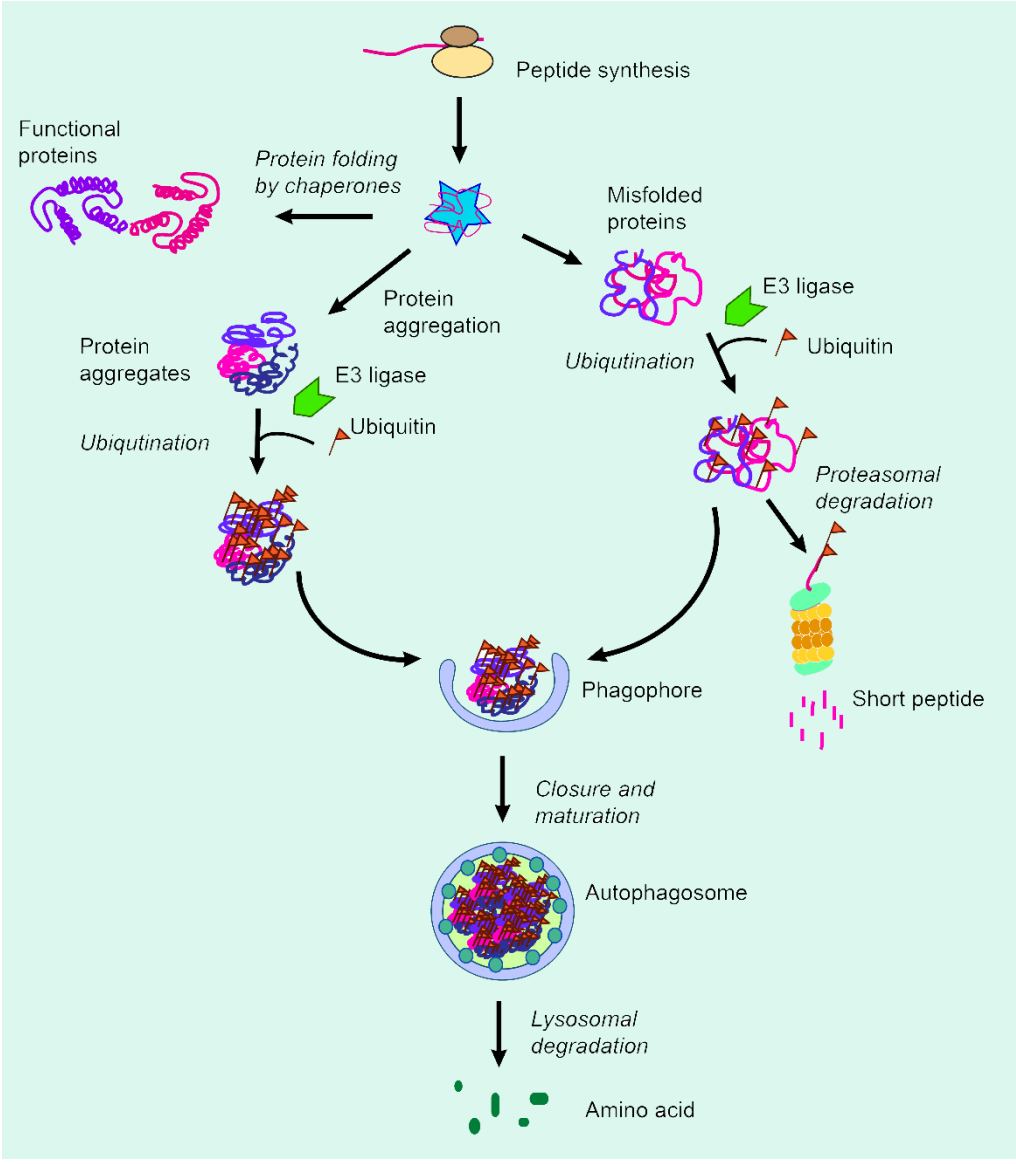
Peptide synthesis
Functional proteins
Protein folding by chaperones
Misfolded proteins
Protein aggregation
Protein aggregates
E3 ligase
Ubiquitin
Ubiquitination
E3 ligase
Ubiquitin
Ubiquitination
Proteasomal degradation
Phagophore
Short peptide
Closure and maturation
Autophagosome
Lysosomal degradation
Amino acid

Figure 2. A schematic diagram of N-end rule pathway. Upon proteasomal degradation, a single amino acid exposed on N-terminus of protein is identified by UBR box of N-recognins, mainly E3 ligases, and ubiquitin (Ub) is tagged on the protein body. Ub-conjugated proteins are delivered to proteasome and degraded into short peptides. However, cellular stresses are accumulated in cells, N-terminus of autophagic substrates are recognized by autophagic receptors, such as p62, and the substrates are undergone autophagic proteolysis.

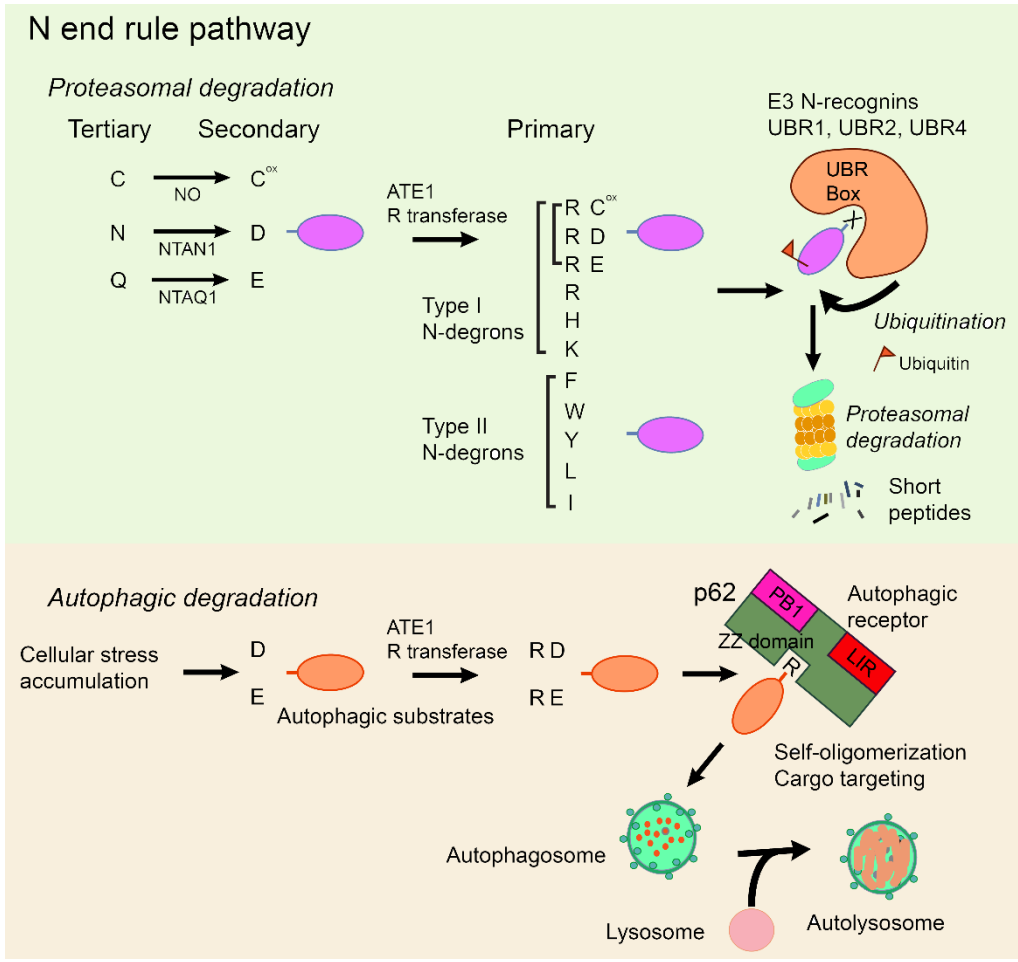
N end rule pathway
Proteasomal degradation
Tertiary
Secondary
Primary
C
NO
C^ox
N
NTAN1
D
Q
NTAQ1
E
ATE1
R transferase
R C^ox
R D
R E
R
H
K
Type I
N-degrons
F
W
Y
L
I
Type II
N-degrons
E3 N-recognins
UBR1, UBR2, UBR4
UBR
Box
Ubiquitination
Ubiquitin
Proteasomal
degradation
Short
peptides
Autophagic degradation
Cellular stress
accumulation
D
E
ATE1
R transferase
R D
R E
Autophagic substrates
p62
PB1
ZZ domain
LIR
R
Autophagic
receptor
Self-oligomerization
Cargo targeting
Autophagosome
Lysosome
Autolysosome

Figure 3. A schematic diagram of autophagic mechanism. A brief model for autophagic proteolysis has been illustrated. When cells encounter cellular stress, autophagy is induced, and autophagic machinery form membrane structure called phagophore, and protein cargos are delivered to autophagic membranes. When cargo proteins are fully loaded, a phagophore is matured and closed and it is referred as matured autophagosome. After the maturation of autophagosome, lysosome is recruited and fused with autophagosome and this fusion forms autolysosome which is a final step for the degradation.

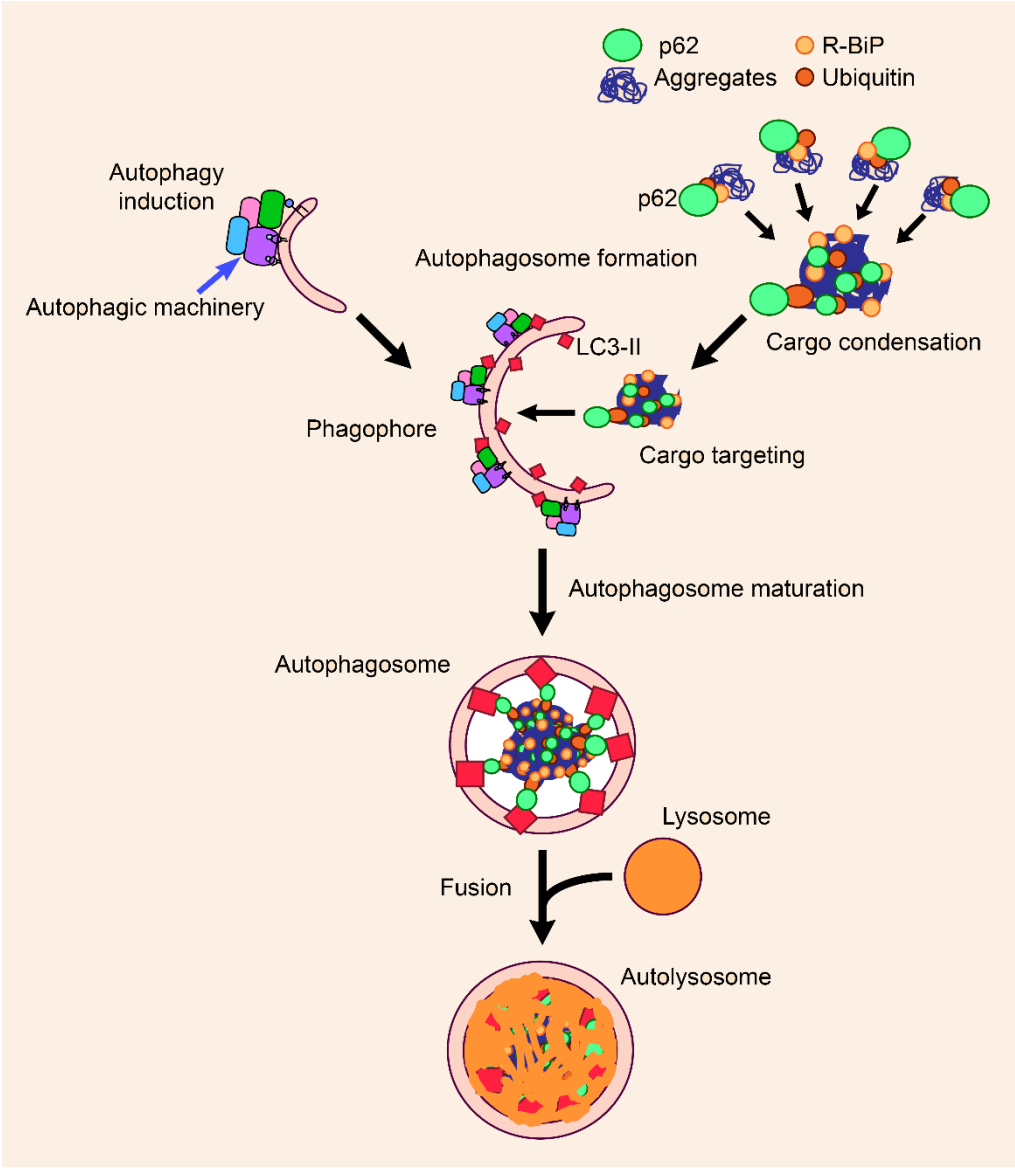
p62
R-BiP
Aggregates
Ubiquitin
Autophagy induction
Autophagic machinery
p62
Autophagosome formation
Cargo condensation
LC3-II
Phagophore
Cargo targeting
Autophagosome maturation
Autophagosome
Lysosome
Fusion
Autolysosome

Figure 4. A schematic diagram of general and selective autophagy. A brief model for comparing general (bulk, non-selective) autophagy and selective autophagy has been illustrated. Upon the starvation, cells non-selectively degrade proteins or cellular substances. but cells encounter specific stress, protein aggregates are generated and specific autophagic receptor recognizes cargo proteins. Therefore, unlike non-selective autophagy, selective autophagy responses for particular stress and cargos by autophagic receptors.

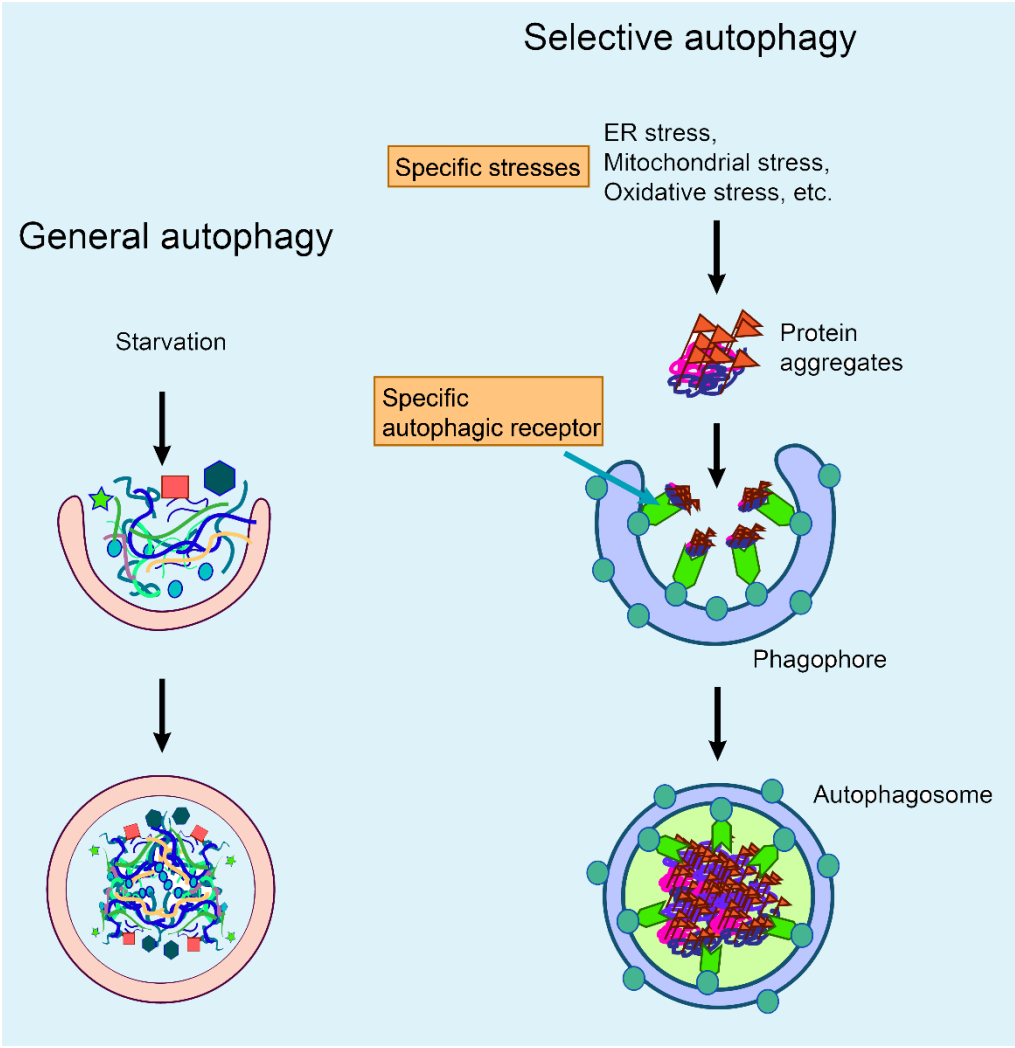
Selective autophagy
Specific stresses
ER stress,
Mitochondrial stress,
Oxidative stress, etc.
General autophagy
Protein
aggregates
Starvation
Specific
autophagic receptor
Phagophore
Autophagosome

Figure 5. A schematic diagram of Hsp70 modulation. A brief model for functional modulation of Hsp70 family has been described. When newly synthesized peptide are identified by molecular chaperone Hsp70, the molecular chaperone complex recruits Hip and Hop and constitutes folding machinery; however, if the peptide is needed to be degraded, Hsp70 complex forms the degrading machinery to process the peptide. Therefore, through the changing of its binding partner, Hsp70 complex alters the function according to the cellular circumstances.

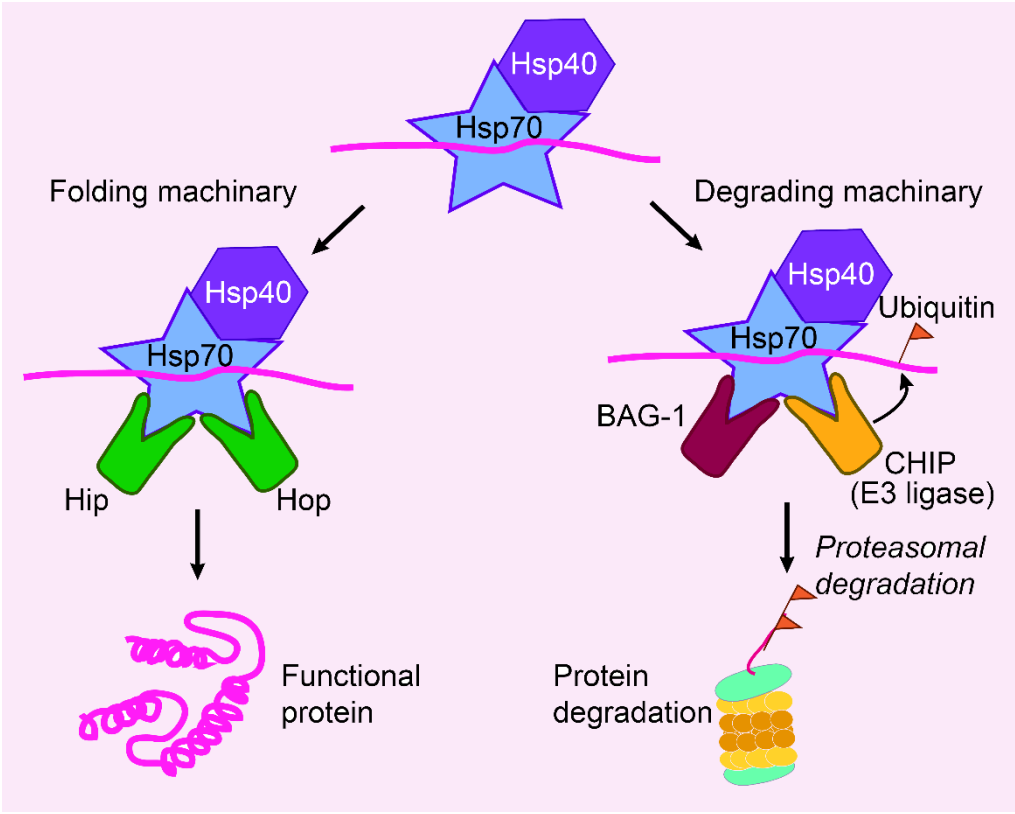
Hsp40
Hsp70
Folding machinary
Degrading machinary
Hsp40
Hsp70
Hip
Hop
Hsp40
Hsp70
Ubiquitin
BAG-1
CHIP
(E3 ligase)
Proteasomal
degradation
Functional
protein
Protein
degradation

Figure 6. A schematic diagram of DJ-1 oxidation. A brief model for DJ-1 oxidation has been described. DJ-1 recognizes cellular ROS and observes oxygen at 106^{th} of cysteine (Cys106). When single oxygen binds to Cys106 of DJ-1, Cys106 may abolish the excessive oxygen, but if the oxidation is accumulated, it turns to be irreversible and further detailed mechanism is still known.

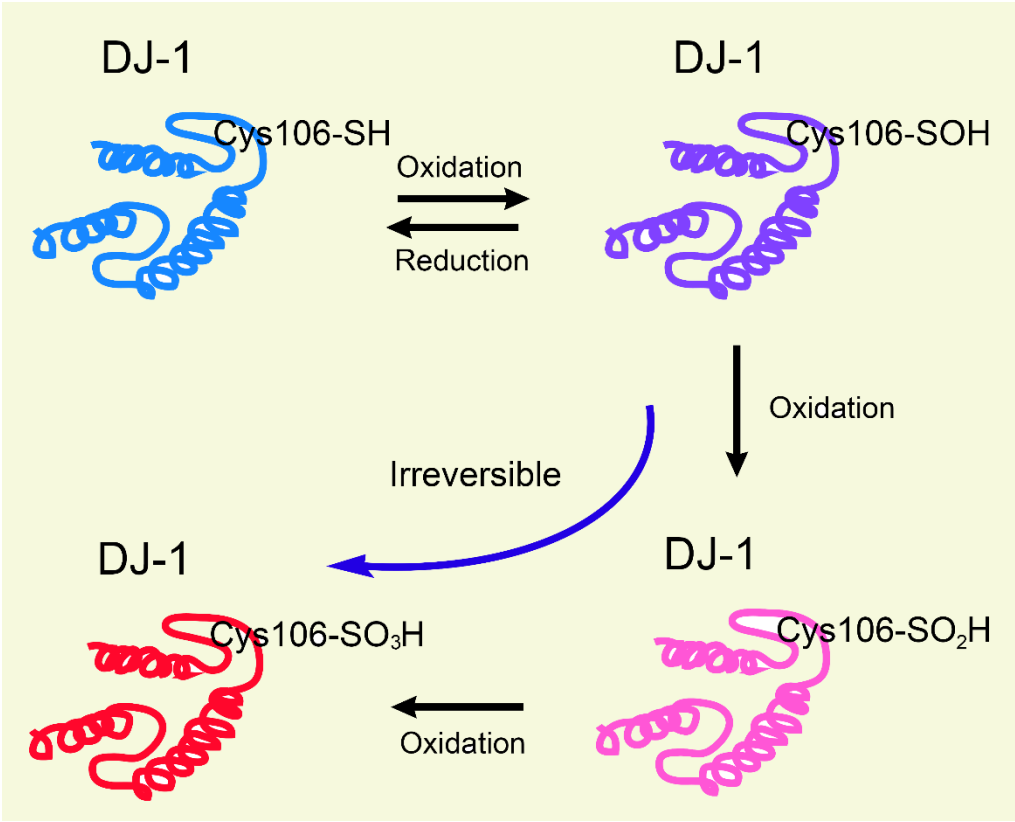
DJ-1
Cys106-SH
Oxidation
Reduction
DJ-1
Cys106-SOH
Oxidation
Irreversible
DJ-1
Cys106-SO3H
Oxidation
DJ-1
Cys106-SO2H

Figure 7. Mitochondrial ROS generation by TRAIL treatment. (**A**) TRAIL was treated to HCT116 cells were treated with different concentrations (1-10 ng/ml) for 4 h and traced with MitoSOX. The intensity of MitoSOX Red was measured using FACS. (**B**) Quantitation of A. Error bars represent the mean ± SEM from three separate experiments (*$p < 0.05$).

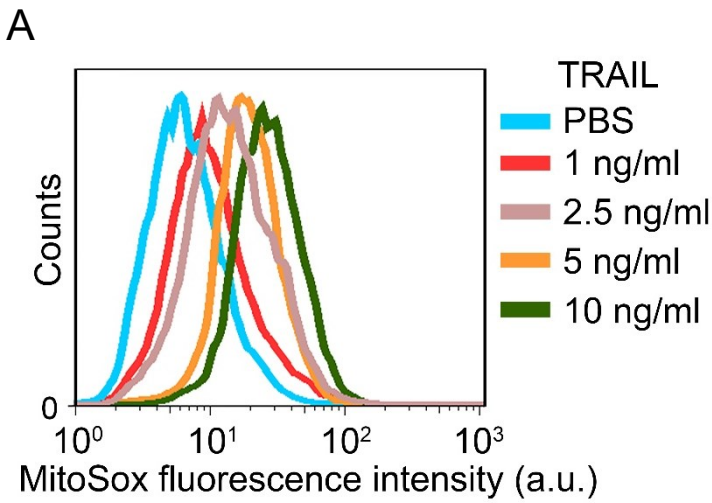
A
TRAIL
PBS
1 ng/ml
2.5 ng/ml
5 ng/ml
10 ng/ml
Counts
0
10^0
10^1
10^2
10^3
MitoSox fluorescence intensity (a.u.)

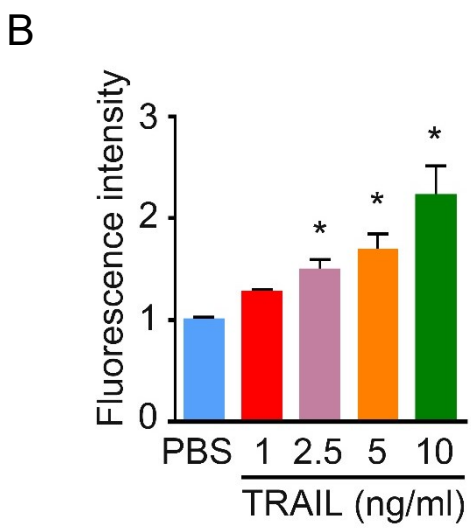
B
Fluorescence intensity
0
1
2
3
*
*
*
PBS
1
2.5
5
10
TRAIL (ng/ml)

Figure 8. The location of TRAIL-induced mitochondrial ROS and detection of cytosolic ROS by CM-H2-DCFDA. (**A**) TRAIL was treated to the cells were stably transfected with sh*DJ-1* or its control shRNA (shScramble) with 10 ng/ml for 4 h. Then cells were stained with MitoTracker and MitoSOX. Mitochondria (green) and mitochondrial superoxide anion (red) were detected using confocal microscopy. Scale bar, 10 μm. (**B**) Cells with stably expressing shScramble or sh*DJ-1* were treated with 4 h of 2.5 mM NAC, 10 ng/ml TRAIL or in combination. Cells were subsequently stained with CM-H_2-DCFDA for 30 min. Green signals indicate ROS in the cytosol. Scale bar, 200 μm.

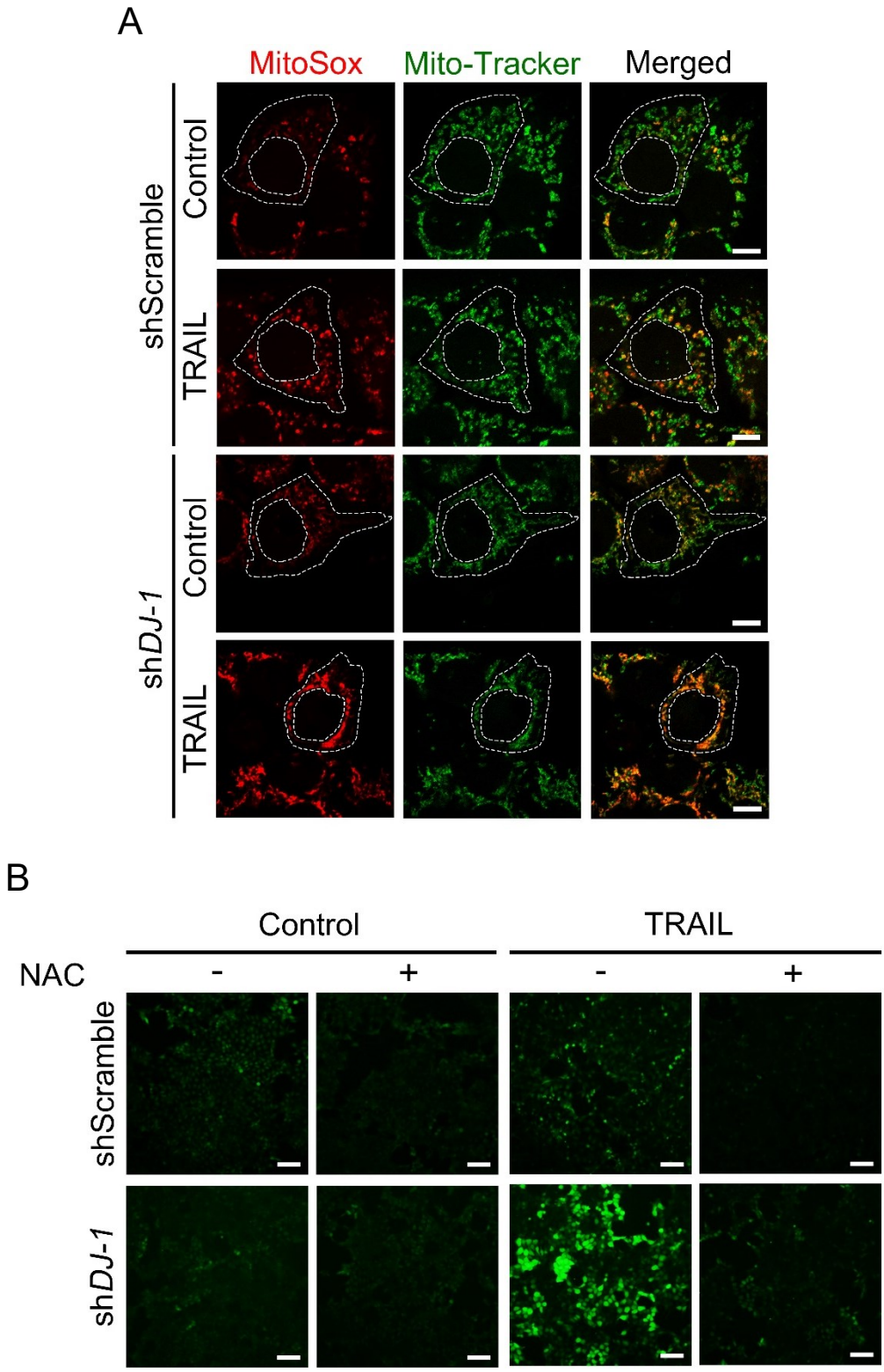
A
MitoSox
Mito-Tracker
Merged
shScramble
Control
TRAIL
shDJ-1
Control
TRAIL
B
Control
TRAIL
NAC
-
+
-
+
shScramble
shDJ-1

Figure 9. DJ-1 effects on mitochondrial ROS generation induced by TRAIL. (**A**) Cells with stably expressing control shRNA (shScram.) or *DJ-1* shRNA (sh*DJ-1*), were treated with 10 ng/ml of TRAIL for 4 h. Cells were subsequently labeled with MitoSOX, and the intensity of fluorescence was analyzed using FACS. (**B**) Quantitation of E. Error bars represent the mean ± SEM from three separate experiments (**$p < 0.01$).

A

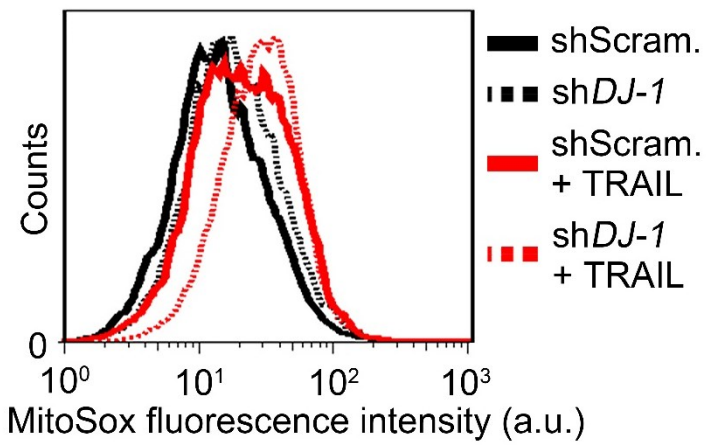
Counts
0
10^0
10^1
10^2
10^3
MitoSox fluorescence intensity (a.u.)
shScram.
sh*DJ-1*
shScram. + TRAIL
sh*DJ-1* + TRAIL

B

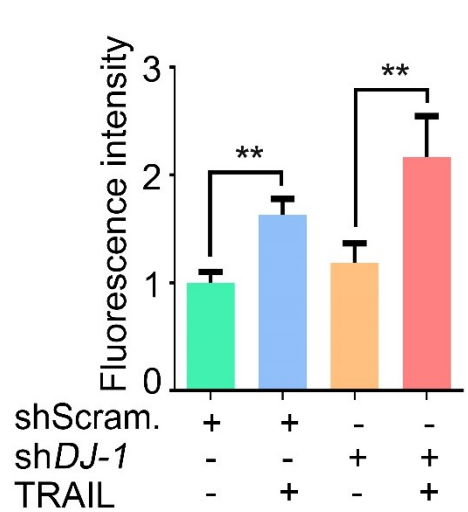
Fluorescence intensity
0
1
2
3
**
**
shScram. + + - -
sh*DJ-1* - - + +
TRAIL - + - +

Figure 10. Silver staining of DJ-1 overexpression cells with TRAIL treatment and the interaction of DJ-1 and BiP by using reciprocal immunoprecipitation assay. (**A**) Cells were manipulated to stably express either p3x-FLAG (transfected with control vector) or FLAG-tagged DJ-1 (FLAG-DJ-1) and treated with 5 ng/ml TRAIL for 4 h. Cell lysates were immunoprecipitated using anti-FLAG antibody, as a bait, and the precipitated proteins were visualized using silver staining. (**B**) With using transiently expressing either FLAG-DJ-1 and HA-BiP in HCT116 cells, protein complexs were pulled out by anti-HA antibody, followed by immunoblotting with anti-FLAG or anti-HA antibody (top). The presence of FLAG-DJ-1 and HA-BiP in the cell lysates was verified by immunoblotting (bottom). (**C**) Cells were treated with 5 ng/ml TRAIL for 3 h, and lysates were immunoprecipitated with anti-DJ-1 antibody or mock antibody (rabbit IgG) for the control, followed by immunoblotting with anti-BiP or anti-DJ-1 antibody (top). The presence of BiP and DJ-1 was shown in the total cell lysates using immunoblotting (bottom).

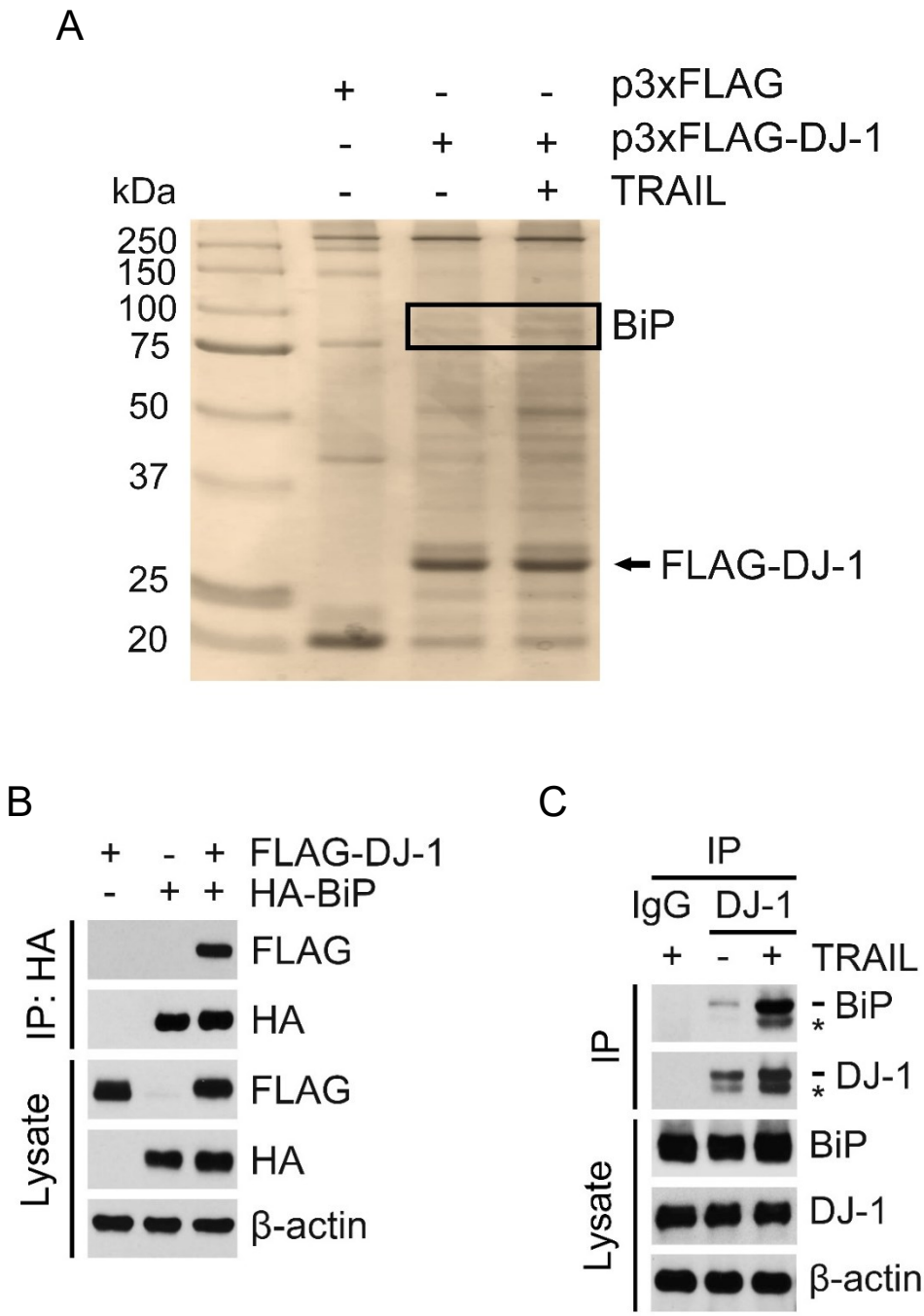
A
+ - - p3xFLAG
- + + p3xFLAG-DJ-1
kDa - - + TRAIL
250
150
100
75
50
37
25
20
BiP
FLAG-DJ-1
B
+ - + FLAG-DJ-1
- + + HA-BiP
IP: HA
FLAG
HA
Lysate
FLAG
HA
β-actin
C
IP
IgG DJ-1
+ - + TRAIL
IP
BiP
DJ-1
Lysate
BiP
DJ-1
β-actin

Figure 11. A schematic diagram in which TRAIL induces the Nt-arginylation of BiP. According to the mechanism, BiP, which has been produced in cytosol, translocates into the ER lumen, then its signal peptide is getting rid of by the signal peptide peptidase, resulting in mature BiP. The results suggest that TRAIL mediates the cytosolic retrotranslocation of BiP and Nt-arginylation of translocated BiP, finally resulting in the accumulation of R-BiP in cytosol.

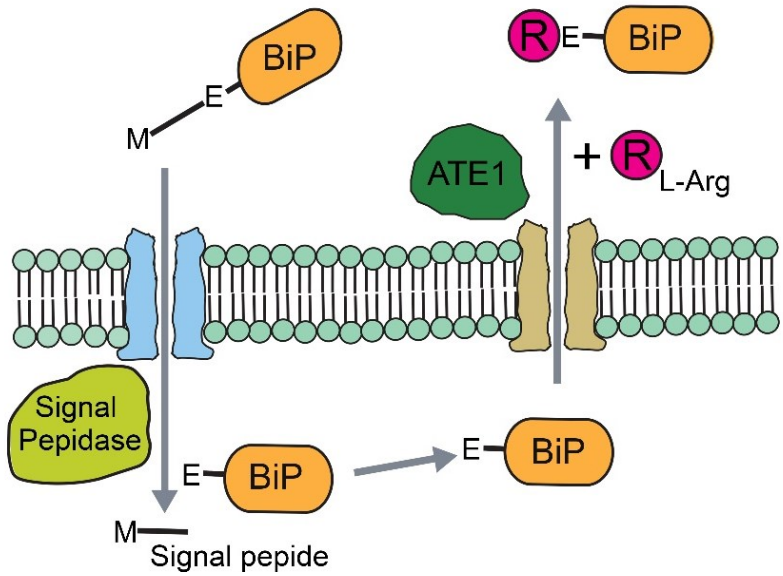
BiP
E
M
R
E
BiP
ATE1
+
R
L-Arg
Signal
Pepidase
E
BiP
E
BiP
M
Signal pepide

Figure 12. R-BiP induction of TRAIL and the location of the process.

(**A**) HCT116 cells were treated with 10 ng/ml TRAIL in time dependent, followed by immunoblotting of R-BiP, BiP, and ATE1. (**B**) Cells were treated with 5 ng/ml TRAIL for 4 h. The lysates were fractionated to the cytosol, mitochondria, and ER. Fractionated solutions were immunoblotted for R-BiP, DJ-1, BiP, the mitochondrial channel VDAC 1 (voltage-dependent anion channel), the ER chaperone calnexin. (Conducted by D.H. Lee)

A

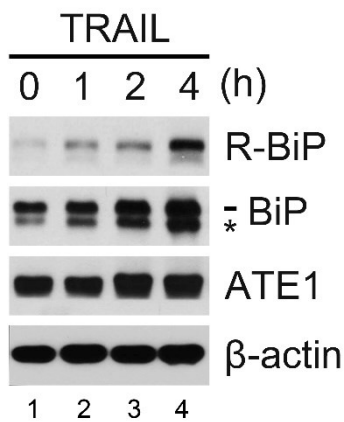
TRAIL
0 1 2 4 (h)
R-BiP
BiP
ATE1
β-actin
1 2 3 4

B

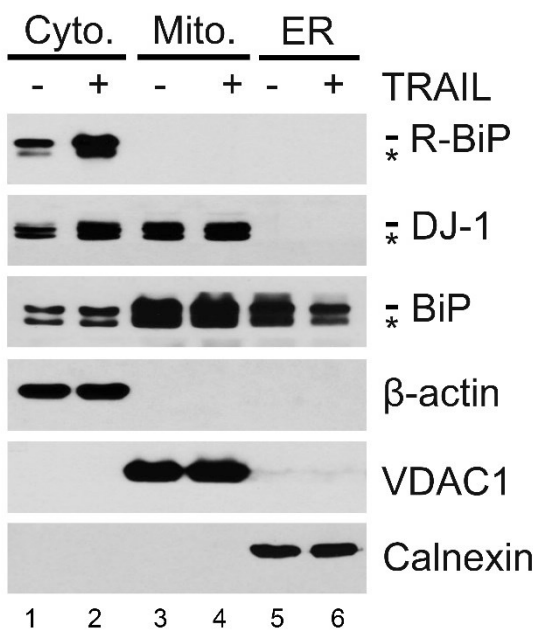
Cyto.
Mito.
ER
- + - + - +
TRAIL
R-BiP
DJ-1
BiP
β-actin
VDAC1
Calnexin
1 2 3 4 5 6

Figure 13. TRAIL induced interaction of DJ-1 with R-BiP and p62.

(**A**) HCT116 cells were transfected with FLAG or FLAG-DJ-1 plasmid. After 48 h of transfection, cells were treated with 10 ng/ml TRAIL for 4 h. The lysates were pull out with anti-FLAG antibody, followed by immunoblotting with the indicated antibodies. (**B**) Hela cells were transfected with FLAG-DJ-1 plasmid. After 48 h of transfection, cells were treated with 100 ng/ml TRAIL for 4 h. The lysates were immunoprecipitated with anti-FLAG antibody or mock antibody (rabbit IgG) for the control, followed by immunoblotting with the indicated antibodies. (**C**) HCT116 cells stably expressing FLAG or FLAG-DJ-1 were treated with 5 ng/ml TRAIL for 4 h. Cell lysates were incubated with *E. coli* derived GST-DJ-1 proteins for 2h then immunoprecipitated with glutathione bead, followed by immunoblotting with the indicated antibodies.

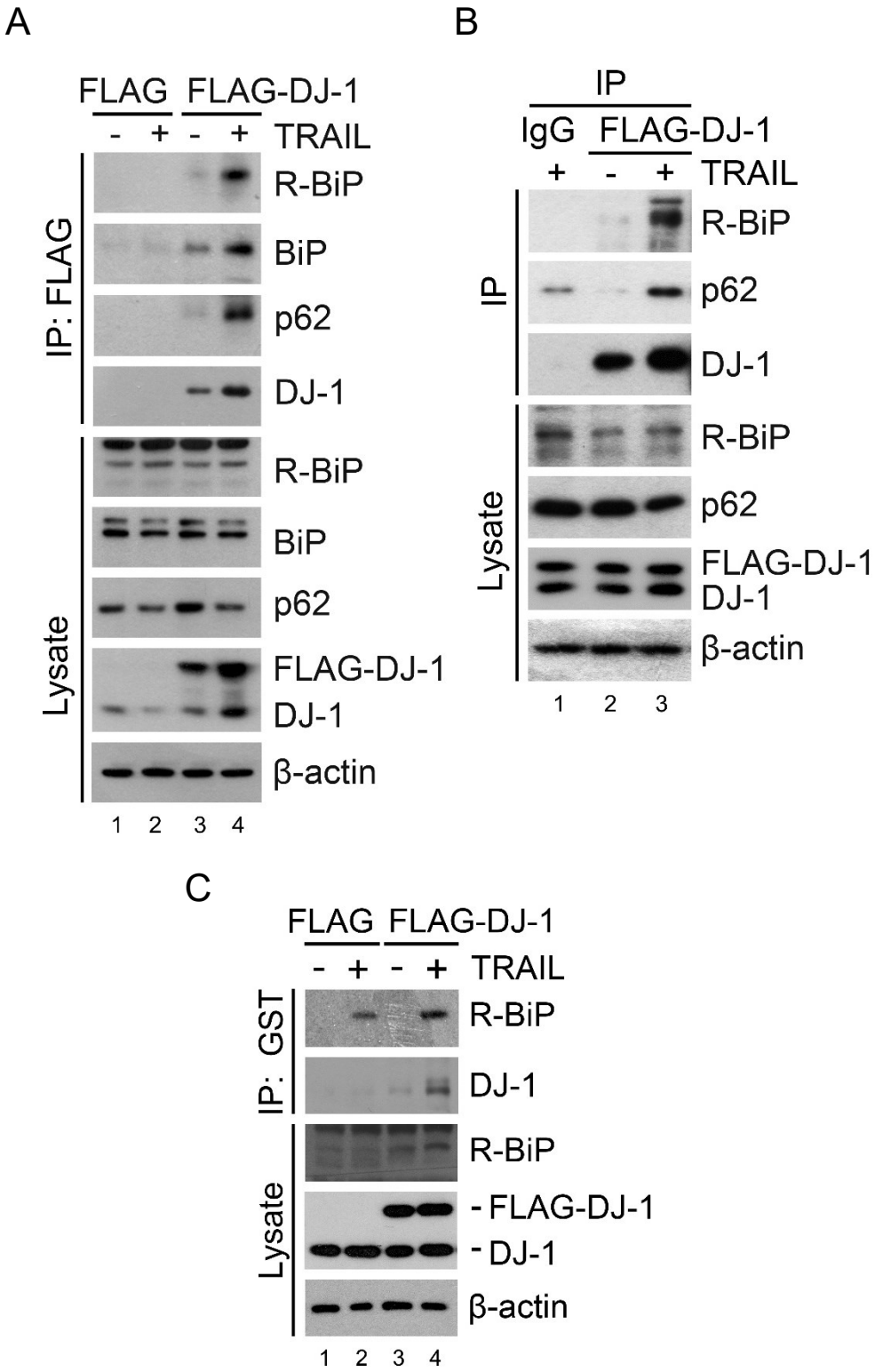
A
FLAG
FLAG-DJ-1
- + - +
TRAIL
IP: FLAG
R-BiP
BiP
p62
DJ-1
Lysate
R-BiP
BiP
p62
FLAG-DJ-1
DJ-1
β-actin
1 2 3 4
B
IP
IgG
FLAG-DJ-1
+ - +
TRAIL
IP
R-BiP
p62
DJ-1
Lysate
R-BiP
p62
FLAG-DJ-1
DJ-1
β-actin
1 2 3
C
FLAG
FLAG-DJ-1
- + - +
TRAIL
IP: GST
R-BiP
DJ-1
Lysate
R-BiP
FLAG-DJ-1
DJ-1
β-actin
1 2 3 4

Figure 14. A schematic diagram in which recombinant Ub-R/V-BiP-GFP proteins are processed by deubiquitylation enzyme (DUB). (**A**) In this mechanism, Ub-R/V-BiP-GFP are transiently expressed in HCT116 cells and its ubiquitin is cleaved by DUB and arginine or valine is exposed on their N-terminal, as a result of cleavage as shown. (**B**) HCT116 cells were co-transfected with plasmids encoding FLAG-DJ-1 and Ub-R-BiP-GFP or Ub-V-BiP-GFP. After 48 h, the cells were treated with 10 ng/ml TRAIL for 4 h. Cell lysates were immunoprecipitated with anti-FLAG antibody followed by immunoblotting with anti-GFP or anti-FLAG antibody.

A

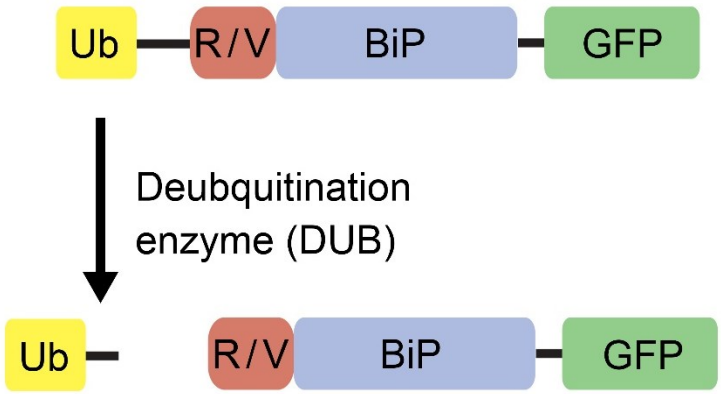
Ub
R/V
BiP
GFP
Deubquitination
enzyme (DUB)
Ub
R/V
BiP
GFP

B

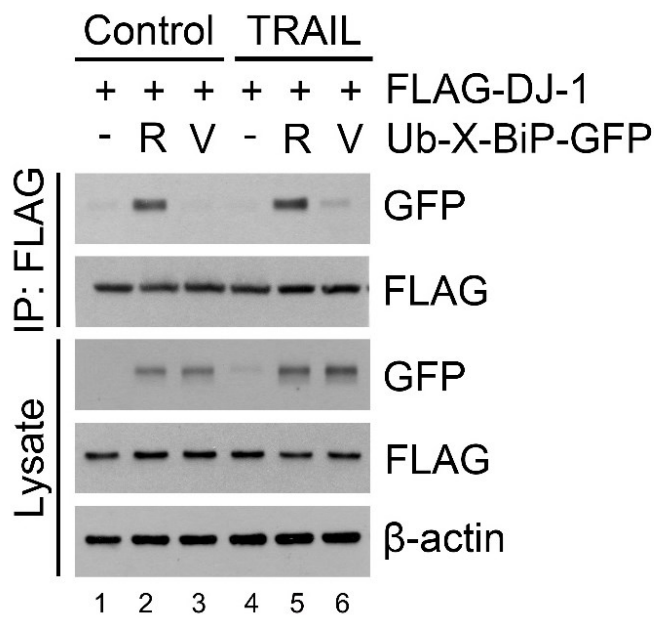
Control
TRAIL
+ + + + + + FLAG-DJ-1
- R V - R V Ub-X-BiP-GFP
IP: FLAG
GFP
FLAG
Lysate
GFP
FLAG
β-actin
1 2 3 4 5 6

Figure 15. DJ-1 oxidation by TRAIL and tBHP. (**A**) HCT116 cells were treated with 10 ng/ml TNFSF10 for 4 h, followed by immunoblotting of specific antibodies for oxidized PARK7 and PARK7. (**B**) HCT116 cells were treated with 10 ng/ml TRAIL for 4 h or co-treated with 10 ng/ml TRAIL and 2.5 mM NAC, followed by immunoblotting of indicated antibodies. (**C**) HCT116 cells were treated with 250 μM tert-butyl hydroperoxide (tBHP) for 3 h or co-treated with 250 μM tBHP and 2.5 mM NAC, followed by immunoblotting of indicated antibodies.

.

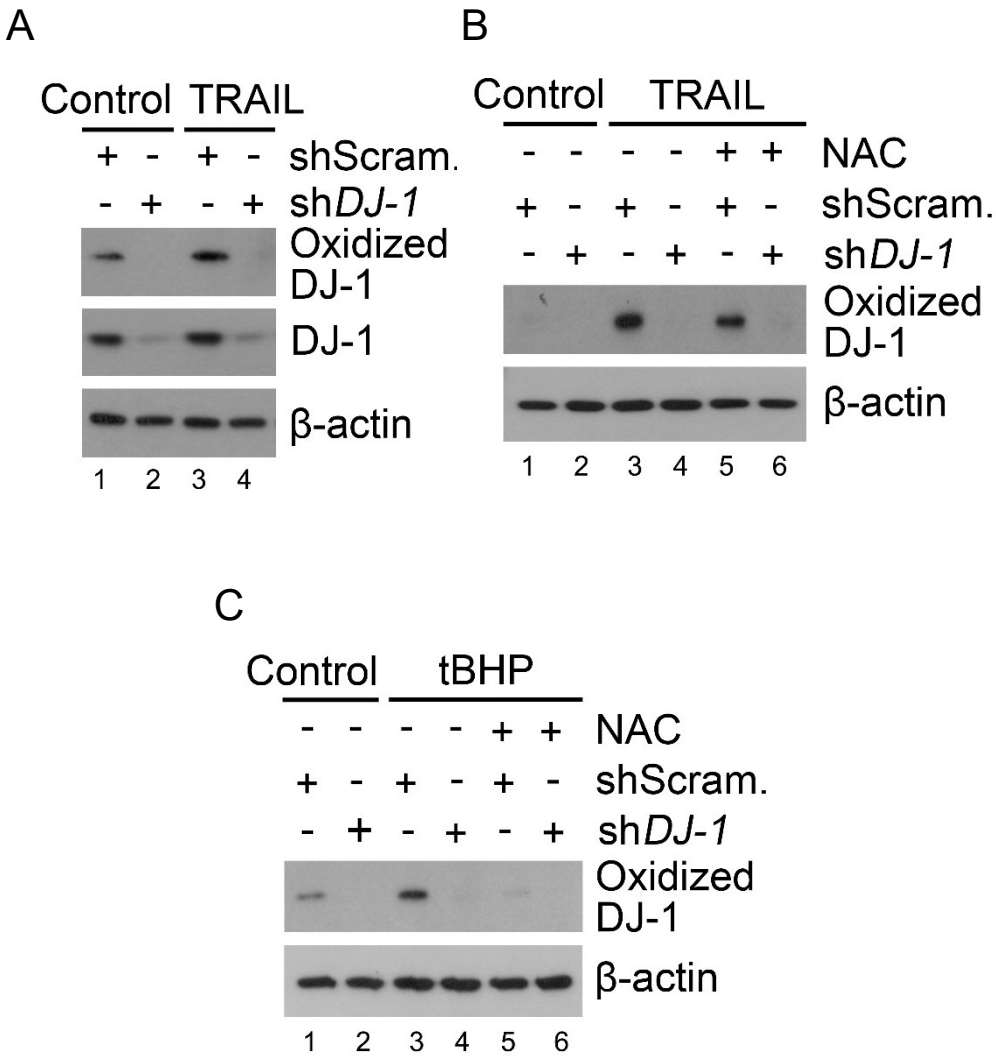
A
Control
TRAIL
+ - + - shScram.
- + - + sh*DJ-1*
Oxidized DJ-1
DJ-1
β-actin
1 2 3 4
B
Control
TRAIL
- - - - + + NAC
+ - + - + - shScram.
- + - + - + sh*DJ-1*
Oxidized DJ-1
β-actin
1 2 3 4 5 6
C
Control
tBHP
- - - - + + NAC
+ - + - + - shScram.
- + - + - + sh*DJ-1*
Oxidized DJ-1
β-actin
1 2 3 4 5 6

Figure 16. The effect of DJ-1 oxidation on DJ-1/R-BiP interaction.

(**A**) HCT116 cells were co-transfected with plasmids encoding Ub-R-BiP-GFP and one of followings: FLAG-DJ-1 and its C46A, C53A, and C106A mutants. After 48 h, the cells were treated with 10 ng/ml TRAIL for 4 h. Cell lysates were immunoprecipitated with anti-FLAG antibody followed by immunoblotting with anti-GFP or anti-FLAG antibody. (**B**) HCT116 cells were transfected with one of following plasmids encoding FLAG, FLAG-DJ-1, or FLAG-DJ-1^{C106A}. After 48 h of transient transfection, cells were treated with 20 ng/ml TRAIL for 2 h. The lysates were immunoprecipitated with the anti-FLAG antibody and then immunoblotted with indicated antibodies.

A

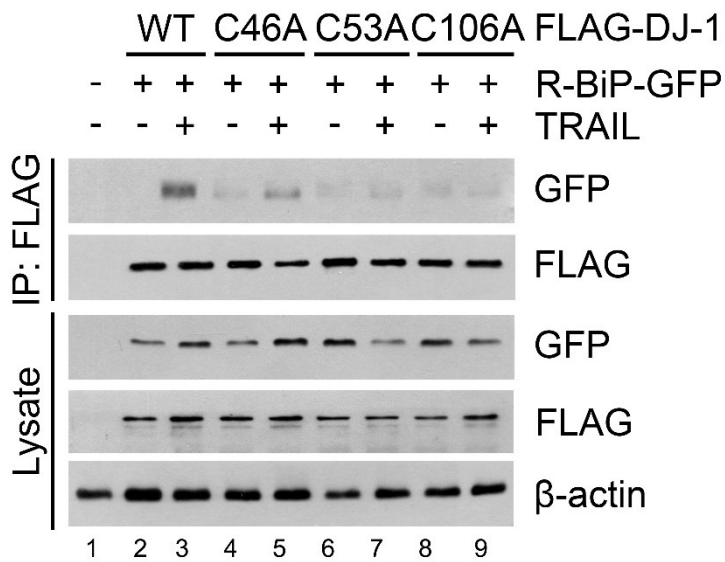
WT
C46A
C53A
C106A
FLAG-DJ-1
- + + + + + + + + R-BiP-GFP
- - + - + - + - + TRAIL
IP: FLAG
GFP
FLAG
Lysate
GFP
FLAG
β-actin
1 2 3 4 5 6 7 8 9

B

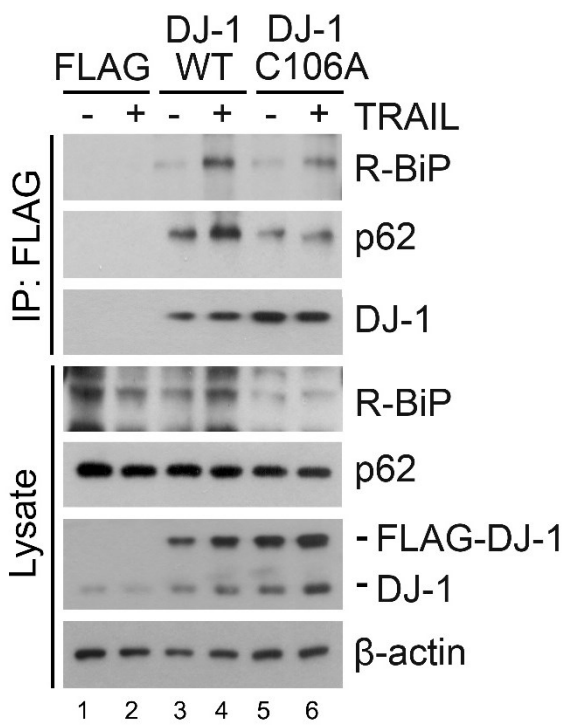
FLAG
DJ-1 WT
DJ-1 C106A
- + - + - + TRAIL
IP: FLAG
R-BiP
p62
DJ-1
Lysate
R-BiP
p62
- FLAG-DJ-1
- DJ-1
β-actin
1 2 3 4 5 6

Figure 17. The role of DJ-1 on DJ-1/R-BiP/p62 interaction. (**A**) HCT116 cells were treated with 10 ng/ml TRAIL for 4 h. Cell lysates were immunoprecipitated with anti-p62 antibody, followed by immunoblotting analysis. (**B**) HCT116 cells were treated with 200 nM bafilomycin A1 (Baf. A1) for 6 h or cultured in the presence of 200 nM bafilomycin A1 for 2 h then additionally treated with 10 ng/ml TRAIL for 4 h. The lysates were immunoprecipitated with anti-p62 antibody, followed by immunoblotting analysis.

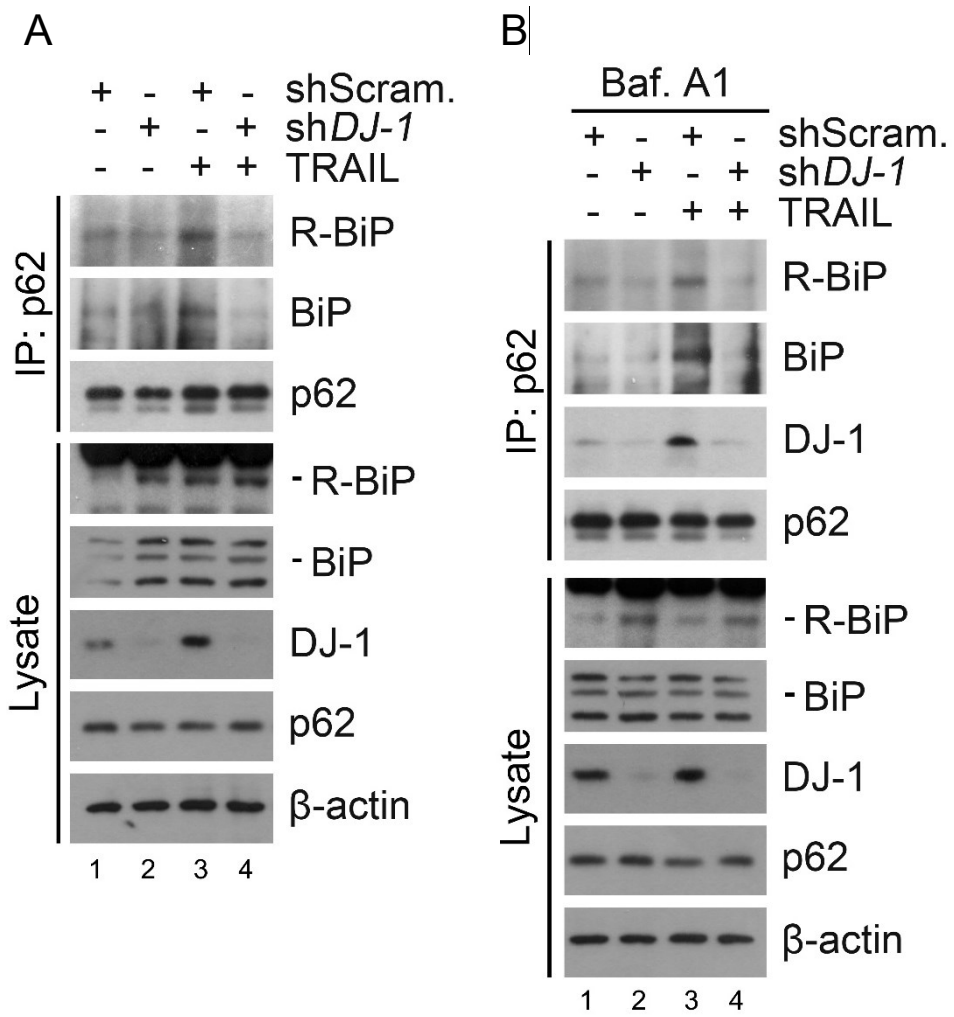
A
+ - + - shScram.
- + - + shDJ-1
- - + + TRAIL
IP: p62
R-BiP
BiP
p62
Lysate
- R-BiP
- BiP
DJ-1
p62
β-actin
1 2 3 4
B
Baf. A1
+ - + - shScram.
- + - + shDJ-1
- - + + TRAIL
IP: p62
R-BiP
BiP
DJ-1
p62
Lysate
- R-BiP
- BiP
DJ-1
p62
β-actin
1 2 3 4

Figure 18. A schematic diagram presenting the interaction between arginylated BiP (R-BiP), oxidized DJ-1 (oxDJ-1), and activated p62. In this mechanism, BiP, DJ-1 and p62 are modified by each of modulation under the stress, and through the modification of these 3 components constitute the complex of 3-way interaction.

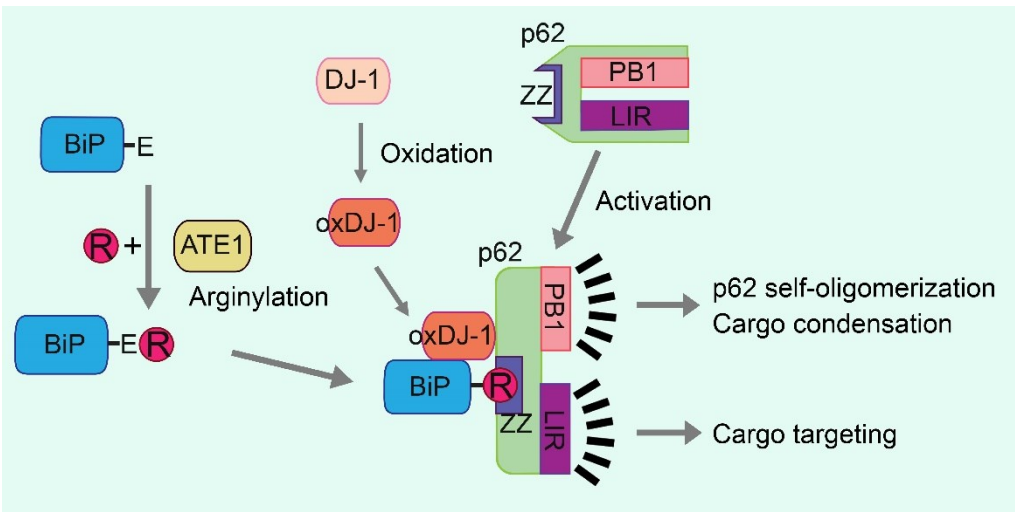
p62
PB1
ZZ
LIR
DJ-1
Oxidation
BiP
E
Activation
oxDJ-1
R
+
ATE1
p62
Arginylation
PB1
p62 self-oligomerization
Cargo condensation
BiP
E
R
oxDJ-1
BiP
R
ZZ
LIR
Cargo targeting

Figure 19. R-BiP and p62 puncta induction by TRAIL. Cells were treated with 200 nM bafilomycin A1 for 6 h or 10 ng/ml TRAIL for 4 h, or the cells cultured in the presence of 200 nM bafilomycin A1 for 2 h were additionally treated with 10 ng/ml TRAIL for 4 h. Immunostaining analysis was performed using antibodies to R-BiP (red) and p62 (green), followed by confocal microscopy. Scale bar, 10 μm.

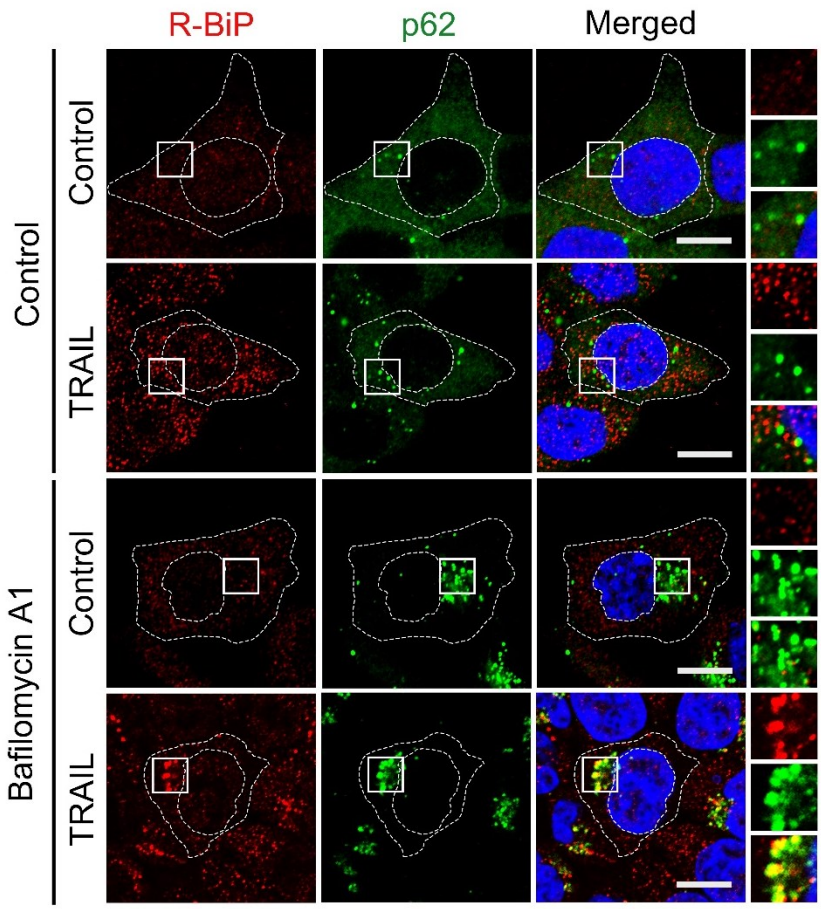
R-BiP
p62
Merged
Control
Control
TRAIL
Bafilomycin A1
Control
TRAIL

Figure 20. The DJ-1 effect on R-BiP and p62 puncta formation.

(A) HCT116 cells stably expressing sh*DJ-1* or its control shRNA were treated with 10 ng/ml TRAIL for 4 h or 200 nM bafilomycin A1 for 2 h were additionally treated with 10 ng/ml TRAIL for 4 h as described in Figure 13. **(B)** Quantitation of R-BiP cytosolic puncta in A. Error bars represent the mean ± SEM from each cells (***$p < 0.001$, n = 50). (**C**) Quantitation of p62 cytosolic puncta in A. Error bars represent the mean ± SEM from each cells (***$p < 0.001$, n = 50). (**D**) Quantitation of the colocalization of p62 cytosolic puncta in A with R-BiP puncta. Error bars represent the mean ± SEM from each cells (***$p < 0.001$, n = 50).

A

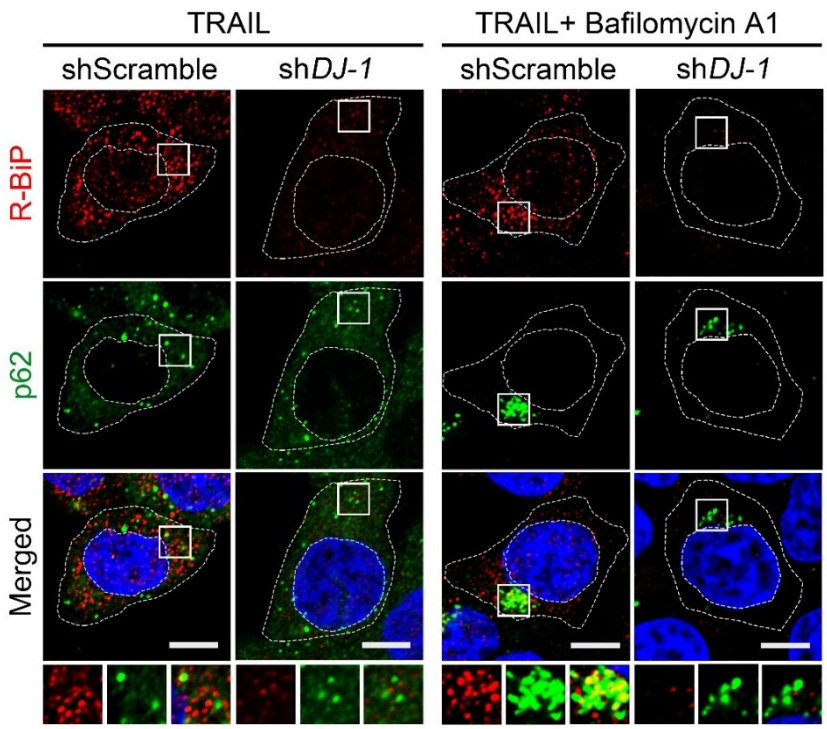
TRAIL
TRAIL+ Bafilomycin A1
shScramble
shDJ-1
shScramble
shDJ-1
R-BiP
p62
Merged

B

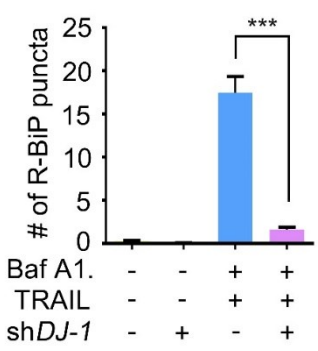
# of R-BiP puncta
25
20
15
10
5
0
***
Baf A1. - - + +
TRAIL - - + +
shDJ-1 - + - +

C

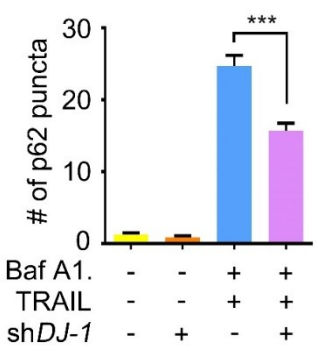
# of p62 puncta
30
20
10
0
***
Baf A1. - - + +
TRAIL - - + +
shDJ-1 - + - +

D

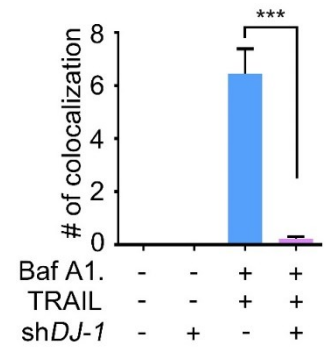
# of colocalization
8
6
4
2
0
***
Baf A1. - - + +
TRAIL - - + +
shDJ-1 - + - +

Figure 21. The DJ-1 effect on p62 oligomerization by TRAIL and the oligomerization of DJ-1. (A) Cells were treated with 10 ng/ml TRAIL for 4 h or 200 nM bafilomycin A1 for 6 h. Alternatively, the cells cultured in the presence of 200 nM bafilomycin A1 for 2 h were additionally treated with 10 ng/ml TRAIL for 4 h. The p62 and DJ-1 oligomerization assay was followed by non-reducing SDS-PAGE and immunoblotting using antibodies to p62 and DJ-1. **(B)** Cells were treated with tBHP indicated concentration. DJ-1 oligomerization assay was followed by non-reducing SDS-PAGE and immunoblotting using an antibody to DJ-1.

A

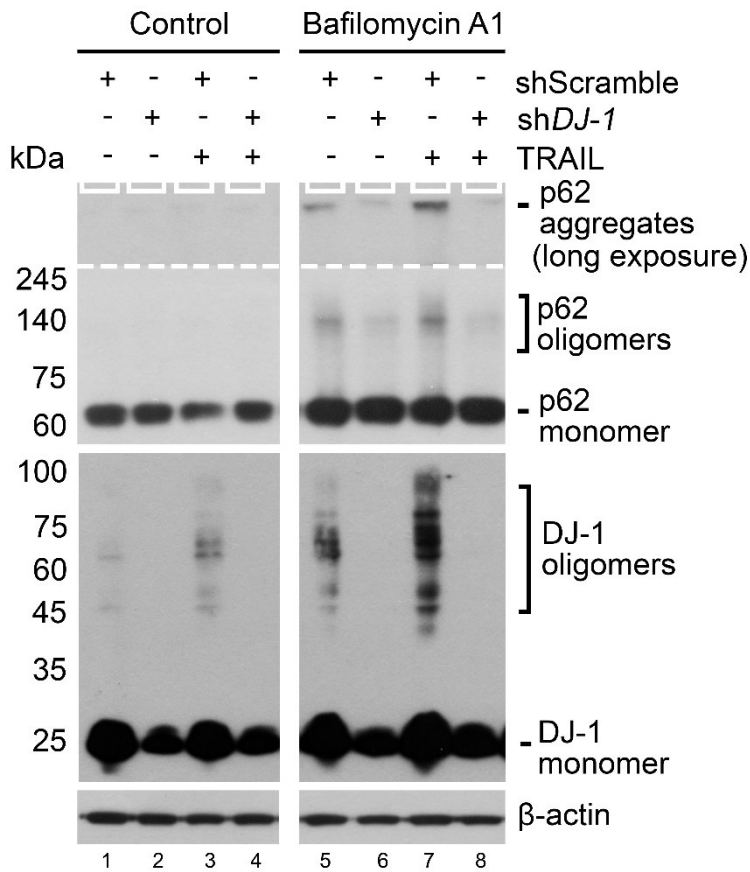
Control
Bafilomycin A1
+ - + - + - + - shScramble
- + - + - + - + shDJ-1
kDa - - + + - - + + TRAIL
p62 aggregates (long exposure)
245
140
p62 oligomers
75
60
p62 monomer
100
75
60
45
DJ-1 oligomers
35
25
DJ-1 monomer
β-actin
1 2 3 4 5 6 7 8

B

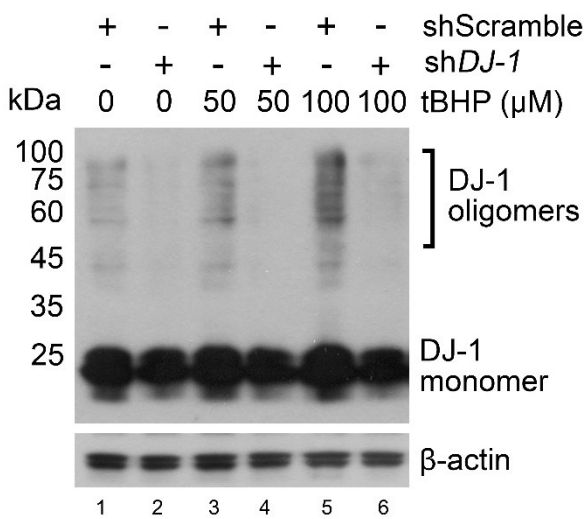
+ - + - + - shScramble
- + - + - + shDJ-1
kDa 0 0 50 50 100 100 tBHP (μM)
100
75
60
45
DJ-1 oligomers
35
25
DJ-1 monomer
β-actin
1 2 3 4 5 6

Figure 22. The impairment of LC3-II puncta formation in DJ-1 deficient cells. (**A**) HCT116 cells stably expressing scrambled shRNA or sh*DJ-1* were treated with 200 nM bafilomycin A1 for 6 h and immunostained for LC3-II (red) or DJ-1 (green). LC3-II-positive autophagic vacuoles were examined using confocal microscopy. Scale bar, 10 μm. (**B**) Quantitation of the number of LC3-II puncta in A. Error bars represent the mean ± SEM from each cell (***$p < 0.001$, n = 50). (**C**) HCT116 cells stably expressing scrambled shRNA or sh*DJ-1* were treated with 200 nM bafilomycin A1 for 2 h, followed by the treatment with 10 ng/ml TRAIL for 4 h. The cells were immunostained for LC3-II (red) or p62 (green). Puncta formation and co-localization of LC3-II and p62 were examined using confocal microscopy. Scale bar, 10 μm.

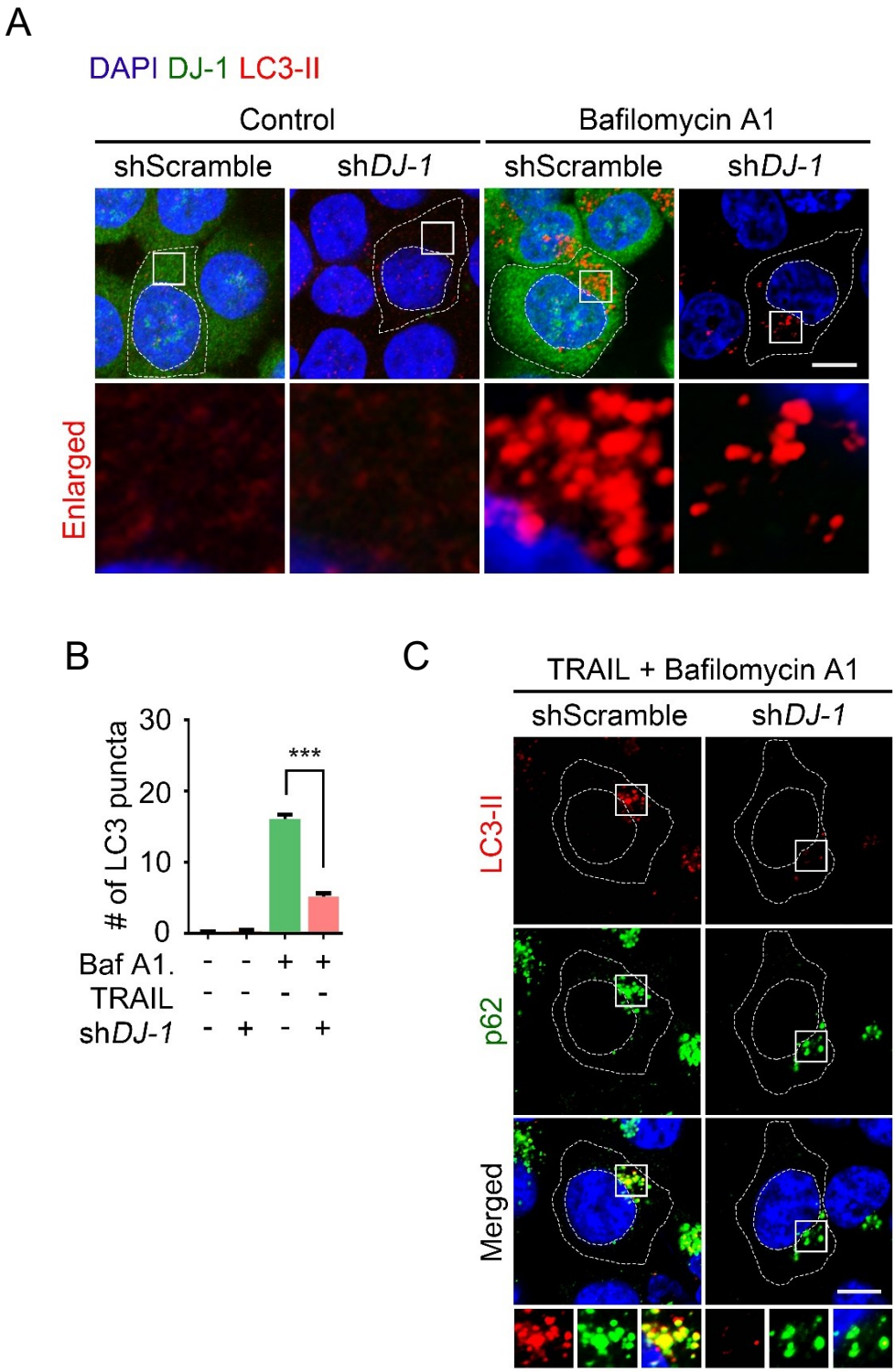
A
DAPI DJ-1 LC3-II
Control
Bafilomycin A1
shScramble
shDJ-1
shScramble
shDJ-1
Enlarged
B
# of LC3 puncta
30
20
10
0
***
Baf A1. - - + +
TRAIL - - - -
shDJ-1 - + - +
C
TRAIL + Bafilomycin A1
shScramble
shDJ-1
LC3-II
p62
Merged

Figure 23. The impairment of the formation of autolysosome in DJ-1 deficient cells. (**A**) HCT116 cells stably expressing scrambled shRNA or sh*DJ-1* were treated with 200 nM bafilomycin A1 for 2 h, followed by the treatment with 10 ng/ml TRAIL for 4 h. The cells were immunostained for PLEKHM1 (green). Puncta formation of PLEKHM1 was examined using confocal microscopy. Scale bar, 10 μm. (**B**) HCT116 cells stably expressing scrambled shRNA or sh*PARK7* were treated with 200 nM bafilomycin A1 for 6 h and immunoblotted with indicated antibodies. (**C**) HCT116 cells stably expressing scrambled shRNA or sh*DJ-1* were treated with 200 nM bafilomycin A1 for 6 h and immunostained for WIPI2 (red). WIPI2-positive autophagic vacuoles were examined using confocal microscopy. Scale bar, 10 μm.

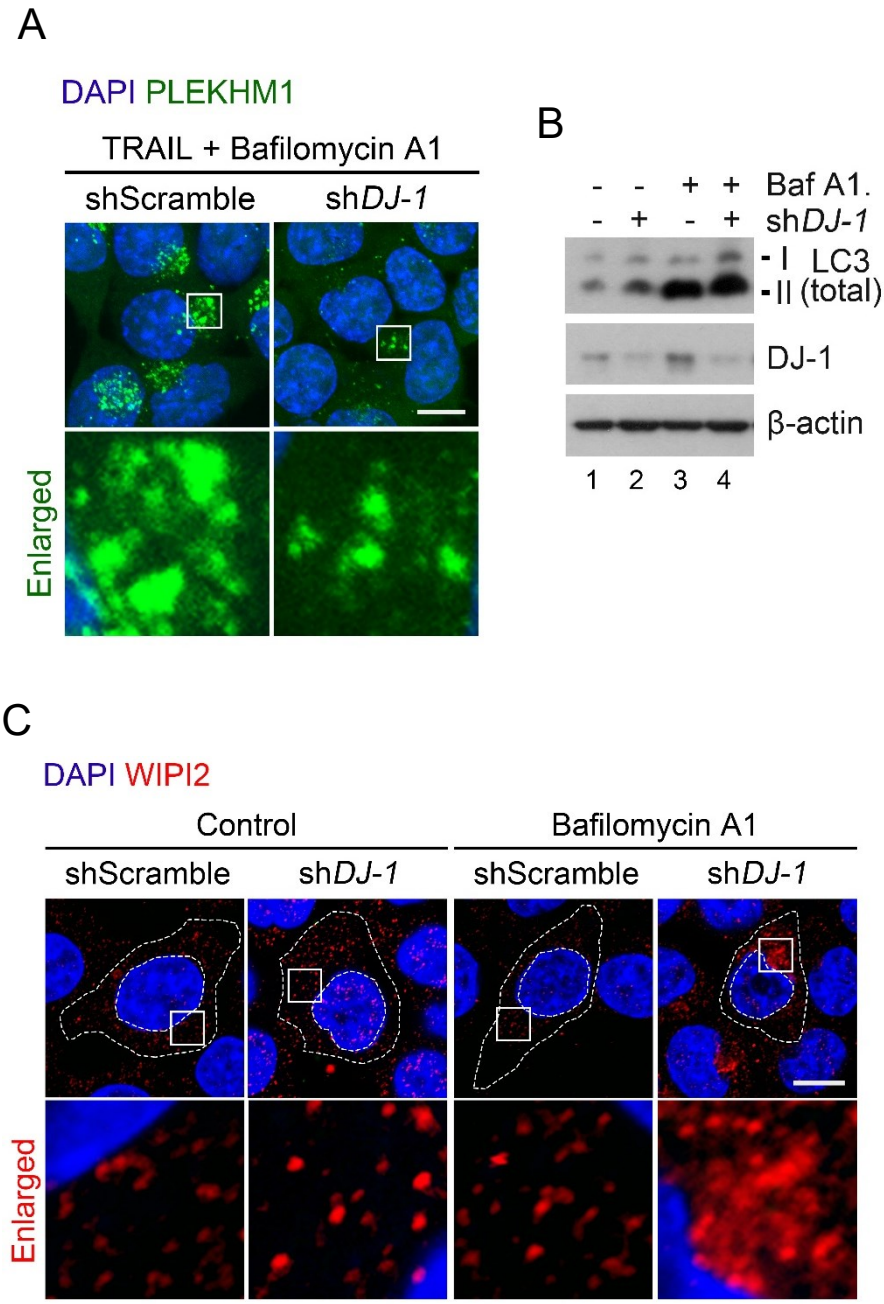
A
DAPI PLEKHM1
TRAIL + Bafilomycin A1
shScramble
shDJ-1
Enlarged
B
- - + + Baf A1.
- + - + shDJ-1
I LC3
II (total)
DJ-1
β-actin
1 2 3 4
C
DAPI WIPI2
Control
Bafilomycin A1
shScramble
shDJ-1
shScramble
shDJ-1
Enlarged

Figure 24. The accumulation of cargo proteins in DJ-1 deficient cells.

(**A**) HCT116 cells stably expressing scrambled shRNA or sh*DJ-1* were treated with the presence of 200 nM bafilomycin A1 for 2 h and were additionally treated with 10 ng/ml TRAIL for 4 h. Cell lysates were subjected to immunoblotting analysis using FK2 antibody specific to Ub-conjugated proteins. (**B**) HCT116 cells stably expressing scrambled shRNA or sh*PARK7* were treated with 10 ng/ml TRAIL for 4 h alone or were pretreated with bafilomycin A1 for 2 h, followed by the treatment with 10 ng/ml TRAIL for 4 h, followed by immunostaining analysis using FK2 antibody (red). Scale bar, 10 μm. (**C**) Quantitation of the intensity of Ub-positive puncta as visualized using FK2 antibody. Error bars represent the mean ± SEM from each cells (***$p < 0.001$, n = 50). (**D**) Quantitation of the number of Ub-positive puncta as visualized using FK2 antibody. Error bars represent the mean ± SEM from each cells (***$p < 0.001$, n = 50).

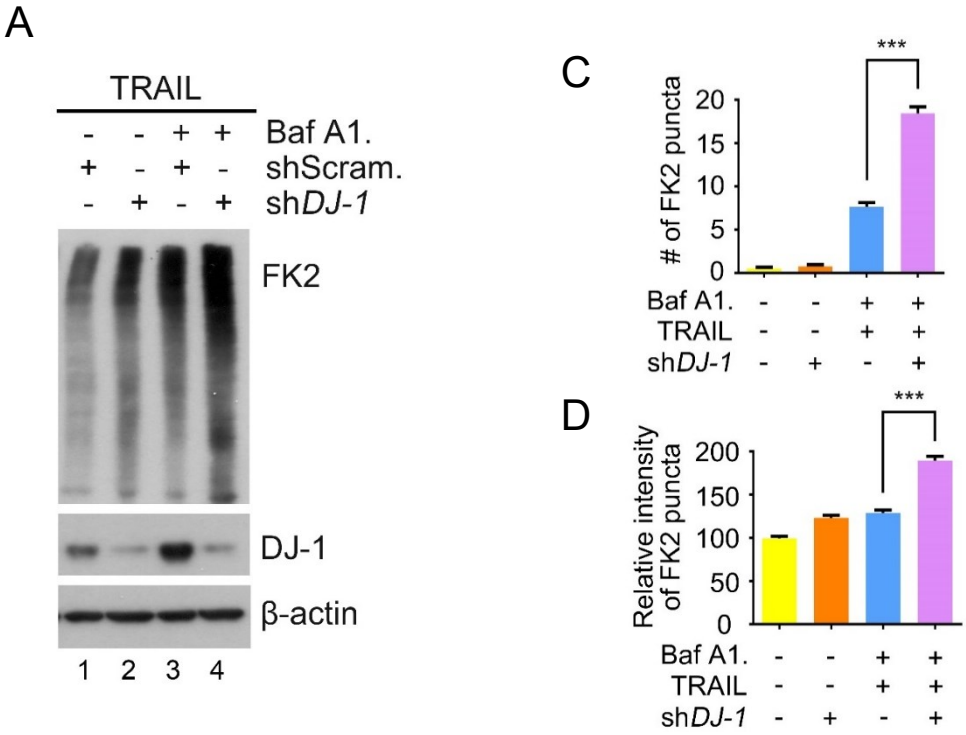
A
TRAIL
- - + + Baf A1.
+ - + - shScram.
- + - + shDJ-1
FK2
DJ-1
β-actin
1 2 3 4
C
# of FK2 puncta
20
15
10
5
0
***
Baf A1. - - + +
TRAIL - - + +
shDJ-1 - + - +
D
Relative intensity of FK2 puncta
200
150
100
50
0
***
Baf A1. - - + +
TRAIL - - + +
shDJ-1 - + - +

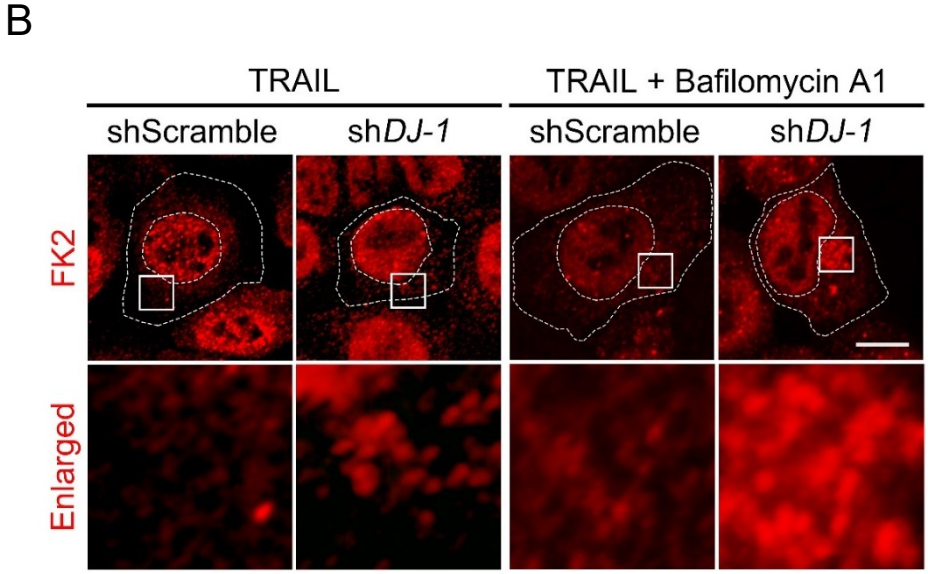
B
TRAIL
TRAIL + Bafilomycin A1
shScramble
shDJ-1
shScramble
shDJ-1
FK2
Enlarged

Figure 25. The impairment of autophagic cargo targeting in DJ-1 deficient cells. (**A**) HCT116 cells stably expressing scrambled shRNA or sh*DJ-1* were treated with 200 nM bafilomycin A1 for 2 h, followed by the treatment with 10 ng/ml TRAIL for 4 h. The cells were immunostained using FK2 (red) or p62 (green) antibodies. Puncta formation and co-localization of FK2 and p62 signals were examined using confocal microscopy. Scale bar, 10 μm. (**B**) Same condition has been used as A except that FK2 (red) or LC3 (green) antibodies were used.

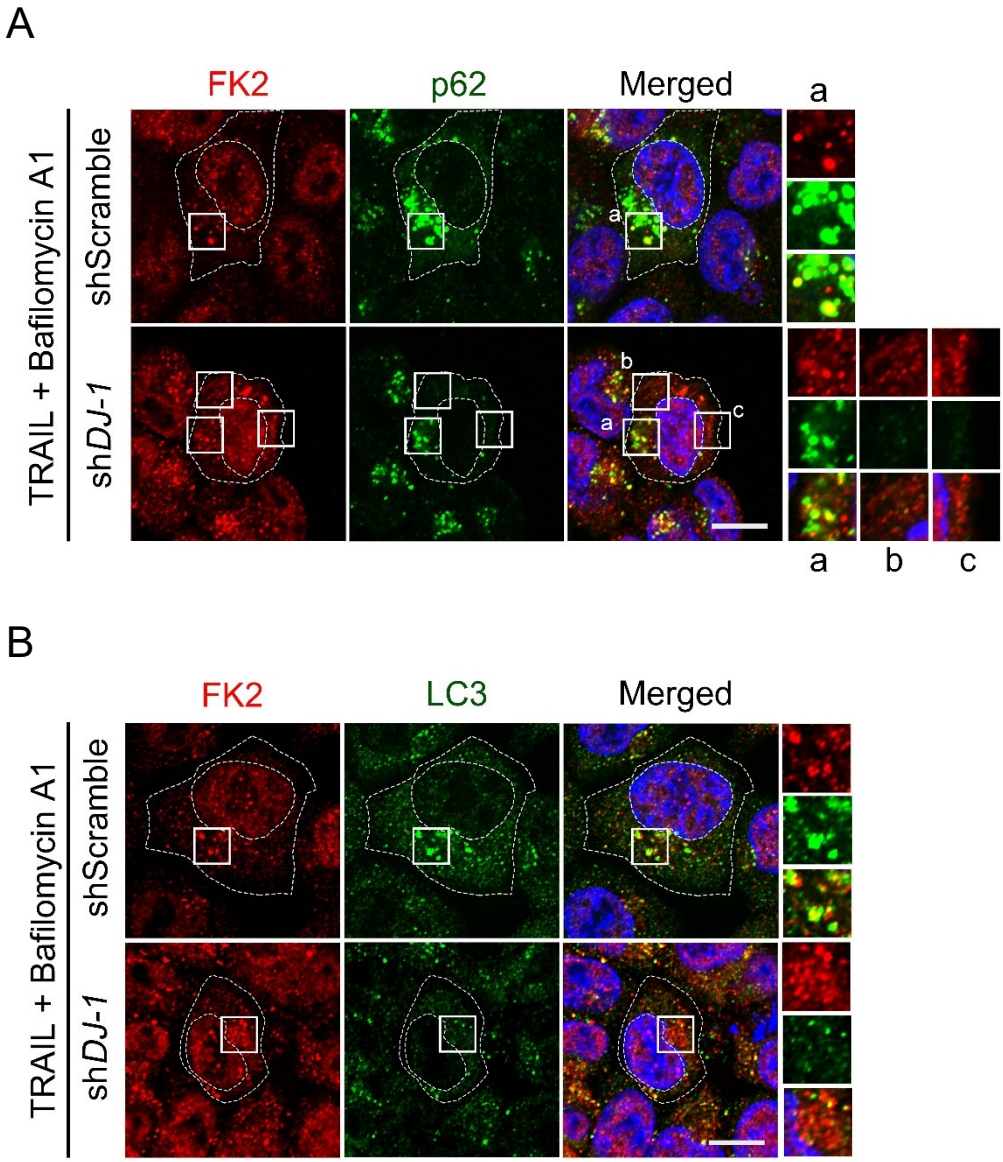
A
FK2
p62
Merged
a
TRAIL + Bafilomycin A1
shScramble
shDJ-1
a
b
c
a
b
c
B
FK2
LC3
Merged
TRAIL + Bafilomycin A1
shScramble
shDJ-1

Figure 26. The impairment on autophagic targeting of Keap1 in response to TRAIL induced oxidative stress. (**A**) HCT116 cells stably expressing scrambled shRNA or sh*DJ-1* were treated with 200 nM bafilomycin A1 for 2 h, followed by the treatment with 10 ng/ml TRAIL for 4 h. The cells were immunostained using Keap1 (red) or p62 (green) antibodies. Puncta formation and co-localization of Keap1 and p62 signals were examined using confocal microscopy. Scale bar, 10 μm. (**B**) HCT116 Cells were cultured in the presence of 200 nM bafilomycin A1 for 2 h were additionally treated with 10 ng/ml TRAIL for 4 h. The cells were immunoblotted with indicated antibodies.

A

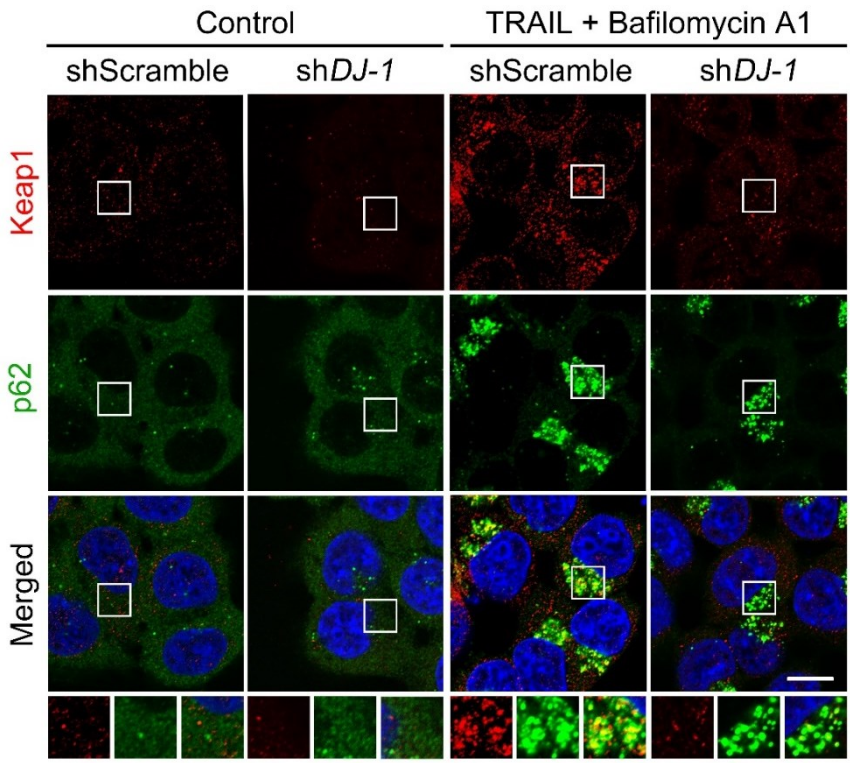
Control
TRAIL + Bafilomycin A1
shScramble
shDJ-1
shScramble
shDJ-1
Keap1
p62
Merged

B

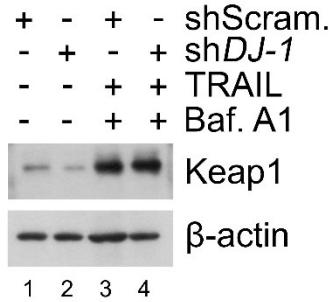
+ - + - shScram.
- + - + shDJ-1
- - + + TRAIL
- - + + Baf. A1
Keap1
β-actin
1 2 3 4

Figure 27. The impairment on autophagic targeting of Keap1 in response to tBHP induced oxidative stress. Cells were cultured in the presence of 200 nM bafilomycin A1 for 3 h were additionally treated with 250 μM tBHP for 3 h. The cells were immunostained for Keap1 (red) and p62 (green), and examined using confocal microscopy. Scale bar, 10 μm

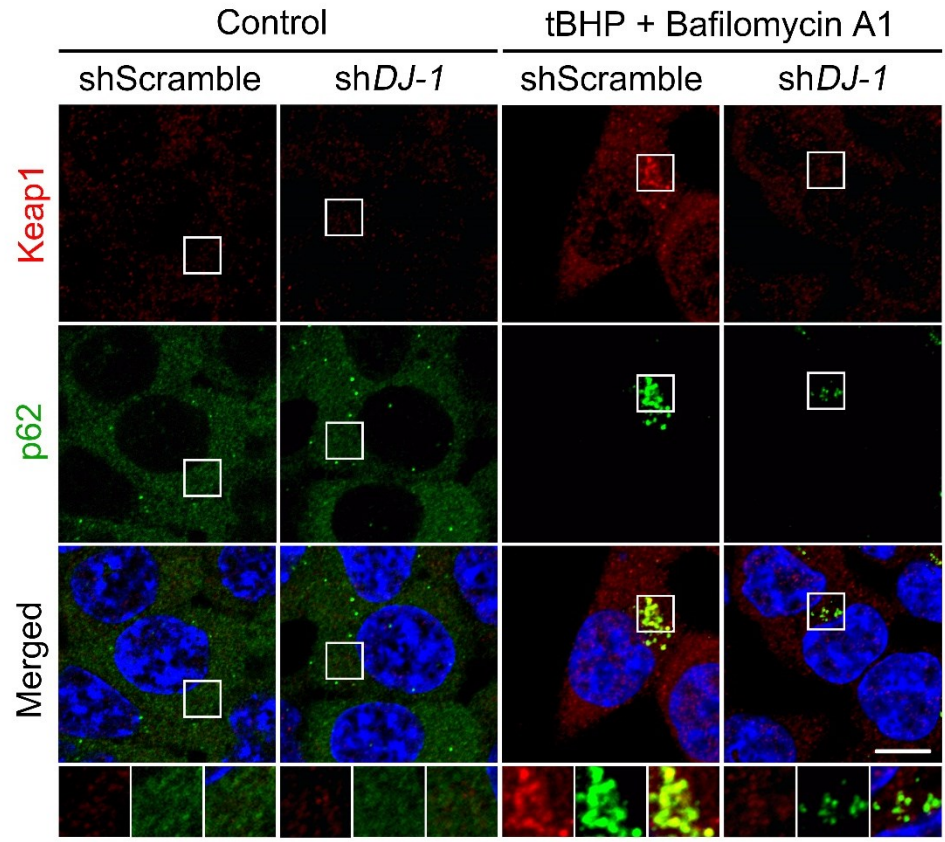
Control
tBHP + Bafilomycin A1
shScramble
shDJ-1
shScramble
shDJ-1
Keap1
p62
Merged

Figure 28. The protective role of DJ-1 against mitochondrial damage by TRAIL in HCT116 cells. (**A)** HCT116 cells stably expressing scrambled shRNA or sh*DJ-1* were treated with 5 ng/ml TRAIL for 4 h. After treatment, the cells were stained with JC-1 and analyzed using FACS to measure the depolarization of mitochondrial membranes. (**B**) Quantitation of A. Error bars represent the mean ± SEM from three independent experiments (**P* < 0.05). (**C**) Immunoblotting analysis of A.

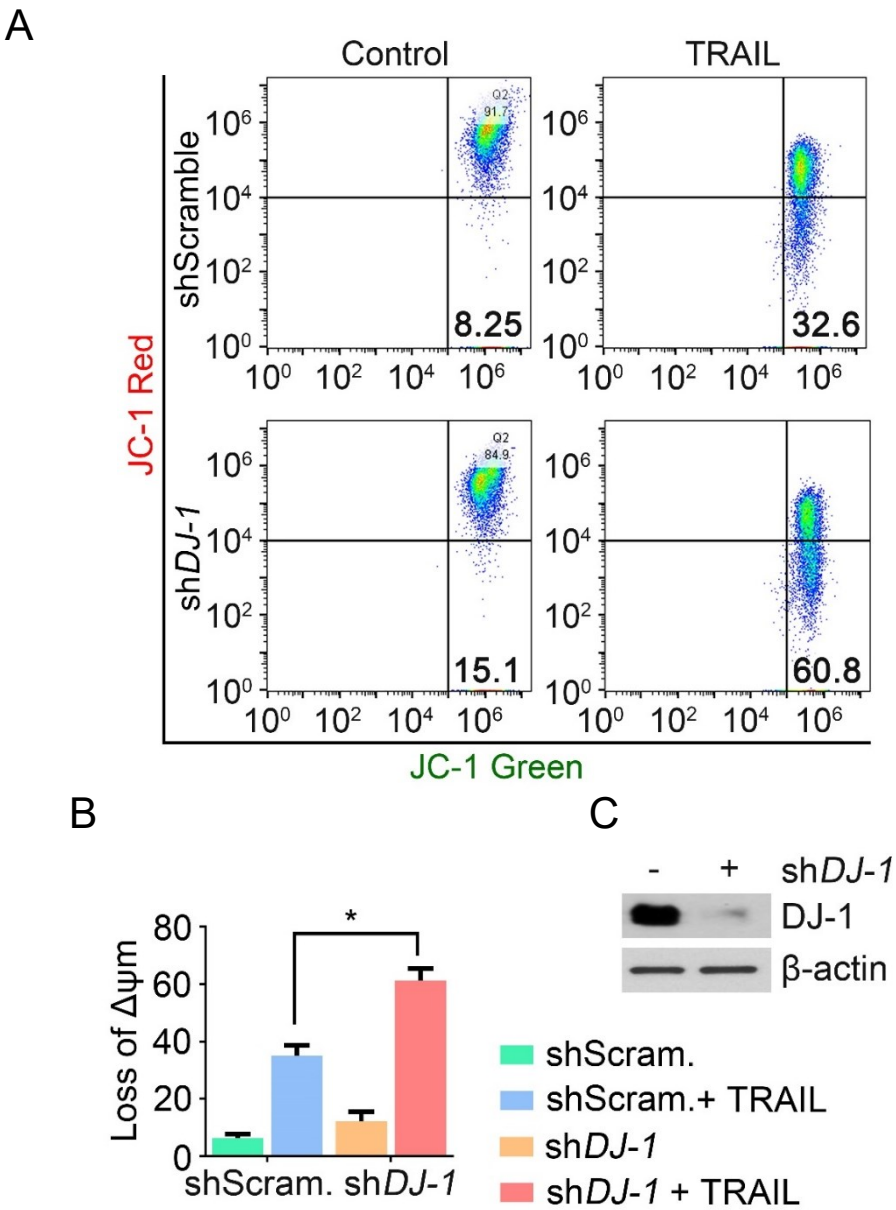
A
Control
TRAIL
shScramble
shDJ-1
JC-1 Red
JC-1 Green
Q2
91.7
8.25
Q2
84.9
15.1
32.6
60.8
B
Loss of Δψm
80
60
40
20
0
*
shScram.
shDJ-1
shScram.
shScram.+ TRAIL
shDJ-1
shDJ-1 + TRAIL
C
-
+
shDJ-1
DJ-1
β-actin

Figure 29. The protective role of DJ-1 against mitochondrial damage by vvmTRAIL in MEFs. (**A)** Wild-type and *DJ-1*$^{-/-}$ MEFs were infected with vvmTRAIL (MOI = 1) for 24 h in comparison with the control vaccinia virus vJS6 (MOI = 1). The cells were stained with JC-1 and analyzed using FACS to measure the depolarization of mitochondrial membranes. (**B**) Quantitation of A. Error bars represent the mean ± SEM from three independent experiments (*$P < 0.05$). (**C**) Immunoblotting analysis of A. (Conducted by D.H. Lee)

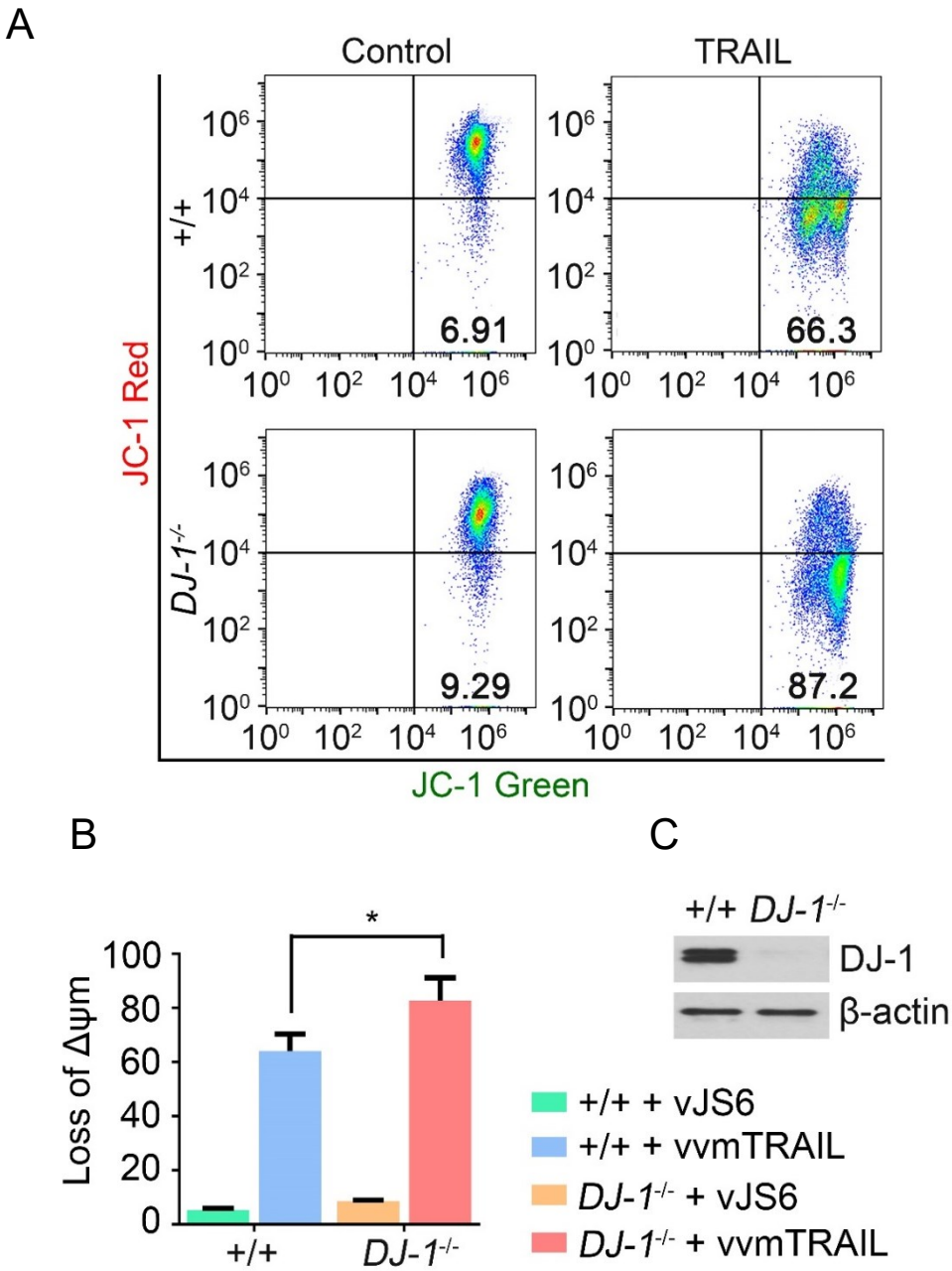
A
Control
TRAIL
+/+
DJ-1-/-
JC-1 Red
JC-1 Green
6.91
66.3
9.29
87.2
B
Loss of Δψm
*
+/+
DJ-1-/-
C
+/+ DJ-1-/-
DJ-1
β-actin
+/+ + vJS6
+/+ + vvmTRAIL
DJ-1-/- + vJS6
DJ-1-/- + vvmTRAIL

Figure 30. Dissociation of lumenal BiP during TRAIL-induced stress.

(**A**, **B**) HCT116 cells were treated with 5 ng/ml TRAIL for 4 h. Cell lysates were subjected to IP with BiP or mock antibody (IgG), followed by immunoblotting as indicated. (Conducted by D.H. Lee)

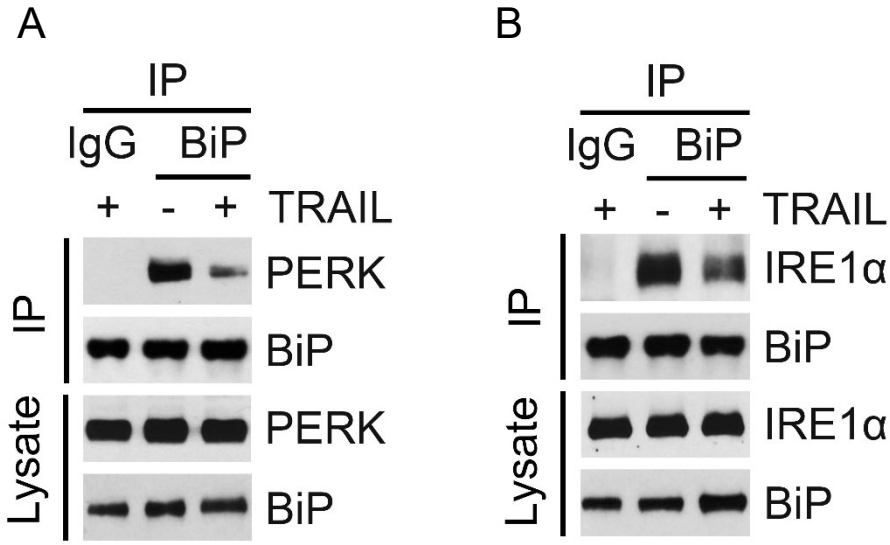
A
IP
IgG
BiP
+
-
+
TRAIL
IP
PERK
BiP
Lysate
PERK
BiP
B
IP
IgG
BiP
+
-
+
TRAIL
IP
IRE1α
BiP
Lysate
IRE1α
BiP

Figure 31. ER stress response of DJ-1 deficient cells.

(**A**) Wild-type and *DJ-1*$^{-/-}$ MEFs were infected with vvmTRAIL (MOI = 1) for 24 h in comparison with the control vaccinia virus vJS6 (MOI = 1), followed by immunoblotting analysis. (**B**) The cells in A were subjected to the MTT assay. Error bars represent the mean ± SEM from three independent experiments (*$P < 0.05$). (**C**) The cells were analyzed using quantitative RT-PCR. The levels of *ATF4*, *CHOP*, and *BiP* mRNA were normalized to the level of GAPDH. Error bars represent the mean ± SEM from three independent experiments (*$P < 0.05$). (Conducted by D.H. Lee)

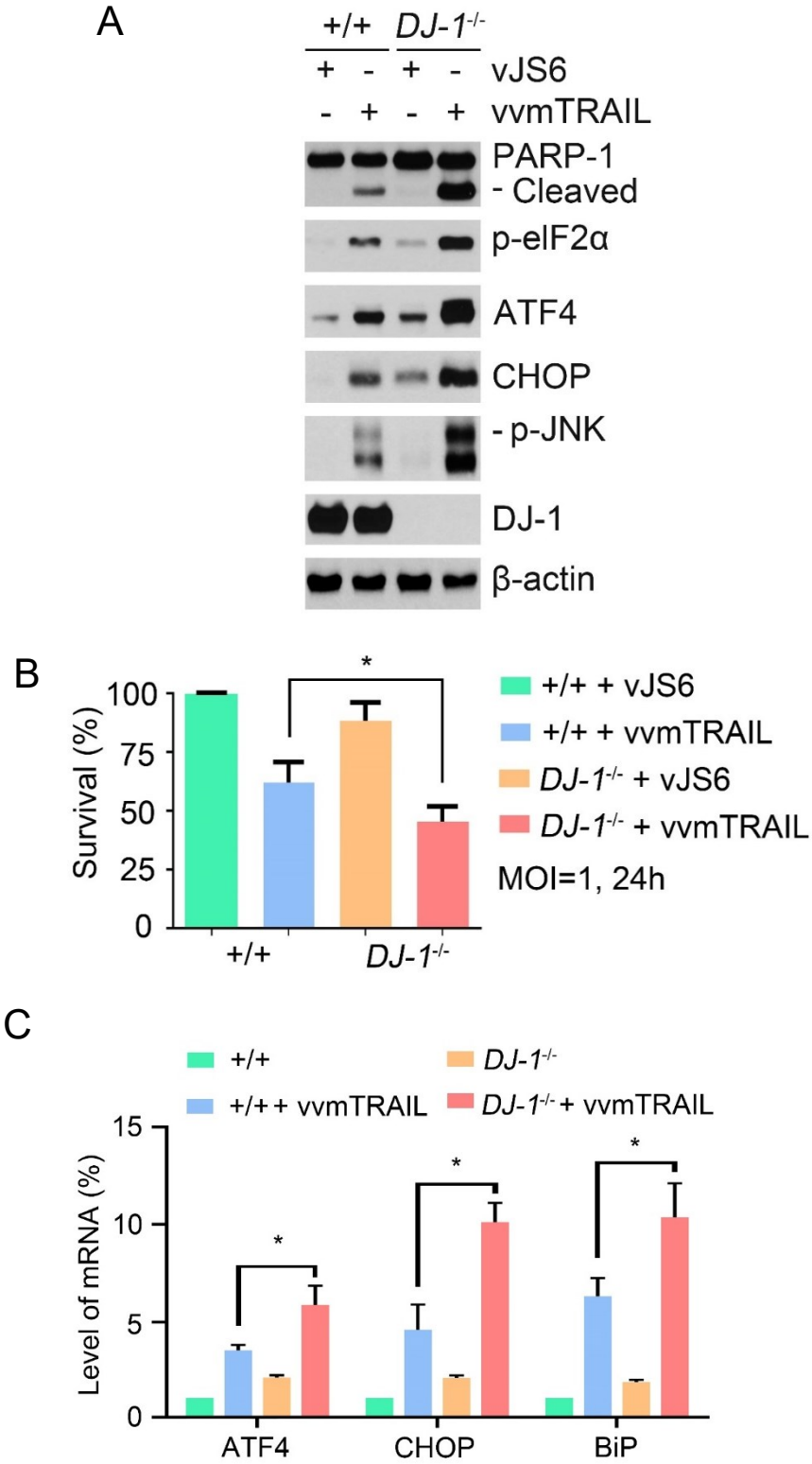
A
+/+
DJ-1-/-
+ - + - vJS6
- + - + vvmTRAIL
PARP-1
- Cleaved
p-eIF2α
ATF4
CHOP
- p-JNK
DJ-1
β-actin
B
Survival (%)
100
75
50
25
0
*
+/+
DJ-1-/-
+/+ + vJS6
+/+ + vvmTRAIL
DJ-1-/- + vJS6
DJ-1-/- + vvmTRAIL
MOI=1, 24h
C
+/+
DJ-1-/-
+/+ + vvmTRAIL
DJ-1-/- + vvmTRAIL
Level of mRNA (%)
15
10
5
0
*
*
*
ATF4
CHOP
BiP

Figure 32. The comparison of effects of DJ-1 deficient and overexpression. (**A**) HCT116 cells transfected with scrambled or DJ-1 siRNA (si*DJ-1*) were cultured for 48 h and subsequently treated with 5 ng/ml TRAIL for 4 h, followed by immunoblotting analysis. (**B**) HCT116 cells transiently expressing EGFP (GFP) or DJ-1-GFP were cultured for 48 h and subsequently treated with 5 ng/ml TRAIL for 4 h, followed by immunoblotting analysis. (**C**) The cells in A were subjected to the MTT assay. Error bars represent the mean ± SEM from three independent experiments (**P* < 0.05). (**D**) The cells in B was followed by the MTT assay. Error bars represent the mean ± SEM from three independent experiments (**P* < 0.05). (Conducted by D.H. Lee)

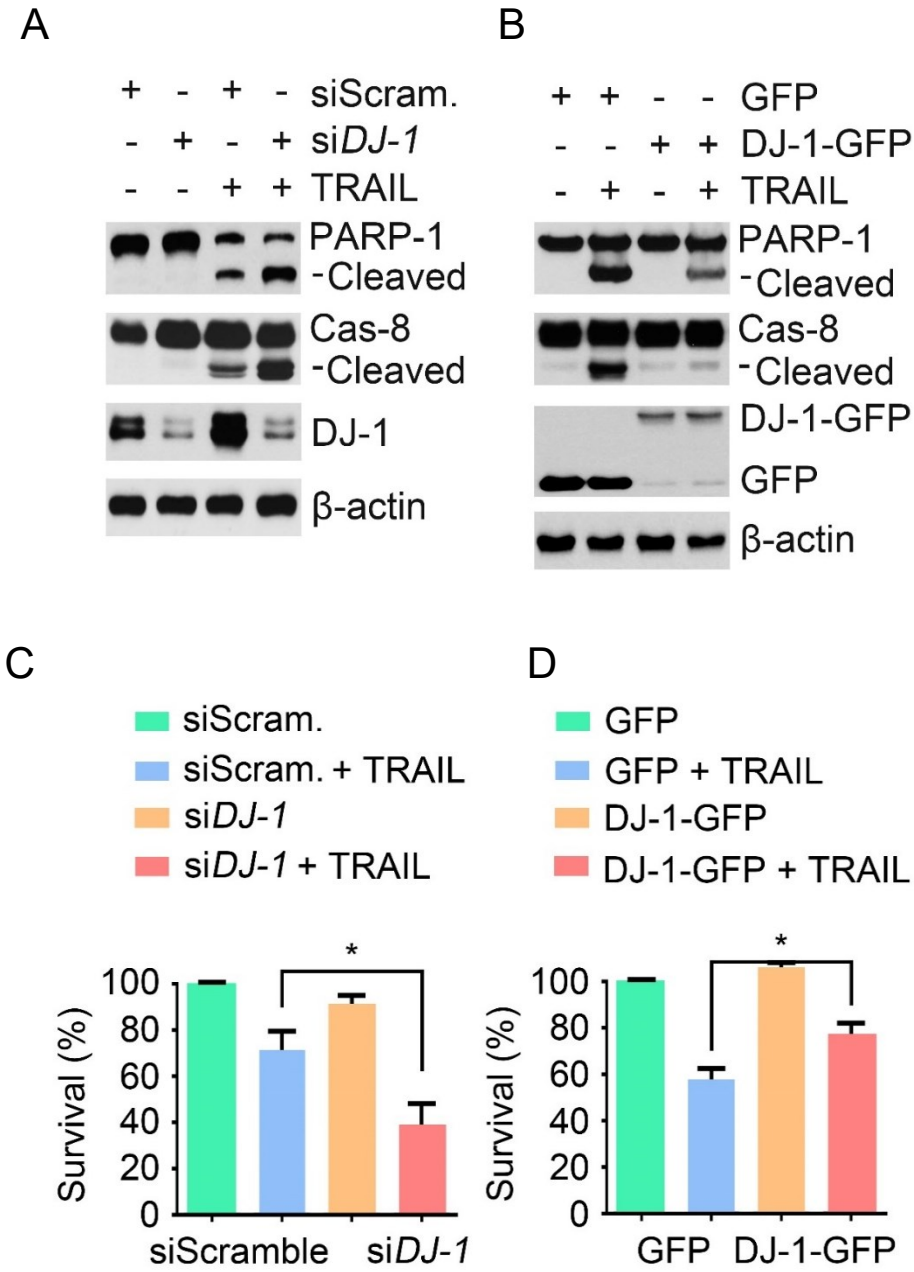
A
+ - + - siScram.
- + - + siDJ-1
- - + + TRAIL
PARP-1
-Cleaved
Cas-8
-Cleaved
DJ-1
β-actin
B
+ + - - GFP
- - + + DJ-1-GFP
- + - + TRAIL
PARP-1
-Cleaved
Cas-8
-Cleaved
DJ-1-GFP
GFP
β-actin
C
siScram.
siScram. + TRAIL
siDJ-1
siDJ-1 + TRAIL
Survival (%)
100
80
60
40
20
0
*
siScramble
siDJ-1
D
GFP
GFP + TRAIL
DJ-1-GFP
DJ-1-GFP + TRAIL
Survival (%)
100
80
60
40
20
0
*
GFP
DJ-1-GFP

Figure 33. The comparison of apoptosis in DJ-1 deficient cells and normal cells during TRAIL treatment. (**A**) HCT116 cells transfected with scrambled or DJ-1 siRNA (si*DJ-1*) were cultured for 48 h and subsequently treated with 5 ng/ml TRAIL for 4 h. The cells were stained with annexin V and propidium iodide, followed by flow cytometric analysis. (**B**) Quantitation of A. Data were calculated from three independent experiments and analyzed by one-way analysis of variance. Data shown are the means ± SEM, $*P < 0.05$. (Conducted by D.H. Lee)

A

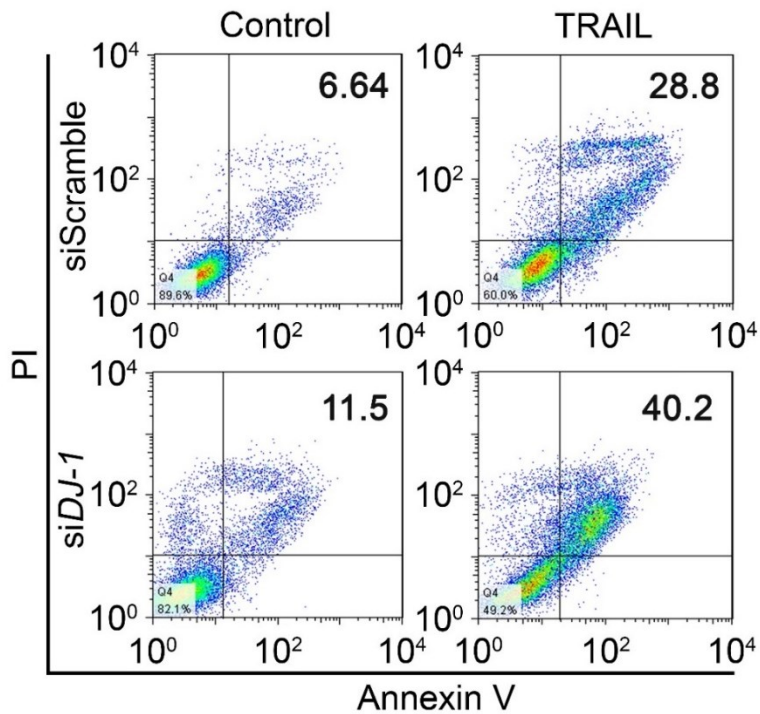
Control
TRAIL
siScramble
siDJ-1
PI
Annexin V
6.64
28.8
11.5
40.2
89.6%
60.0%
82.1%
49.2%

B

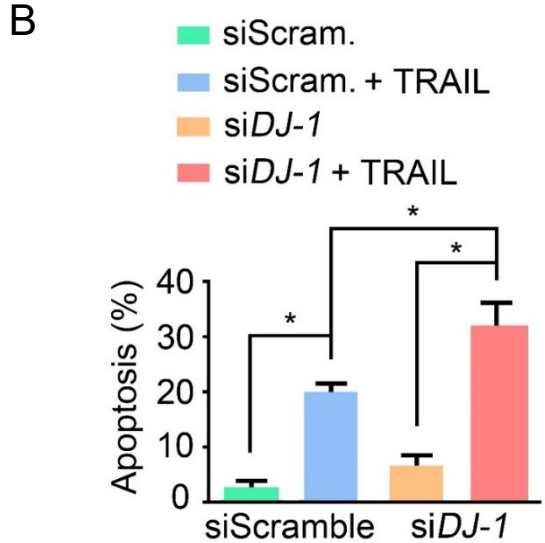
siScram.
siScram. + TRAIL
siDJ-1
siDJ-1 + TRAIL
Apoptosis (%)
siScramble
siDJ-1

Figure 34. The response of DJ-1 deficient cells under the general ER stressor. (**A**) Wild-type and and *DJ-1*$^{-/-}$ MEFs were treated with 2.5 μM thapsigargin. Cell lysates were subjected to immunoblot analysis as indicated to the right. (**B**) The cells in A were subjected to the MTT assay. Error bars represent the mean ± SEM from three independent experiments (*$P < 0.05$).

A

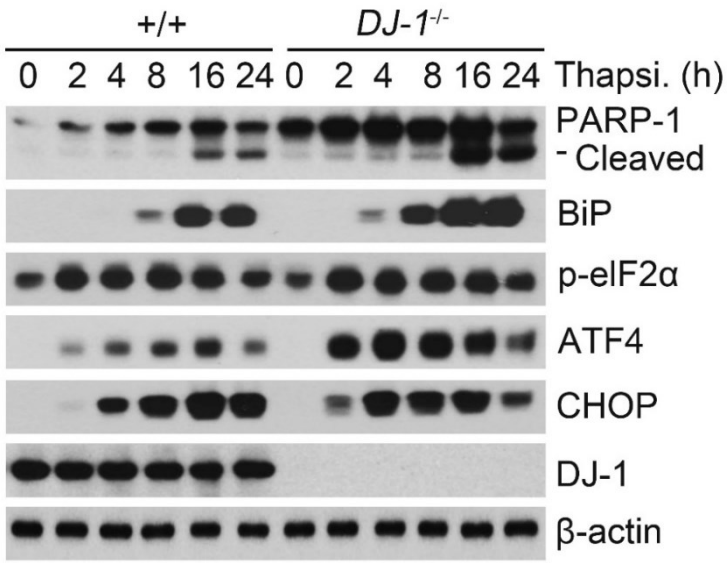
+/+
DJ-1-/-
0 2 4 8 16 24 0 2 4 8 16 24 Thapsi. (h)
PARP-1
Cleaved
BiP
p-eIF2α
ATF4
CHOP
DJ-1
β-actin

B

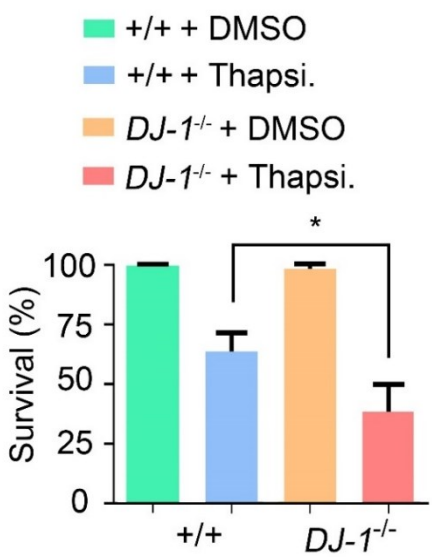
+/+ + DMSO
+/+ + Thapsi.
DJ-1-/- + DMSO
DJ-1-/- + Thapsi.
*
Survival (%)
100
75
50
25
0
+/+
DJ-1-/-

Figure 35. The protective role of ATE1 and BiP from TRAIL-induced stress in HCT116 cells. (**A**) HCT116 cells transfected with scrambled or ATE1 siRNA (si*ATE1*) were cultured for 48 h and subsequently treated with 5 ng/ml TRAIL for 4 h. Cell lysates were subjected to immunoblotting analysis. (**B**) The MTT assay of A. Error bars represent the mean ± SEM from three independent experiments (**P* < 0.05). (**C**) HCT116 cells transfected with scrambled or BiP siRNA (si*BiP*) were cultured for 48 h and subsequently treated with 5 ng/ml TRAIL for 4 h. Cell lysates were subjected to immunoblotting analysis. (**D**) The cells in C were used for the MTT assay. Error bars represent the mean ± SEM from three independent experiments (**P* < 0.05). (**E**) Cells transiently expressing HA-BiP or HA were cultured for 48 h and subsequently treated with 5 ng/ml TRAIL for 4 h, followed by immunoblotting analysis. (**F**) The MTT assay of E. Error bars represent the mean ± SEM from three independent experiments (**P* < 0.05).

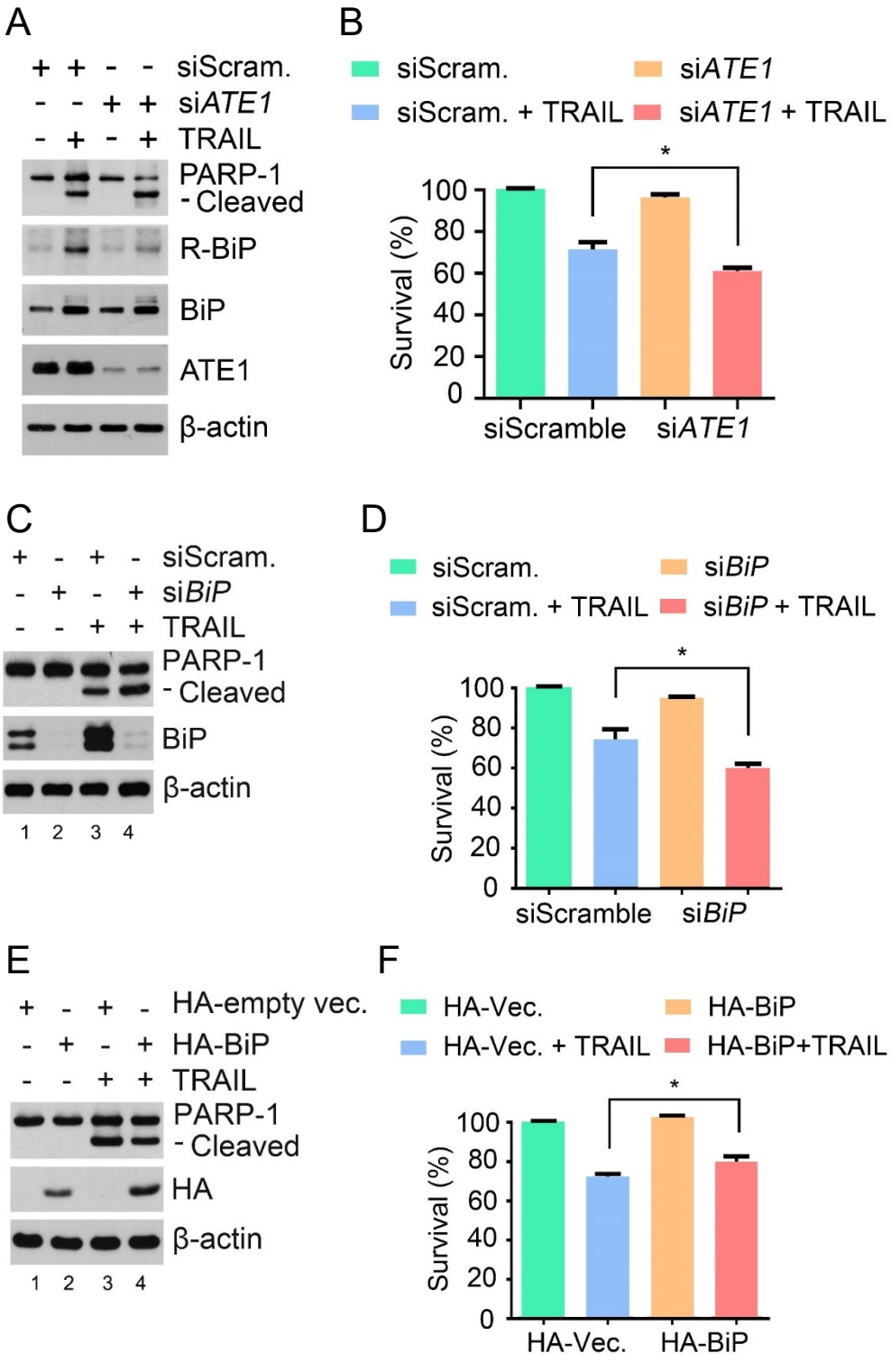
A
+ + - - siScram.
- - + + siATE1
- + - + TRAIL
PARP-1
- Cleaved
R-BiP
BiP
ATE1
β-actin
B
siScram.
siATE1
siScram. + TRAIL
siATE1 + TRAIL
Survival (%)
100
80
60
40
20
0
*
siScramble
siATE1
C
+ - + - siScram.
- + - + siBiP
- - + + TRAIL
PARP-1
- Cleaved
BiP
β-actin
1 2 3 4
D
siScram.
siBiP
siScram. + TRAIL
siBiP + TRAIL
Survival (%)
100
80
60
40
20
0
*
siScramble
siBiP
E
+ - + - HA-empty vec.
- + - + HA-BiP
- - + + TRAIL
PARP-1
- Cleaved
HA
β-actin
1 2 3 4
F
HA-Vec.
HA-BiP
HA-Vec. + TRAIL
HA-BiP+TRAIL
Survival (%)
100
80
60
40
20
0
*
HA-Vec.
HA-BiP

Figure 36. Hypothetical models for the role of DJ-1 in autophagic protein quality control. (A) In this model, TRAIL leads mitochondrial dysfunction and oxidative stress according to the excessive generation of ROS. This phenomenon induces the production of misfolded proteins in cytosol which are not able to be degraded by the UPS, canonical mechanism for protein quality control (Step 1). In response to the stress, cells initiates autophagic protein quality control with N-terminal arginylation of BiP which translocated from endoplasmic reticulum (Step 2). Meanwhile, DJ-1 recognizes the excessive ROS in cytosol and is oxidized under the condition that cells are engaged in (Step 3). The oxidized DJ-1 interacts with Nt-arginylated BiP and functions as if a cofactor or co-chaperone for BiP and through the interaction, the interaction between oxidized DJ-1 and Nt-arginylated BiP mediates the binding affinity of Ub-tagged misfolded protein clients (Step 4) and enhances the ability to activate p62 by their complex (Step 5). The previous report has reported that p62 is activated by stress and during the activation, the arginine exposed in N-terminus of R-BiP binds to ZZ domain of p62 and stimulates conformational change of p62. Through the change of the structure of p62, oligomerzation domain (PB1) and LC3 interacting region (LIR) of p62 are exposed (Step 6). As a result of allosteric change of p62, PB1 mediated self-oligomerization forms aggregation and condensation of Ub-conjugated misfolded cargo proteins that have been recruited during such mechanism (Step 7). In addition to cargo collection, LIR of p62 facilitates the interaction

between p62 aggregates and LC3 which is embedded in autophagic membrane (Step 8) and targeting misfolded proteins to lysosomal degradation. In this R-BiP-p62 circuit, DJ-1 functions as a co-factor or a co-chaperone to R-BiP and it may mediate cargo condensation and further modulates autophagic proteolysis under TRAIL induced oxidative stress.

(B) For the further model for DJ-1, DJ-1 is oxidized by oxidative stress in cytosol. Almost simultaneously, Keap1 is also oxidized by oxidative stress with similar mechanism with DJ-1, and through the oxidation on Keap1, binding affinity to p62 has been increased. In addition to oxidations of these proteins, p62 is phosphorylated on its S349 located in Keap1 interaction region, and the phosphorylation is affected by the concentration of cytosolic ROS; all the sequences lead the targeting Keap1 to autophagic degradation. Upon the mechanism, DJ-1 has a potential to modulate the targeting of autophagic substrates.

A

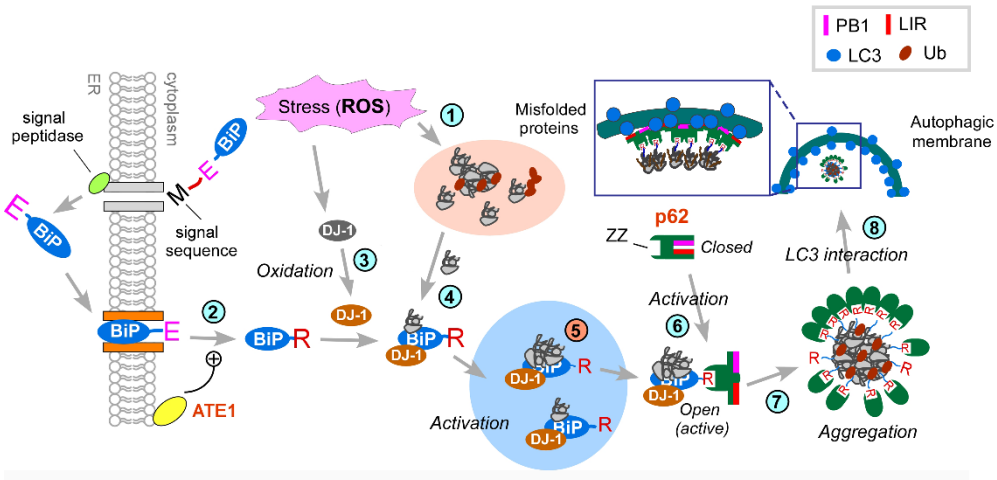
PB1
LIR
LC3
Ub
ER
cytoplasm
signal peptidase
signal sequence
Stress (ROS)
Misfolded proteins
Autophagic membrane
BiP
DJ-1
Oxidation
ATE1
p62
ZZ
Closed
LC3 interaction
Activation
Open (active)
Aggregation

B

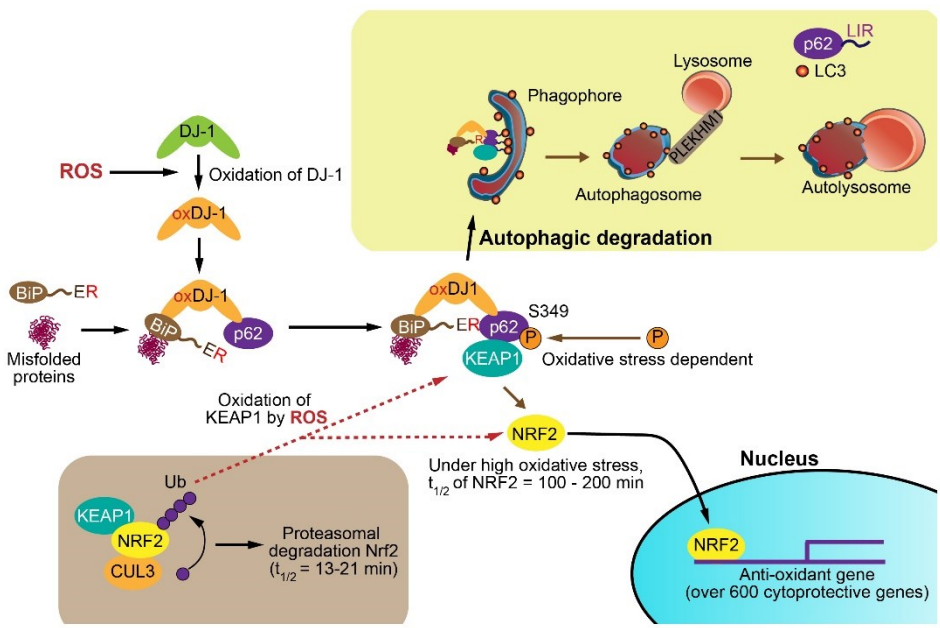
ROS
DJ-1
Oxidation of DJ-1
oxDJ-1
BiP
ER
p62
Misfolded proteins
Lysosome
LIR
LC3
Phagophore
Autophagosome
Autolysosome
PLEKHM1
Autophagic degradation
S349
KEAP1
Oxidative stress dependent
Oxidation of KEAP1 by ROS
NRF2
Under high oxidative stress, t1/2 of NRF2 = 100 - 200 min
Nucleus
Ub
CUL3
Proteasomal degradation Nrf2 (t1/2 = 13-21 min)
Anti-oxidant gene (over 600 cytoprotective genes)

Table 1. The proteins identified in the mass spectrometric analysis using DJ-1 as a bait.

Identified proteins	Number of matched peptide
Hsc70	21
Hsp90 (90 kDa)	18
BiP (78 kDa)	11
E3 ubiquitin-protein ligase TRIM21 (52 kDa)	8
Hsp70 (70 kDa)	6
40S ribosomal protein S3 (27 kDa)	8
eIF4B (70 kDa)	14
14-3-3 protein zeta/delta (27 kDa)	2
Guanine nucleotide-binding protein subunit beta-2-like 1 (70 kDa)	5
Peroxiredoxin-6 (25 kDa)	5

Discussion

Selective autophagy is a cellular mechanism that resolves cytotoxic substances which have been accumulated during cellular stress (Fimia, Kroemer, & Piacentini, 2013; Xie & Klionsky, 2007; Zaffagnini & Martens, 2016). Autophagic cargos are selectively chosen by specific autophagy adaptors and receptors such as BiP or p62, constituting autophagosome and delivered to lysosome for lysosomal degradation (Cha-Molstad et al., 2015; Cha-Molstad et al., 2017; Ji & Kwon, 2017). The key point of the mechanism is how cells keenly recognize the several different types of stresses encountered from their specific sensors, and, after sensing the stress properly (Figure 3 and 4), it is important that cells need to induce the autophagy when it is required.

In this study, I found another important function of peroxiredoxin-like protein, DJ-1 (Andres-Mateos et al., 2007; McCoy & Cookson, 2011), when cells are undergoing oxidative stress. DJ-1 has been known as anti-oxidative responses to mitochondrial ROS (Andres-Mateos et al., 2007; Girotto et al., 2012; Taira et al., 2004). Also may of studies reported that DJ-1 participates in many important mechanisms in cells, which includes cell proliferation, differentiation, transcriptional regulation, oxidative stress protection, and mitochondrial function maintenance (Hayashi et al., 2009; Kim et al., 2012; Lev et al., 2009; Martinat et al., 2004; Wang et al., 2016; Won et al., 2013). To the date, molecular mechanisms underlying these functions of DJ-1 still remain unclear, or studies limitedly was focused on the activity absorbing the excessive oxygen (Kinumi et al., 2004; Mitsumoto et al., 2001; Taira et al., 2004), or the transcription factor for activating oxidative stress related genes (Clements, McNally, Conti, Mak, &

Ting, 2006), as a matter fact, DJ-1 is modulating autophagic proteolysis which is processing protein aggregates generated by TRAIL induced oxidative stress (Figure 36A).

Upon TRAIL treatment, ER residing molecular chaperone BiP translocates to cytoplasm and is arginylated by ATE1 R-transferase (Figure 12A and 12B). Accumulated R-BiP binds to DJ-1 and the interaction of R-BiP and DJ-1 facilitates delivery of R-BiP to autophagosome with baring cargos on R-BiP. (Figures 13, 19, and 24). Through the binding with BiP, DJ-1 is seemingly having an indirect interaction with p62; in addition, as BiP belongs to Hsp70 family and their reactions of these family proteins is modulated by co-chaperones (Figure 5), I can propose that DJ-1 also can be function as a stress specific modulator for the cargo collection of arginylated BiP and targeting to autophagosome.

DJ-1 is an atypical peroxiredoxin-like protein baring the oxidation its three cysteines (Andres-Mateos et al., 2007; Wilson, 2011) and it has been known as a reservoir for excessive ROS in cells (Ren et al., 2011; Saito, 2014) However, in this study, I have found that the oxidation is rather important because of the regulation on the interaction among the R-BiP, p62 and DJ-1 itself. The result of oxidation assay shows that the impairment of oxidation on Cys106 down-regulated bindings of three components and it is indeed meaningful for understanding the role and physiological aspect of DJ-1 during oxidative stress (Figure 6). But, to understand the function of DJ-1 in cells more clear, it still is needed to perform for further experiments which are to be examined whether to suppress the influence of deficiency of DJ-1 by recombinant DJ-1 proteins.

Considering that DJ-1 has a role in puncta formation of R-BiP and p62 during oxidative stress, it has been shown that DJ-1 may form oligomer itself (Figures 21) as well as p62; thereby, it is giving a clue that DJ-1 can be functioning as a seed during R-BiP and p62 interaction, and it results a hiding of DJ-1 into the complex, which is the reason of poorly detection of DJ-1 puncta in immunostaining analyses. Even it is hardly detected in such way of the experiment, it still can be the evidence of modulation for autophagy.

During the experiment focusing on the function of DJ-1, p62 and R-BiP puncta was decreased when DJ-1 was knock down (Figure 16). But the total level of LC3-II in cells has not been decreased while autophagic was pharmaceutically blocked by bafilomycin A1 (Figure 23B). Correlating the result of immunoblotting assay of LC3, WIPI2 puncta which indicate the formation of phagophores, precursors of autophagosomes, also was not decreased during autophagy blockage, and the aspect can be considered that total number of phagophores and LC3-II embedded phagophores were not affected by deficiency of DJ-1 and only the number of autophagic puncta were concerned by DJ-1 (Figures 24). Thereby, DJ-1 is engaged in constituting autophagic puncta formation and cargo targeting to autophagosome, which is different from autophagosome biogenesis, the generation of phagophore and autophagosome structures.

Intriguingly, Keap1 Nrf2 one of axis of managing oxidative stress and it regulates the metabolic fate of Keap1 that mainly degraded by autophagy when cells are undergone the oxidative stress (Ichimura et al., 2013; Komatsu et al., 2010; Rojo de la Vega, Dodson, Chapman, & Zhang, 2016). However, Keap1^{+} puncta were down-regulated during TRAIL treatment (Figure 26), and similar aspect has been shown in tBHP treatment to DJ-1 deficient cells (Figure 27). These results indicate that DJ-1

influences on not only on the cargo delivery for misfolded proteins or unfolded protein needed to be resolved but it regulates the protein that along with one of the mechanism in response to oxidative stress; therefore, DJ-1 has rather important role in cells as well as it has been implicated by the abundancy in various cells. Moreover, in other recent studies, in the Keap1 Nrf2 mechanism, p62 phosphorylation on its S349 is important factor for the activation of p62, and the site of phosphorylation is in the middle of Keap1 recognition site of p62 (Ichimura et al., 2013; Rojo de la Vega et al., 2016). The S349 phosphorylation has been considered as a noteworthy factor for oxidative stress sensing (Figure 36B), therefore, it could be a clue for applying this R-BiP/p62/DJ-1 circuit for solving the other side of aspect indwelled (Ichimura et al., 2013; Watanabe, Tsujimura, Taguchi, & Tanaka, 2017).

TRAIL has been broadly used for specifically targeting cancers by recognizing cell surface-associated pro-apoptotic receptors (S. Wang & El-Deiry, 2003; Ziauddin et al., 2010) and triggering impairment in the function of mitochondrial enzymes. A few studies reported the effect of TRAIL in the cell (J. Cao, Lou, Ying, & Yang, 2015; Inoue & Suzuki-Karasaki, 2013; Suzuki-Karasaki et al., 2014), but in this study, I elucidated the correlation of mitochondria derived oxidative stress and cytoplasmic oxidative stress by comparing the effect of DJ-1 and finding that TRAIL caused the dissociation of ER lumenal BiP from PERK and IRE1α, two sensors of the UPR (Figure 30) and N-terminal arginylation which have not been comprehended. Importantly, DJ-1 has a cyto-protective role in stresses caused by apoptotic cell death, ER and mitochondrial dysfunctions, but when it comes to the targeting cancer cells, DJ-1 may hinder the cytotoxic effect of anti-cancer reagent that needs to work on killing the cancer cells. It

should be determined more about how well the activity of DJ-1 and R-BiP take a place in cyto-protection against stresses.

The N-end rule was considered as a way of protein degradation system for tightly controlling the half-life of certain protein by recognition of N-terminal residue of protein. Interestingly, according to resent studies, N-recognin includes not only E3 ligases but an autophagic receptor p62 may be belonged to the recognin, and identify N-terminal arginylated BiP during cellular stress; thereby, I could say that the N-end rule has further biological meaning on its mechanism and assume that p62 and R-BiP is not only the case of comprehensive crosstalk for those two different mechanisms. In addition, DJ-1 has been found as a co-factor for the modulation of the activity of R-BiP as well as p62 under oxidative stress; therefore, there might be some other co-factors that involving in response of various cellular stress encountered. Given that the there is a co-factor that regulates the interaction between N-recognins and N-degrons in biological processes, the research was mainly conducted in human colon tumor cells and cancer specific ligand; however, there is still other possibility that the interaction of N-recognins and N-degrons is not only related to stress response mechanism but it may also participate in other biological processes within the different cellular environment or during the various stages of the development of embryos or other human organs; therefore, perhaps, the research may be expend to other systems in development in response for stress or other stimuli that cells encounter.

Reference

Altman, B. J., & Rathmell, J. C. (2012). Metabolic stress in autophagy and cell death pathways. *Cold Spring Harb Perspect Biol, 4*(9), a008763. doi:10.1101/cshperspect.a008763

Andres-Mateos, E., Perier, C., Zhang, L., Blanchard-Fillion, B., Greco, T. M., Thomas, B., . . . Dawson, V. L. (2007). DJ-1 gene deletion reveals that DJ-1 is an atypical peroxiredoxin-like peroxidase. *Proc Natl Acad Sci U S A, 104*(37), 14807-14812. doi:10.1073/pnas.0703219104

Ardail, D., Popa, I., Bodennec, J., Louisot, P., Schmitt, D., & Portoukalian, J. (2003). The mitochondria-associated endoplasmic-reticulum subcompartment (MAM fraction) of rat liver contains highly active sphingolipid-specific glycosyltransferases. *Biochem J, 371*(Pt 3), 1013-1019. doi:10.1042/BJ20021834

Ariga, H., Takahashi-Niki, K., Kato, I., Maita, H., Niki, T., & Iguchi-Ariga, S. M. (2013). Neuroprotective function of DJ-1 in Parkinson's disease. *Oxid Med Cell Longev, 2013*, 683920. doi:10.1155/2013/683920

Balchin, D., Hayer-Hartl, M., & Hartl, F. U. (2016). In vivo aspects of protein folding and quality control. *Science, 353*(6294), aac4354. doi:10.1126/science.aac4354

Bonifati, V., Rizzu, P., Squitieri, F., Krieger, E., Vanacore, N., van Swieten, J. C., . . . Heutink, P. (2003). DJ-1(PARK7), a novel gene for autosomal recessive, early onset parkinsonism. *Neurol Sci, 24*(3), 159-160. doi:10.1007/s10072-003-0108-0

Broadley, S. A., & Hartl, F. U. (2009). The role of molecular chaperones in human

misfolding diseases. *FEBS Lett, 583*(16), 2647-2653. doi:10.1016/j.febslet.2009.04.029

Buchberger, A., Bukau, B., & Sommer, T. (2010). Protein quality control in the cytosol and the endoplasmic reticulum: brothers in arms. *Mol Cell, 40*(2), 238-252. doi:10.1016/j.molcel.2010.10.001

Bukau, B., Weissman, J., & Horwich, A. (2006). Molecular chaperones and protein quality control. *Cell, 125*(3), 443-451. doi:10.1016/j.cell.2006.04.014

Canet-Aviles, R. M., Wilson, M. A., Miller, D. W., Ahmad, R., McLendon, C., Bandyopadhyay, S., . . . Cookson, M. R. (2004). The Parkinson's disease protein DJ-1 is neuroprotective due to cysteine-sulfinic acid-driven mitochondrial localization. *Proc Natl Acad Sci U S A, 101*(24), 9103-9108. doi:10.1073/pnas.0402959101

Cao, J., Lou, S., Ying, M., & Yang, B. (2015). DJ-1 as a human oncogene and potential therapeutic target. *Biochem Pharmacol, 93*(3), 241-250. doi:10.1016/j.bcp.2014.11.012

Cao, S. S., & Kaufman, R. J. (2014). Endoplasmic reticulum stress and oxidative stress in cell fate decision and human disease. *Antioxid Redox Signal, 21*(3), 396-413. doi:10.1089/ars.2014.5851

Carrara, M., Prischi, F., Nowak, P. R., Kopp, M. C., & Ali, M. M. (2015). Noncanonical binding of BiP ATPase domain to Ire1 and Perk is dissociated by unfolded protein CH1 to initiate ER stress signaling. *Elife, 4*. doi:10.7554/eLife.03522

Cha-Molstad, H., Lee, S. H., Kim, J. G., Sung, K. W., Hwang, J., Shim, S. M., . . . Kwon, Y. T. (2018). Regulation of autophagic proteolysis by the N-recognin

SQSTM1/p62 of the N-end rule pathway. *Autophagy, 14*(2), 359-361. doi:10.1080/15548627.2017.1415190

Cha-Molstad, H., Sung, K. S., Hwang, J., Kim, K. A., Yu, J. E., Yoo, Y. D., . . . Kwon, Y. T. (2015). Amino-terminal arginylation targets endoplasmic reticulum chaperone BiP for autophagy through p62 binding. *Nat Cell Biol, 17*(7), 917-929. doi:10.1038/ncb3177

Cha-Molstad, H., Yu, J. E., Feng, Z., Lee, S. H., Kim, J. G., Yang, P., . . . Kim, B. Y. (2017). p62/SQSTM1/Sequestosome-1 is an N-recognin of the N-end rule pathway which modulates autophagosome biogenesis. *Nat Commun, 8*(1), 102. doi:10.1038/s41467-017-00085-7

Chance, B., Boveris, A., Oschino, N., & Loschen, G. (1973). The nature of the catalase intermediate in its biological function. *Oxidases and Related Redox Systems*, 350-353.

Chen, B., Retzlaff, M., Roos, T., & Frydman, J. (2011). Cellular strategies of protein quality control. *Cold Spring Harb Perspect Biol, 3*(8), a004374. doi:10.1101/cshperspect.a004374

Chen, Y., Azad, M. B., & Gibson, S. B. (2009). Superoxide is the major reactive oxygen species regulating autophagy. *Cell Death Differ, 16*(7), 1040-1052. doi:10.1038/cdd.2009.49

Chien, V., Aitken, J. F., Zhang, S., Buchanan, C. M., Hickey, A., Brittain, T., . . . Loomes, K. M. (2010). The chaperone proteins HSP70, HSP40/DnaJ and GRP78/BiP suppress misfolding and formation of beta-sheet-containing aggregates by human amylin: a potential role for defective chaperone biology in Type 2 diabetes. *Biochem*

J, 432(1), 113-121. doi:10.1042/BJ20100434

Choi, J., Sullards, M. C., Olzmann, J. A., Rees, H. D., Weintraub, S. T., Bostwick, D. E., . . . Li, L. (2006). Oxidative damage of DJ-1 is linked to sporadic Parkinson and Alzheimer diseases. *J Biol Chem, 281*(16), 10816-10824. doi:10.1074/jbc.M509079200

Ciechanover, A., & Kwon, Y. T. (2015). Degradation of misfolded proteins in neurodegenerative diseases: therapeutic targets and strategies. *Exp Mol Med, 47*, e147. doi:10.1038/emm.2014.117

Ciechanover, A., & Kwon, Y. T. (2017). Protein Quality Control by Molecular Chaperones in Neurodegeneration. *Front Neurosci, 11*, 185. doi:10.3389/fnins.2017.00185

Clements, C. M., McNally, R. S., Conti, B. J., Mak, T. W., & Ting, J. P. (2006). DJ-1, a cancer- and Parkinson's disease-associated protein, stabilizes the antioxidant transcriptional master regulator Nrf2. *Proc Natl Acad Sci U S A, 103*(41), 15091-15096. doi:10.1073/pnas.0607260103

Day, A. M., Brown, J. D., Taylor, S. R., Rand, J. D., Morgan, B. A., & Veal, E. A. (2012). Inactivation of a peroxiredoxin by hydrogen peroxide is critical for thioredoxin-mediated repair of oxidized proteins and cell survival. *Mol Cell, 45*(3), 398-408. doi:10.1016/j.molcel.2011.11.027

Deshmukh, P., Unni, S., Krishnappa, G., & Padmanabhan, B. (2017). The Keap1-Nrf2 pathway: promising therapeutic target to counteract ROS-mediated damage in cancers and neurodegenerative diseases. *Biophys Rev, 9*(1), 41-56. doi:10.1007/s12551-016-0244-4

Dickinson, B. C., Srikun, D., & Chang, C. J. (2010). Mitochondrial-targeted fluorescent probes for reactive oxygen species. *Curr Opin Chem Biol, 14*(1), 50-56. doi:10.1016/j.cbpa.2009.10.014

Dikic, I. (2017). Proteasomal and Autophagic Degradation Systems. *Annu Rev Biochem, 86*, 193-224. doi:10.1146/annurev-biochem-061516-044908

Dikic, I., & Elazar, Z. (2018). Mechanism and medical implications of mammalian autophagy. *Nat Rev Mol Cell Biol, 19*(6), 349-364. doi:10.1038/s41580-018-0003-4

Dooley, H. C., Razi, M., Polson, H. E., Girardin, S. E., Wilson, M. I., & Tooze, S. A. (2014). WIPI2 links LC3 conjugation with PI3P, autophagosome formation, and pathogen clearance by recruiting Atg12-5-16L1. *Mol Cell, 55*(2), 238-252. doi:10.1016/j.molcel.2014.05.021

Duncan, E. J., Cheetham, M. E., Chapple, J. P., & van der Spuy, J. (2015). The role of HSP70 and its co-chaperones in protein misfolding, aggregation and disease. *Subcell Biochem, 78*, 243-273. doi:10.1007/978-3-319-11731-7_12

Eruslanov, E., & Kusmartsev, S. (2010). Identification of ROS using oxidized DCFDA and flow-cytometry. *Methods Mol Biol, 594*, 57-72. doi:10.1007/978-1-60761-411-1_4

Filomeni, G., De Zio, D., & Cecconi, F. (2015). Oxidative stress and autophagy: the clash between damage and metabolic needs. *Cell Death Differ, 22*(3), 377-388. doi:10.1038/cdd.2014.150

Fimia, G. M., Kroemer, G., & Piacentini, M. (2013). Molecular mechanisms of selective autophagy. *Cell Death Differ, 20*(1), 1-2. doi:10.1038/cdd.2012.97

Fu, K., Ren, H., Wang, Y., Fei, E., Wang, H., & Wang, G. (2012). DJ-1 inhibits

TRAIL-induced apoptosis by blocking pro-caspase-8 recruitment to FADD. *Oncogene, 31*(10), 1311-1322. doi:10.1038/onc.2011.315

Fujimoto, M., & Hayashi, T. (2011). New insights into the role of mitochondria-associated endoplasmic reticulum membrane. *Int Rev Cell Mol Biol, 292*, 73-117. doi:10.1016/B978-0-12-386033-0.00002-5

Gething, M. J. (1999). Role and regulation of the ER chaperone BiP. *Semin Cell Dev Biol, 10*(5), 465-472. doi:10.1006/scdb.1999.0318

Giaime, E., Yamaguchi, H., Gautier, C. A., Kitada, T., & Shen, J. (2012). Loss of DJ-1 does not affect mitochondrial respiration but increases ROS production and mitochondrial permeability transition pore opening. *PLoS One, 7*(7), e40501. doi:10.1371/journal.pone.0040501

Gibbs, D. J., Bacardit, J., Bachmair, A., & Holdsworth, M. J. (2014). The eukaryotic N-end rule pathway: conserved mechanisms and diverse functions. *Trends Cell Biol, 24*(10), 603-611. doi:10.1016/j.tcb.2014.05.001

Gibson, S. B. (2013). Investigating the role of reactive oxygen species in regulating autophagy. *Methods Enzymol, 528*, 217-235. doi:10.1016/B978-0-12-405881-1.00013-6

Gonzalez-Gronow, M., Selim, M. A., Papalas, J., & Pizzo, S. V. (2009). GRP78: a multifunctional receptor on the cell surface. *Antioxid Redox Signal, 11*(9), 2299-2306. doi:10.1089/ARS.2009.2568

Green, D. R., & Levine, B. (2014). To be or not to be? How selective autophagy and cell death govern cell fate. *Cell, 157*(1), 65-75. doi:10.1016/j.cell.2014.02.049

Guicciardi, M. E., & Gores, G. J. (2009). Life and death by death receptors. *FASEB J,*

23(6), 1625-1637. doi:10.1096/fj.08-111005

Guzman, J. N., Sanchez-Padilla, J., Wokosin, D., Kondapalli, J., Ilijic, E., Schumacker, P. T., & Surmeier, D. J. (2010). Oxidant stress evoked by pacemaking in dopaminergic neurons is attenuated by DJ-1. *Nature, 468*(7324), 696-700. doi:10.1038/nature09536

Hayashi, T., Ishimori, C., Takahashi-Niki, K., Taira, T., Kim, Y. C., Maita, H., . . . Iguchi-Ariga, S. M. (2009). DJ-1 binds to mitochondrial complex I and maintains its activity. *Biochem Biophys Res Commun, 390*(3), 667-672. doi:10.1016/j.bbrc.2009.10.025

Hu, H., Jiang, C., Schuster, T., Li, G. X., Daniel, P. T., & Lu, J. (2006). Inorganic selenium sensitizes prostate cancer cells to TRAIL-induced apoptosis through superoxide/p53/Bax-mediated activation of mitochondrial pathway. *Mol Cancer Ther, 5*(7), 1873-1882. doi:10.1158/1535-7163.MCT-06-0063

Huber, L. A., & Teis, D. (2016). Lysosomal signaling in control of degradation pathways. *Curr Opin Cell Biol, 39*, 8-14. doi:10.1016/j.ceb.2016.01.006

Ichimura, Y., Waguri, S., Sou, Y. S., Kageyama, S., Hasegawa, J., Ishimura, R., . . . Komatsu, M. (2013). Phosphorylation of p62 activates the Keap1-Nrf2 pathway during selective autophagy. *Mol Cell, 51*(5), 618-631. doi:10.1016/j.molcel.2013.08.003

Im, J. Y., Lee, K. W., Junn, E., & Mouradian, M. M. (2010). DJ-1 protects against oxidative damage by regulating the thioredoxin/ASK1 complex. *Neurosci Res, 67*(3), 203-208. doi:10.1016/j.neures.2010.04.002

Inoue, T., & Suzuki-Karasaki, Y. (2013). Mitochondrial superoxide mediates

mitochondrial and endoplasmic reticulum dysfunctions in TRAIL-induced apoptosis in Jurkat cells. *Free Radic Biol Med, 61*, 273-284. doi:10.1016/j.freeradbiomed.2013.04.020

Ishdorj, G., Li, L., & Gibson, S. B. (2012). Regulation of autophagy in hematological malignancies: role of reactive oxygen species. *Leuk Lymphoma, 53*(1), 26-33. doi:10.3109/10428194.2011.604752

Ji, C. H., & Kwon, Y. T. (2017). Crosstalk and Interplay between the Ubiquitin-Proteasome System and Autophagy. *Mol Cells, 40*(7), 441-449. doi:10.14348/molcells.2017.0115

Johnstone, R. W., Frew, A. J., & Smyth, M. J. (2008). The TRAIL apoptotic pathway in cancer onset, progression and therapy. *Nat Rev Cancer, 8*(10), 782-798. doi:10.1038/nrc2465

Kahle, P. J., Waak, J., & Gasser, T. (2009). DJ-1 and prevention of oxidative stress in Parkinson's disease and other age-related disorders. *Free Radic Biol Med, 47*(10), 1354-1361. doi:10.1016/j.freeradbiomed.2009.08.003

Katsuragi, Y., Ichimura, Y., & Komatsu, M. (2015). p62/SQSTM1 functions as a signaling hub and an autophagy adaptor. *FEBS J, 282*(24), 4672-4678. doi:10.1111/febs.13540

Kiffin, R., Bandyopadhyay, U., & Cuervo, A. M. (2006). Oxidative stress and autophagy. *Antioxid Redox Signal, 8*(1-2), 152-162. doi:10.1089/ars.2006.8.152

Kim, R. H., Smith, P. D., Aleyasin, H., Hayley, S., Mount, M. P., Pownall, S., . . . Mak, T. W. (2005). Hypersensitivity of DJ-1-deficient mice to 1-methyl-4-phenyl-1,2,3,6-tetrahydropyrindine (MPTP) and oxidative stress. *Proc Natl Acad Sci U S A,*

102(14), 5215-5220. doi:10.1073/pnas.0501282102

Kim, S. T., Tasaki, T., Zakrzewska, A., Yoo, Y. D., Sa Sung, K., Kim, S. H., . . . Kwon, Y. T. (2013). The N-end rule proteolytic system in autophagy. *Autophagy, 9*(7), 1100-1103. doi:10.4161/auto.24643

Kinumi, T., Kimata, J., Taira, T., Ariga, H., & Niki, E. (2004). Cysteine-106 of DJ-1 is the most sensitive cysteine residue to hydrogen peroxide-mediated oxidation in vivo in human umbilical vein endothelial cells. *Biochem Biophys Res Commun, 317*(3), 722-728. doi:10.1016/j.bbrc.2004.03.110

Kolisek, M., Montezano, A. C., Sponder, G., Anagnostopoulou, A., Vormann, J., Touyz, R. M., & Aschenbach, J. R. (2015). PARK7/DJ-1 dysregulation by oxidative stress leads to magnesium deficiency: implications in degenerative and chronic diseases. *Clin Sci (Lond), 129*(12), 1143-1150. doi:10.1042/CS20150355

Komatsu, M., Kurokawa, H., Waguri, S., Taguchi, K., Kobayashi, A., Ichimura, Y., . . . Yamamoto, M. (2010). The selective autophagy substrate p62 activates the stress responsive transcription factor Nrf2 through inactivation of Keap1. *Nat Cell Biol, 12*(3), 213-223. doi:10.1038/ncb2021

Kriegenburg, F., Ellgaard, L., & Hartmann-Petersen, R. (2012). Molecular chaperones in targeting misfolded proteins for ubiquitin-dependent degradation. *FEBS J, 279*(4), 532-542. doi:10.1111/j.1742-4658.2011.08456.x

Kuang, A. A., Diehl, G. E., Zhang, J., & Winoto, A. (2000). FADD is required for DR4- and DR5-mediated apoptosis: lack of trail-induced apoptosis in FADD-deficient mouse embryonic fibroblasts. *J Biol Chem, 275*(33), 25065-25068. doi:10.1074/jbc.C000284200

Kwon, Y. T., Reiss, Y., Fried, V. A., Hershko, A., Yoon, J. K., Gonda, D. K., . . . Varshavsky, A. (1998). The mouse and human genes encoding the recognition component of the N-end rule pathway. *Proc Natl Acad Sci U S A, 95*(14), 7898-7903.

Lee, A. S. (2005). The ER chaperone and signaling regulator GRP78/BiP as a monitor of endoplasmic reticulum stress. *Methods, 35*(4), 373-381. doi:10.1016/j.ymeth.2004.10.010

Lee, D. H., Sung, K. S., Bartlett, D. L., Kwon, Y. T., & Lee, Y. J. (2015). HSP90 inhibitor NVP-AUY922 enhances TRAIL-induced apoptosis by suppressing the JAK2-STAT3-Mcl-1 signal transduction pathway in colorectal cancer cells. *Cell Signal, 27*(2), 293-305. doi:10.1016/j.cellsig.2014.11.013

Lee, D. H., Sung, K. S., Guo, Z. S., Kwon, W. T., Bartlett, D. L., Oh, S. C., . . . Lee, Y. J. (2016). TRAIL-Induced Caspase Activation Is a Prerequisite for Activation of the Endoplasmic Reticulum Stress-Induced Signal Transduction Pathways. *J Cell Biochem, 117*(5), 1078-1091. doi:10.1002/jcb.25289

Lev, N., Barhum, Y., Pilosof, N. S., Ickowicz, D., Cohen, H. Y., Melamed, E., & Offen, D. (2013). DJ-1 protects against dopamine toxicity: implications for Parkinson's disease and aging. *J Gerontol A Biol Sci Med Sci, 68*(3), 215-225. doi:10.1093/gerona/gls147

Lev, N., Ickowicz, D., Barhum, Y., Lev, S., Melamed, E., & Offen, D. (2009). DJ-1 protects against dopamine toxicity. *J Neural Transm (Vienna), 116*(2), 151-160. doi:10.1007/s00702-008-0134-4

Li, H. M., Niki, T., Taira, T., Iguchi-Ariga, S. M., & Ariga, H. (2005). Association of DJ-1 with chaperones and enhanced association and colocalization with

mitochondrial Hsp70 by oxidative stress. *Free Radic Res, 39*(10), 1091-1099. doi:10.1080/10715760500260348

Li, J., & Lee, A. S. (2006). Stress induction of GRP78/BiP and its role in cancer. *Curr Mol Med, 6*(1), 45-54.

Lim, J., Lachenmayer, M. L., Wu, S., Liu, W., Kundu, M., Wang, R., . . . Yue, Z. (2015). Proteotoxic stress induces phosphorylation of p62/SQSTM1 by ULK1 to regulate selective autophagic clearance of protein aggregates. *PLoS Genet, 11*(2), e1004987. doi:10.1371/journal.pgen.1004987

Ling, L. U., Tan, K. B., Lin, H., & Chiu, G. N. (2011). The role of reactive oxygen species and autophagy in safingol-induced cell death. *Cell Death Dis, 2*, e129. doi:10.1038/cddis.2011.12

Lodhi, I. J., & Semenkovich, C. F. (2014). Peroxisomes: a nexus for lipid metabolism and cellular signaling. *Cell Metab, 19*(3), 380-392. doi:10.1016/j.cmet.2014.01.002

Marwaha, R., Arya, S. B., Jagga, D., Kaur, H., Tuli, A., & Sharma, M. (2017). The Rab7 effector PLEKHM1 binds Arl8b to promote cargo traffic to lysosomes. *J Cell Biol, 216*(4), 1051-1070. doi:10.1083/jcb.201607085

McCoy, M. K., & Cookson, M. R. (2011). DJ-1 regulation of mitochondrial function and autophagy through oxidative stress. *Autophagy, 7*(5), 531-532.

McEwan, D. G., Popovic, D., Gubas, A., Terawaki, S., Suzuki, H., Stadel, D., . . . Dikic, I. (2015). PLEKHM1 regulates autophagosome-lysosome fusion through HOPS complex and LC3/GABARAP proteins. *Mol Cell, 57*(1), 39-54. doi:10.1016/j.molcel.2014.11.006

Meulener, M. C., Xu, K., Thomson, L., Ischiropoulos, H., & Bonini, N. M. (2006).

Mutational analysis of DJ-1 in Drosophila implicates functional inactivation by oxidative damage and aging. *Proc Natl Acad Sci U S A, 103*(33), 12517-12522. doi:10.1073/pnas.0601891103

Mitsumoto, A., Nakagawa, Y., Takeuchi, A., Okawa, K., Iwamatsu, A., & Takanezawa, Y. (2001). Oxidized forms of peroxiredoxins and DJ-1 on two-dimensional gels increased in response to sublethal levels of paraquat. *Free Radic Res, 35*(3), 301-310.

Muller, P., Ruckova, E., Halada, P., Coates, P. J., Hrstka, R., Lane, D. P., & Vojtesek, B. (2013). C-terminal phosphorylation of Hsp70 and Hsp90 regulates alternate binding to co-chaperones CHIP and HOP to determine cellular protein folding/degradation balances. *Oncogene, 32*(25), 3101-3110. doi:10.1038/onc.2012.314

Murphy, M. P. (2009). How mitochondria produce reactive oxygen species. *Biochem J, 417*(1), 1-13. doi:10.1042/BJ20081386

Nakatani, Y., & Ogryzko, V. (2003). Immunoaffinity purification of mammalian protein complexes. *Methods Enzymol, 370*, 430-444. doi:10.1016/S0076-6879(03)70037-8

Patella, F., Neilson, L. J., Athineos, D., Erami, Z., Anderson, K. I., Blyth, K., . . . Zanivan, S. (2016). In-Depth Proteomics Identifies a Role for Autophagy in Controlling Reactive Oxygen Species Mediated Endothelial Permeability. *J Proteome Res, 15*(7), 2187-2197. doi:10.1021/acs.jproteome.6b00166

Perelman, A., Wachtel, C., Cohen, M., Haupt, S., Shapiro, H., & Tzur, A. (2012). JC-1: alternative excitation wavelengths facilitate mitochondrial membrane potential

cytometry. *Cell Death Dis, 3*, e430. doi:10.1038/cddis.2012.171

Polson, H. E., de Lartigue, J., Rigden, D. J., Reedijk, M., Urbe, S., Clague, M. J., & Tooze, S. A. (2010). Mammalian Atg18 (WIPI2) localizes to omegasome-anchored phagophores and positively regulates LC3 lipidation. *Autophagy, 6*(4), 506-522. doi:10.4161/auto.6.4.11863

Ramis, M. R., Esteban, S., Miralles, A., Tan, D. X., & Reiter, R. J. (2015). Protective Effects of Melatonin and Mitochondria-targeted Antioxidants Against Oxidative Stress: A Review. *Curr Med Chem, 22*(22), 2690-2711.

Ray, P. D., Huang, B. W., & Tsuji, Y. (2012). Reactive oxygen species (ROS) homeostasis and redox regulation in cellular signaling. *Cell Signal, 24*(5), 981-990. doi:10.1016/j.cellsig.2012.01.008

Ren, H., Fu, K., Wang, D., Mu, C., & Wang, G. (2011). Oxidized DJ-1 interacts with the mitochondrial protein BCL-XL. *J Biol Chem, 286*(40), 35308-35317. doi:10.1074/jbc.M110.207134

Rojo de la Vega, M., Dodson, M., Chapman, E., & Zhang, D. D. (2016). NRF2-targeted therapeutics: New targets and modes of NRF2 regulation. *Curr Opin Toxicol, 1*, 62-70. doi:10.1016/j.cotox.2016.10.005

Rudner, J., Jendrossek, V., Lauber, K., Daniel, P. T., Wesselborg, S., & Belka, C. (2005). Type I and type II reactions in TRAIL-induced apoptosis -- results from dose-response studies. *Oncogene, 24*(1), 130-140. doi:10.1038/sj.onc.1208191

Saito, Y. (2014). Oxidized DJ-1 as a possible biomarker of Parkinson's disease. *J Clin Biochem Nutr, 54*(3), 138-144. doi:10.3164/jcbn.13-108

Saito, Y., Miyasaka, T., Hatsuta, H., Takahashi-Niki, K., Hayashi, K., Mita, Y., . . .

Noguchi, N. (2014). Immunostaining of oxidized DJ-1 in human and mouse brains. *J Neuropathol Exp Neurol, 73*(7), 714-728. doi:10.1097/NEN.0000000000000087

Scherz-Shouval, R., Shvets, E., Fass, E., Shorer, H., Gil, L., & Elazar, Z. (2007). Reactive oxygen species are essential for autophagy and specifically regulate the activity of Atg4. *EMBO J, 26*(7), 1749-1760. doi:10.1038/sj.emboj.7601623

Schneider-Brachert, W., Heigl, U., & Ehrenschwender, M. (2013). Membrane trafficking of death receptors: implications on signalling. *Int J Mol Sci, 14*(7), 14475-14503. doi:10.3390/ijms140714475

Shevchenko, A., Tomas, H., Havlis, J., Olsen, J. V., & Mann, M. (2006). In-gel digestion for mass spectrometric characterization of proteins and proteomes. *Nat Protoc, 1*(6), 2856-2860. doi:10.1038/nprot.2006.468

Shim, S. M., Choi, H. R., Sung, K. W., Lee, Y. J., Kim, S. T., Kim, D., . . . Kwon, Y. T. (2018). The endoplasmic reticulum-residing chaperone BiP is short-lived and metabolized through N-terminal arginylation. *Sci Signal, 11*(511). doi:10.1126/scisignal.aan0630

Silva, B. R., Pernomian, L., & Bendhack, L. M. (2012). Contribution of oxidative stress to endothelial dysfunction in hypertension. *Front Physiol, 3*, 441. doi:10.3389/fphys.2012.00441

Suliman, A., Lam, A., Datta, R., & Srivastava, R. K. (2001). Intracellular mechanisms of TRAIL: apoptosis through mitochondrial-dependent and -independent pathways. *Oncogene, 20*(17), 2122-2133. doi:10.1038/sj.onc.1204282

Suzuki-Karasaki, M., Ochiai, T., & Suzuki-Karasaki, Y. (2014). Crosstalk between mitochondrial ROS and depolarization in the potentiation of TRAIL-induced

apoptosis in human tumor cells. *Int J Oncol, 44*(2), 616-628. doi:10.3892/ijo.2013.2215

Suzuki, Y., Inoue, T., Murai, M., Suzuki-Karasaki, M., Ochiai, T., & Ra, C. (2012). Depolarization potentiates TRAIL-induced apoptosis in human melanoma cells: role for ATP-sensitive K+ channels and endoplasmic reticulum stress. *Int J Oncol, 41*(2), 465-475. doi:10.3892/ijo.2012.1483

Taira, T., Saito, Y., Niki, T., Iguchi-Ariga, S. M., Takahashi, K., & Ariga, H. (2004). DJ-1 has a role in antioxidative stress to prevent cell death. *EMBO Rep, 5*(2), 213-218. doi:10.1038/sj.embor.7400074

Tasaki, T., Mulder, L. C., Iwamatsu, A., Lee, M. J., Davydov, I. V., Varshavsky, A., . . . Kwon, Y. T. (2005). A family of mammalian E3 ubiquitin ligases that contain the UBR box motif and recognize N-degrons. *Mol Cell Biol, 25*(16), 7120-7136. doi:10.1128/MCB.25.16.7120-7136.2005

Thomas, K. J., McCoy, M. K., Blackinton, J., Beilina, A., van der Brug, M., Sandebring, A., . . . Cookson, M. R. (2011). DJ-1 acts in parallel to the PINK1/parkin pathway to control mitochondrial function and autophagy. *Hum Mol Genet, 20*(1), 40-50. doi:10.1093/hmg/ddq430

Tsutsui, H., Kinugawa, S., & Matsushima, S. (2011). Oxidative stress and heart failure. *Am J Physiol Heart Circ Physiol, 301*(6), H2181-2190. doi:10.1152/ajpheart.00554.2011

Varshavsky, A. (2011). The N-end rule pathway and regulation by proteolysis. *Protein Sci, 20*(8), 1298-1345. doi:10.1002/pro.666

Wadas, B., Borjigin, J., Huang, Z., Oh, J. H., Hwang, C. S., & Varshavsky, A. (2016).

Degradation of Serotonin N-Acetyltransferase, a Circadian Regulator, by the N-end Rule Pathway. *J Biol Chem, 291*(33), 17178-17196. doi:10.1074/jbc.M116.734640

Walczak, H., Degli-Esposti, M. A., Johnson, R. S., Smolak, P. J., Waugh, J. Y., Boiani, N., . . . Rauch, C. T. (1997). TRAIL-R2: a novel apoptosis-mediating receptor for TRAIL. *EMBO J, 16*(17), 5386-5397. doi:10.1093/emboj/16.17.5386

Wang, J., Lee, J., Liem, D., & Ping, P. (2017). HSPA5 Gene encoding Hsp70 chaperone BiP in the endoplasmic reticulum. *Gene, 618*, 14-23. doi:10.1016/j.gene.2017.03.005

Wang, J., Pareja, K. A., Kaiser, C. A., & Sevier, C. S. (2014). Redox signaling via the molecular chaperone BiP protects cells against endoplasmic reticulum-derived oxidative stress. *Elife, 3*, e03496. doi:10.7554/eLife.03496

Wang, S., & El-Deiry, W. S. (2003). TRAIL and apoptosis induction by TNF-family death receptors. *Oncogene, 22*(53), 8628-8633. doi:10.1038/sj.onc.1207232

Wang, X., Pattison, J. S., & Su, H. (2013). Posttranslational modification and quality control. *Circ Res, 112*(2), 367-381. doi:10.1161/CIRCRESAHA.112.268706

Wang, X., Petrie, T. G., Liu, Y., Liu, J., Fujioka, H., & Zhu, X. (2012). Parkinson's disease-associated DJ-1 mutations impair mitochondrial dynamics and cause mitochondrial dysfunction. *J Neurochem, 121*(5), 830-839. doi:10.1111/j.1471-4159.2012.07734.x

Watanabe, Y., Tsujimura, A., Taguchi, K., & Tanaka, M. (2017). HSF1 stress response pathway regulates autophagy receptor SQSTM1/p62-associated proteostasis. *Autophagy, 13*(1), 133-148. doi:10.1080/15548627.2016.1248018

Wen, X., Wu, J., Wang, F., Liu, B., Huang, C., & Wei, Y. (2013). Deconvoluting the

role of reactive oxygen species and autophagy in human diseases. *Free Radic Biol Med, 65*, 402-410. doi:10.1016/j.freeradbiomed.2013.07.013

Wiley, S. R., Schooley, K., Smolak, P. J., Din, W. S., Huang, C. P., Nicholl, J. K., . . . Smith, C. A. (1995). Identification and characterization of a new member of the TNF family that induces apoptosis. *Immunity*.

Wilson, M. A. (2011). The role of cysteine oxidation in DJ-1 function and dysfunction. *Antioxid Redox Signal, 15*(1), 111-122. doi:10.1089/ars.2010.3481

Won, K. J., Jung, S. H., Lee, C. K., Na, H. R., Lee, K. P., Lee, D. Y., . . . Kim, B. (2013). DJ-1/park7 protects against neointimal formation via the inhibition of vascular smooth muscle cell growth. *Cardiovasc Res, 97*(3), 553-561. doi:10.1093/cvr/cvs363

Wurzer, B., Zaffagnini, G., Fracchiolla, D., Turco, E., Abert, C., Romanov, J., & Martens, S. (2015). Oligomerization of p62 allows for selection of ubiquitinated cargo and isolation membrane during selective autophagy. *Elife, 4*, e08941. doi:10.7554/eLife.08941

Xie, Z., & Klionsky, D. J. (2007). Autophagosome formation: core machinery and adaptations. *Nat Cell Biol, 9*(10), 1102-1109. doi:10.1038/ncb1007-1102

Zaffagnini, G., & Martens, S. (2016). Mechanisms of Selective Autophagy. *J Mol Biol, 428*(9 Pt A), 1714-1724. doi:10.1016/j.jmb.2016.02.004

Zhang, H., Kong, X., Kang, J., Su, J., Li, Y., Zhong, J., & Sun, L. (2009). Oxidative stress induces parallel autophagy and mitochondria dysfunction in human glioma U251 cells. *Toxicol Sci, 110*(2), 376-388. doi:10.1093/toxsci/kfp101

Zhang, Y., Liu, R., Ni, M., Gill, P., & Lee, A. S. (2010). Cell surface relocalization of

the endoplasmic reticulum chaperone and unfolded protein response regulator GRP78/BiP. *J Biol Chem, 285*(20), 15065-15075. doi:10.1074/jbc.M109.087445

Zhou, W., Zhu, M., Wilson, M. A., Petsko, G. A., & Fink, A. L. (2006). The oxidation state of DJ-1 regulates its chaperone activity toward alpha-synuclein. *J Mol Biol, 356*(4), 1036-1048. doi:10.1016/j.jmb.2005.12.030

Ziauddin, M. F., Guo, Z. S., O'Malley, M. E., Austin, F., Popovic, P. J., Kavanagh, M. A., . . . Bartlett, D. L. (2010). TRAIL gene-armed oncolytic poxvirus and oxaliplatin can work synergistically against colorectal cancer. *Gene Ther, 17*(4), 550-559. doi:10.1038/gt.2010.5

국문 초록

활성 산소체 (Reactive Oxygen Species, ROS) 는 최외각에 잉여 전자를 가지고 있고, 이 특성을 이용하여 세포 내 여러 반응에 전자 공여원으로 이용된다. 하지만 과량의 활성 산소체가 세포 내에 존재 할 경우, 생성된 과량의 활성 산소체는 세포 내 물질과 반응하여 세포 내 산화적 스트레스 (oxidative stress)를 유발한다. 한편 세포 내에는 산화적 스트레스 (oxidative stress)를 제거하는 시스템들 (oxidative stress scavengers) 이 있어서 과량의 ROS를 제거하는 역할을 하고 있지만, 이들 기작은 단지 세포 내 활성 산소체의 농도를 낮추거나 다른 기작에서 부산물로 발생하거나, 반응에 필요한 활성 산소체의 양을 조절하는 역할을 하고 있다. 따라서 이러한 기작은 과량의 활성 산소체로 발생하는 산화적 스트레스를 대응하는 방법에 있어서 충분히 설명할 수 없는 한계점을 가지고 있다.

DJ-1/PARK7은 세포 내에서 다양한 기능을 가진 단백질로서 세포의 발생과 발달, Parkinson's disease와 연관된 미토콘드리아 (mitochondria) 항상성 유지 등의 역할을 하지만 그 중에서도 활성 산소체의 인식 및 제거와 관계된 기능을 가지고 있다. 암세포에 특이적으로 발현하는 수용체를 인식하여 세포 내에서 미토콘드리아 유래 활성 산소체를 생성하는 TRAIL (tumor necrosis factor-related apoptosis-inducing ligand)에 의해 유발된 oxidative stress 상황 하에서 DJ-1은 자식작용 수용체 (autophagy receptor) 로 작용하는 p62

기능을 조절하고 유비퀴틴 (ubiquitin) 이 부착된 단백질의 자식작용 (autophagy) 으로의 전달을 유도하게 된다. 또한 TRAIL에 의한 산화적 스트레스에 반응하는 DJ-1은 46번째, 53번째 및 106번째 cysteine에 활성산소체 유래 산소 원자를 받아들여 산화 (oxidation) 되는데 이 과정을 통해 세포 내 과량의 활성 산소체를 제거하게 된다. 그리고 산화된 DJ-1은 TRAIL이 유발한 스트레스에 의해 세포질로 나와서 N 말단에 아르기닌 (arginine) 이 부착된 소포체 샤페론 BiP (ER chaperone BiP) 과 상호작용하게 되는데 이는 샤페론 (chaperone) 의 기능을 보조하는 보조샤페론 (co-chaperone) 과 흡사하다. 즉 산화된 DJ-1 과 아르기닌화 된 BiP (R-BIP) 은 p62의 자기 중합체화 (self-oligomerization) 를 유도하며 이 과정을 통해 산화적 스트레스로 발생한 변성 단백질 (misfolded protein) 및 적절하게 접히지 않은 단백질 (unfolded protein) 등 세포 내 독성물질을 자식작용을 통해 처리하게 된다.

또한 DJ-1이 결손 된 세포의 경우, TRAIL에 의해 발생한 세포 내 독성물질이 오토파고솜 (autophagosome) 으로 전달되어 최종적으로 리소좀 (lysosome) 에 의해 분해되는 과정이 저해된다. 궁극적으로는 DJ-1이 결여된 세포는 TRAIL 및 기타 스트레스 유발 물질이 유도하는 세포 소기관 내의 스트레스에 취약하고 이는 세포 생존성과 연관되게 된다. 따라서 본 연구에서는 DJ-1의 산화적 스트레스 상황 하에서 발생한 세포 내 독성물질 분해 과정에서의 역할을 확인하였고, DJ-1의 세포 보호기능을 규명하였다.

주요어: 산화적 스트레스 (Oxidative stress), DJ-1, 단백질 분해 과정

(proteolysis), 단백질 품질 관리 (protein quality control), R-BiP, N 말단 규칙 (N-end rule pathway), N-말단 아르기닌화 (N-terminal arginylation), 자식 작용 (macroautophagy), p62.

학번: 2011-22826